



DIPLOMARBEIT

# Leading order HVP Contributions to the Anomalous Magnetic Moment of the Muon from Holographic QCD

zur Erlangung des akademischen Grades

**Diplom-Ingenieur**

im Rahmen des Studiums

**Technische Physik**

eingereicht von

**Michael Stadlbauer**

Matrikelnummer 1609924

ausgeführt am Institut für Theoretische Physik  
der Fakultät für Physik der Technischen Universität Wien

Betreuung  
Betreuer: Univ.-Prof. Dipl.-Ing. Dr. A. Rebhan

Wien, 13.12.2020

\_\_\_\_\_  
(Unterschrift Verfasser)

\_\_\_\_\_  
(Unterschrift Betreuer)



Die approbierte gedruckte Originalversion dieser Diplomarbeit ist an der TU Wien Bibliothek verfügbar  
The approved original version of this thesis is available in print at TU Wien Bibliothek.

Michael Stadlbauer

# Leading order HVP Contributions to the Anomalous Magnetic Moment of the Muon from Holographic QCD

Master Thesis

Institute for Theoretical Physics  
Vienna University of Technology

Supervision

First Supervisor  
Prof. Dr. Anton Rebhan

December 2020



Die approbierte gedruckte Originalversion dieser Diplomarbeit ist an der TU Wien Bibliothek verfügbar  
The approved original version of this thesis is available in print at TU Wien Bibliothek.

# Contents

<b>Abstract</b>	<b>v</b>
<b>Acknowledgments</b>	<b>vi</b>
<b>1 Introduction</b>	<b>1</b>
1.1 A brief history of holography . . . . .	1
1.2 The idea of holographic QCD . . . . .	2
1.3 The HVP in hQCD . . . . .	3
1.4 The anomalous magnetic moment of the muon $a_\mu$ . . . . .	3
1.5 Overview . . . . .	4
<b>2 Gauge/Gravity duality</b>	<b>5</b>
2.1 The holographic principle . . . . .	5
2.2 Anti-de Sitter space . . . . .	6
2.3 Yang-Mills theory . . . . .	8
2.4 $\mathcal{N} = 4$ Super Yang-Mills theory in 3+1 dimensions . . . . .	9
2.5 <i>AdS/CFT</i> correspondence . . . . .	10
2.6 From <i>AdS/CFT</i> to <i>AdS/QCD</i> . . . . .	15
<b>3 The anomalous magnetic moment of the muon</b>	<b>17</b>
3.1 Current status of $a_\mu$ . . . . .	17
3.2 Calculation of leading order HVP contribution to $a_\mu$ . . . . .	18
<b>4 Holographic QCD models and their HVP</b>	<b>23</b>
4.1 Hard-Wall Model (HW) . . . . .	23
4.1.1 HW1 model . . . . .	28
4.1.2 HW2 model . . . . .	28
4.2 Soft-Wall Model (SW) . . . . .	29
4.2.1 The SW two-point correlation function . . . . .	30
4.2.2 Calculating the self energy function for the SW Model . . . . .	31
4.3 Generalized SW Model . . . . .	34
4.4 Interpolating between HW and SW model . . . . .	37
4.4.1 Dilaton background for the HW model . . . . .	38
4.4.2 Improved holographic QCD background . . . . .	40
4.5 Li and Huang dilaton model . . . . .	42
4.5.1 Vector meson states and the HVP . . . . .	45
4.6 Holographic QCD model from Sen's tachyon action . . . . .	48
4.7 Sakai-Sugimoto model . . . . .	55

4.7.1	Background and induced metric . . . . .	56
4.7.2	Meson states . . . . .	57
<b>5</b>	<b>Conclusion and Outlook</b>	<b>61</b>
5.1	Results from holographic QCD . . . . .	61
5.1.1	Anomalous magnetic moment . . . . .	61
5.1.2	Mass spectrum . . . . .	63
5.2	Other results . . . . .	63
5.2.1	Results from lattice QCD . . . . .	63
5.2.2	Results from dispersive calculations . . . . .	63
5.2.3	Experimental vector meson masses . . . . .	64
5.3	Possible improvements . . . . .	65
<b>A</b>	<b>Transformation into Liouville normal form</b>	<b>67</b>
	<b>Bibliography</b>	<b>69</b>

# List of Figures

1.1	Leading order HVP Feynman diagram . . . . .	4
2.1	$AdS_2$ embedded in $\mathbb{R}^{1,2}$ . . . . .	7
2.2	Sketch of the AdS/CFT correspondence . . . . .	12
2.3	Sketch: duality between two theories . . . . .	15
3.1	Pictorial representation of the dressed vertex function . . . . .	18
3.2	Leading order vertex diagram for the HVP . . . . .	19
3.3	The hadronic blob as an exchange of a neutral vector meson . . . . .	21
4.1	Plot of the first five eigenstates for the HW model . . . . .	27
4.2	Plot of the first four eigenstates for the SW model . . . . .	34
4.3	Plot of the dilaton background $e^{-\Phi(z)}$ for the model interpolating between HW and SW model . . . . .	40
4.4	Plot of the metric function $b_s(z) = e^{A_s(z)}$ for the Li-Huang model . . . . .	45
4.5	Plot of the potential $V_v(z)$ for the Li-Huang model . . . . .	46
4.6	Plot of the first four eigenstates for the Li-Huang model . . . . .	47
4.7	Plot of the tachyon field $\tau(z)$ . . . . .	51
4.8	Plot of the coordinate transformation $z \rightarrow u$ . . . . .	52
4.9	Plot of the potential $V(u)$ for the tachyon condensation model . . . . .	52
4.10	Plot of the first four eigenstates for the tachyon condensation model . . . . .	53
4.11	Plot of the first four eigenstates for the Sakai-Sugimoto model . . . . .	59

# List of Tables

2.1	The four laws of black hole mechanics and their thermodynamical counterparts	5
4.1	Field content of the hard-wall model	24
4.2	Vector meson masses $M_{V_n}$ and decay constants $F_{V_n}^{1/2}$ of the HW models	29
4.3	Values of $a_\mu^{\text{HVP,LO}}$ for different parameter fits of the HW model	29
4.4	Vector meson masses $M_{V_n}$ and decay constants $F_{V_n}^{1/2}$ of the standard SW model	34
4.5	Values of $a_\mu^{\text{HVP,LO}}$ from the standard SW model and two generalizations of it	37
4.6	Parameters $\kappa$ and $z_m$ corresponding to the chosen value of $\langle \frac{\alpha}{\pi} G^2 \rangle$	39
4.7	Masses of the first six vector meson state for each value of $\langle \frac{\alpha}{\pi} G^2 \rangle$	40
4.8	Results for $a_\mu^{\text{HVP,LO}}$ for each value of $\langle \frac{\alpha}{\pi} G^2 \rangle$ and $N_f = 2, 3$	40
4.9	Vector meson masses $M_{V_n}$ and decay constants $F_{V_n}^{1/2}$ of a model interpolating between HW and SW model	42
4.10	Values for $a_\mu^{\text{HVP,LO}}$ within a model interpolating between HW and SW model	42
4.11	Parameters for the different Li-Huang models	45
4.12	Calculated masses for the first eight vector mesons in the Li-Huang model	46
4.13	Calculated values for the decay constants of the first eight vector mesons in the Li-Huang model	48
4.14	Results for $a_\mu^{\text{HVP,LO}}$ using the Li-Huang model	48
4.15	Vector meson masses $M_{V_n}$ and decay constants $F_{V_n}^{1/2}$ of the tachyon condensation model	55
4.16	Values for $a_\mu^{\text{HVP,LO}}$ within the tachyon condensation model	55
4.17	Boundary conditions defined by the brane configuration of the Sakai-Sugimoto model	56
4.18	Vector meson masses $M_{V_n}$ and decay constants $F_{V_n}^{1/2}$ of the Sakai-Sugimoto model	60
4.19	Calculated values for $a_\mu^{\text{HVP,LO}}$ within the Sakai-Sugimoto model	60
5.1	Summary of all the calculated values for $a_\mu^{\text{HVP,LO}}$ within the considered hQCD models	62
5.2	Contributions of the different quarks to $a_\mu^{\text{HVP,LO}}$ up to $N_f = 3$ from lattice QCD	63
5.3	Contributions of the different decay channels to $a_\mu^{\text{HVP,LO}}$ in the dispersive approach	64
5.4	Experimentally measured vector meson masses $M_{V_n}$	64



# Abstract

In this thesis the hadronic vacuum polarization (HVP) is calculated using a variety of holographic QCD (hQCD) models. The results are then used to calculate the leading order HVP contributions to the anomalous magnetic moment of the muon  $a_\mu^{\text{HVP,LO}}$ . These hQCD models (sometimes also called *AdS/QCD* models) are based on the gauge/gravity duality (the generalization of the *AdS/CFT* correspondence). Since the low energy regime of QCD is not accessible with perturbation theory, one usually has to rely on lattice QCD (LQCD) or calculations using experimental data (usually cross sections). However, the LQCD calculations and the experimental data give different results. Therefore, it is interesting to see what *AdS/QCD* models predict for the HVP since they provide the possibility of calculating observables in the low energy regime directly.

Both categories of models, the so-called top-down models which are directly based on string theory and the bottom-up models which only use the main ideas from string theory, are studied in this thesis. We begin by giving a broad introduction into the subject of gauge/gravity duality and the motivation for the *AdS/QCD* "correspondence" from the *AdS/CFT* correspondence. Then a detailed overview of the concrete models used for the calculation of the HVP is given. This includes among others the soft-wall (SW) and the hard-wall (HW) model as well as a model interpolating between these two. In addition more advanced models such as a model from tachyon condensation, the Li-Huang dilaton model and the Sakai-Sugimoto model are part of this study. Finally we calculate the numerical values for the HVP and the resulting meson spectrum, compare them with each other and discuss possible further improvements of the models.

# Acknowledgments

I would like to thank Anton Rebhan for supervising this thesis. Additionally, I wish to acknowledge Josef Leutgeb and Jonas Mager for proofreading my thesis and their numerous references to typos and other inaccuracies.

# Chapter 1

## Introduction

### 1.1 A brief history of holography

The idea of holography - the description of everything contained within a spacetime by the information encoded at its surface - goes back to the past century. Originally this idea came from string theory, which at first was developed to describe the strong interaction. The intention was that a description of particles as strings rather than as points would lead to an explanation of the strong nuclear force [1]. That was in the 1960s and early 70s. However, in 1971 Wilczek, Gross [2] and Politzer [3] discovered the asymptotic freedom of  $SU(3)$  Yang-Mills theory (nowadays an important ingredient of QCD) which allows perturbative calculation of observables at large energies. This idea gave a much more suitable description of the strong interaction and the idea of string theory as a description of the strong nuclear force was abandoned. Later in 2004 the three men mentioned above were awarded the Nobel prize in physics for their discovery.

A few years later in 1974 Gerard 't Hooft (also by now a Nobel laureate in physics) published his work on planar diagrams for the strong interaction [4], where he noticed that the expansion of QCD for a large number of colors  $N_c$  is very similar to string theory. In the same year Scherk et al. [5] noticed that every string theory naturally includes a description of gravity and further that string theory could be considered as a theory of quantum gravity. At the same time Hawking et al. published a paper on black hole mechanics, stating that black holes can be described by four laws very similar to the laws of thermodynamics [6]. This discovery formed the basis of the holographic principle, since one can directly conclude from it, that the entropy of a black hole is proportional to its surface area rather than its volume [7]. Also, still in the same year, Kenneth Wilson proposed lattice QCD and showed that quarks can be confined through strings [8]. These discoveries, especially the last one, brought the idea of using string theory as a description of QCD back in the game.

Fast forwarding to the early 1990s Gerard t' Hooft [9] and Leonard Susskind [10] first came up with the idea that one might be able to describe the physics of a  $d$ -dimensional universe entirely by the information encoded in its  $(d - 1)$ -dimensional boundary. A few years later in 1997 - the probably most important year for holography so far - groundbreaking discoveries were made. First Polyakov came to the conclusion that one should use a five dimensional non-compact  $AdS$  like space for string theory in order to obtain a consistent theory which is further dual to a field theory like QCD [11]. Then later that same year Juan

M. Maldacena published his famous paper "The Large N Limit of Superconformal Field Theories and Supergravity" [12], where he gives a concrete example for a duality between a certain string theory in  $AdS$  spacetime and a conformally invariant field theory ( $CFT$ ). Today this is known as  $AdS/CFT$  correspondence (or sometimes Maldacena duality) and is the most cited paper in the history of theoretical physics with approximately 20,000 citations. A few months later in 1998 Edward Witten was the first who noticed that this is precisely the holographic duality proposed by Susskind [13]. Numerous other concrete examples of holographic dualities have been found since then. One of the main features of these dualities is that they enable us to calculate correlation functions on the field theory side by considering the on shell action on the  $AdS$  side. To be more concrete we can identify the generating functional in the exponent of the partition function  $Z[\phi_{(0)}] = e^{-W[\phi_{(0)}]}$  with the on-shell supergravity action evaluated under certain boundary conditions.

$$W[\phi_{(0)}] = \mathcal{S}_{\text{sugra}}[\phi] \Big|_{\lim_{z \rightarrow 0} (\phi(z,x) z^{\Delta-d}) = \phi_{(0)}(x)}. \quad (1.1)$$

This provides the possibility to calculate correlation functions of a strongly coupled  $CFT$  by calculating the variation of the action of the weakly coupled dual theory. For more details see chapter 2 (note that in the stronger form of the duality one directly identifies the partition function of the  $CFT$  and the string theory). Even though there is no rigorous proof of the duality, there is a tremendous amount of evidence that it should be correct.

## 1.2 The idea of holographic QCD

As mentioned above, the description of QCD with string theory is not a new idea. It began by noticing that flux tubes (Wilson lines) are objects behaving very much like strings. So the idea came up to describe QCD with flux tubes realized by strings as basic objects. Briefly after Maldacena published his first paper on  $AdS/CFT$ , Witten was the first to propose a holographic approach to QCD in [13]. This idea has been further developed in the 1999 review paper of the holographic correspondence [14]. After that a broad variety of models has been proposed. In general one distinguishes between the so called bottom-up and top-down models [15].

Top-down models are directly based on string theory and constructed analogously to the  $AdS/CFT$  correspondence. The ultimate goal of such a model would be to find a weakly coupled theory exactly dual to QCD. So far nobody has found such a theory, despite numerous attempts, but there are many theories that can describe certain features of QCD in certain energy regimes very well. One of them is the model of Sakai and Sugimoto [16, 17] discussed in section 4.7.

Bottom-up models on the other hand are models where one only takes some key features of string theory. Essentially one tries to guess the correct dual theory of QCD. There are many bottom-up models which provide results in good agreement with experiment. Such models are for example the hard-wall [18] and the soft-wall model [19] to name only two. Actually all hQCD models we will discuss in chapter 4, except the Sakai-Sugimoto model, are bottom-up models. However, some of them, such as the  $AdS/QCD$  model from tachyon condensation of Kiritsis et al. [20, 21, 22], are very much based on string theory, but not directly obtained from the latter. Also there are a lot of models we do not discuss

in detail in this thesis, as for example [23].

As in the case of the *AdS/CFT* correspondence, the main point for the calculation of observables on the QCD side of the *AdS/QCD* models is that we can calculate correlation functions of the strongly coupled gauge theory (here QCD) by identifying the generating functional with the dual weakly coupled action. For the correlation function this means that

$$\left\langle \exp \left( \int d^d x \mathcal{O} \phi_{(0)} \right) \right\rangle_{\text{QCD}} = e^{-\mathcal{S}_{\text{dual}} \Big|_{\lim_{z \rightarrow 0} (\phi(z,x) z^{\Delta-d}) = \phi_{(0)}(x)}}, \quad (1.2)$$

such that we have to calculate for example the second variation of (1.2) to obtain the two-point correlation function. The left hand side is then per definition the two-point correlator and on the right hand side we are left with the second variation of the action of the dual theory.

### 1.3 The HVP in hQCD

As the title of the thesis suggests, our main goal is to calculate the hadronic vacuum polarization (HVP) using hQCD models and further study their predictions for the leading order HVP contributions to the anomalous magnetic moment of the muon. The vacuum polarization at leading order is determined by the two-point correlation function of the electromagnetic current

$$i \int d^4 x e^{iqx} \langle 0 | T J_V^{a\mu}(x) J_V^{b\nu}(0) | 0 \rangle = \delta^{ab} (q^2 \eta^{\mu\nu} - q^\mu q^\nu) \Pi_V(-q^2). \quad (1.3)$$

In our hQCD picture this means that we have to evaluate the second variation of the dual action  $\mathcal{S}_{\text{dual}}$  with respect to the source  $V_\mu^a$  of the vector current  $J_V^{a\mu}$

$$\frac{\delta^2 \mathcal{S}_{\text{dual}} [V_\mu]}{\delta V_\mu^a(-q) \delta V_\nu^b(q)} = i \int d^4 x e^{iqx} \langle 0 | T J_V^{a\mu}(x) J_V^{b\nu}(0) | 0 \rangle. \quad (1.4)$$

This is not a trivial task to do, as we will see in chapter 4 when we do explicit calculations.

### 1.4 The anomalous magnetic moment of the muon $a_\mu$

Given the vacuum polarization  $\Pi_V(-q^2)$  it is straightforward to calculate the leading order (LO) HVP contribution to the anomalous magnetic moment of the muon  $a_\mu^{\text{HVP,LO}}$ . As we will show in chapter 3,  $a_\mu$  can be calculated from the vertex function by using the projection techniques. The relevant Feynman diagram is given in figure 1.1. With a few pages of calculation one can derive an integral where we just have to plug in  $\Pi_V(-q^2)$  in order to calculate the leading order HVP contribution to  $a_\mu$ .

$$a_\mu^{\text{HVP,LO}} = \left( \frac{\alpha}{\pi} \right)^2 \int_0^\infty dK^2 f(K^2) \hat{\Pi}(K^2) \quad (1.5)$$

In (1.5) we integrate over the Euclidean momentum  $K^2$ .  $f(K^2)$  is an analytic function and  $\hat{\Pi}(K^2)$  depends only on vacuum polarization  $\Pi_V(-q^2)$ , both are explicitly given in section 3.2.

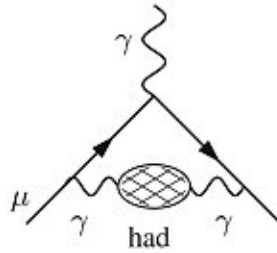


Figure 1.1: Leading order HVP Feynman diagram [24].

The reason why it is interesting to see what results hQCD models provide for the LO HVP contributions to  $a_\mu$  is the following. First of all there is still a discrepancy between the experimentally measured value of  $a_\mu$  and the theoretical predictions, at the level of  $3.7\sigma$  [25]. The highest uncertainties on the side of the theoretical calculations are from the hadronic contributions. A big part of the hadronic contributions are the contributions from the vacuum polarization, which at leading order we are going to calculate in this thesis. Currently there is an ongoing discussion on the value of  $a_\mu^{\text{HVP,LO}}$ . Recent lattice calculations [26] provide a value which is in better agreement with the experimental data than the best calculations using dispersion relation and experimental cross section data. More importantly they managed to shrink the error bar to a level comparable with the dispersive approach. However, they had to correct their initially provided result in an updated version of the paper which brings the predicted value out of the "no new physics area", but it is still closer to the experimental value than the dispersive calculations using cross section data. Moreover, there are still unresolved discrepancies between different approaches within lattice QCD [27]. So it is not only interesting to see what hQCD yields for this value because the discrepancy of the experimental and theoretical result could possibly be a hint for new physics, but also in order to see what it can contribute to the ongoing discussion on the value of  $a_\mu^{\text{HVP,LO}}$ .

For more details on the current values of  $a_\mu$  and  $a_\mu^{\text{HVP,LO}}$  from both experiment and theory see section 3.1.

## 1.5 Overview

This thesis is organized in the following way. In chapter 2 we review the main concepts leading to holographic QCD. Starting from the holographic principle we try to cover everything needed to understand the *AdS/CFT* correspondence and then also the hQCD models. In chapter 3 the current status of the anomalous magnetic moment of the muon is discussed. Also a sketch of the derivation of a compact integral formula for  $a_\mu^{\text{HVP,LO}}$  is presented. In chapter 4, the core part of this thesis, various hQCD models are presented and the HVP is calculated explicitly. At the end of each section we summarize the resulting meson spectra as well as the predicted values for  $a_\mu^{\text{HVP,LO}}$ . In the last chapter, chapter 5, we summarize all our results and compare them with the predictions from other approaches. Also possible improvements are discussed there. In appendix A we give a brief overview of the transformations of a Liouville eigenvalue problem into the Liouville normal form.

## Chapter 2

# Gauge/Gravity duality

### 2.1 The holographic principle

In this section a brief overview of the holographic principle based on [7] and [28] is given. Basically the holographic principle constrains the entropy  $S$  (and therefore the information) of a finite volume  $V$  in spacetime. This bound is called the Bekenstein bound and is proportional to the surface area  $A$  of the boundary  $\partial V$  of the volume  $V$ . This means that all the information in a volume  $V$  can actually be described by just as much information as can fit on the boundary. The amount of information is determined by the number of microstates. One can therefore say that the degrees of freedom of a theory in the bulk are sufficiently described by the degrees of freedom at the boundary. For this section let us set all constants to unity

$$\hbar = G = c = k = 1. \quad (2.1)$$

To motivate this statement let us recapitulate the four laws of black hole mechanics and their thermodynamical counterparts in table 2.1. The right hand side of the table should

	black hole mechanics	thermodynamics
0 <sup>th</sup>	$\kappa = \text{const.}$	$T = \text{const.}$
1 <sup>st</sup>	$\delta M = \frac{\kappa}{8\pi} \delta A + \text{work terms}$	$\delta E = T \delta S + \text{work terms}$
2 <sup>nd</sup>	$\delta A \geq 0$	$\delta S \geq 0$
3 <sup>rd</sup>	$\kappa \rightarrow 0$ impossible	$T \rightarrow 0$ impossible

Table 2.1: The four laws of black hole mechanics and their thermodynamical counterparts.

be clear. The left hand side states from top to bottom that the surface gravity is constant for a stationary black hole, the change of mass is related to a change of the surface area which always has to be non-negative and lastly that the surface gravity cannot vanish. Comparing the two sets of laws we see that we could formally identify the surface gravity  $\kappa$  with the temperature  $T$ , the black hole surface area  $A$  with the entropy  $S$ , and the black hole mass  $M$  with the energy  $E$ . The last one is of course true as  $E = M$  in our units. The laws above are of course only true for black holes and not for arbitrary systems. The Bekenstein entropy bound now states that

$$S \leq \frac{A}{4}. \quad (2.2)$$

For the case of a black hole one can show that  $S_{BH} = \frac{A}{4}$  (the constant  $\frac{1}{4}$  is fixed after consideration of the Hawking temperature  $T = \frac{\kappa}{2\pi}$ ). This means that a black hole is the state of maximum stored information and all other systems contain less information.

In an optical hologram the information stored on a 2-dimensional surface pretends to be 3-dimensional. According to the holographic principle something similar should also be true for our real world. This is where the idea of holographic dualities comes into play. The idea is that a theory living in a  $d$ -dimensional bulk is related to another theory at its  $(d-1)$ -dimensional boundary. This is exactly what we are going to study in this thesis.

## 2.2 Anti-de Sitter space

The  $n$ -dimensional Anti-de Sitter space, or short  $AdS_n$  space, is of great importance for holographic models. Therefore we will give a short overview of its geometry in this subsection by stating some of its most important facts based on [29]. The  $AdS$  metric describes a spacetime which is maximally symmetric and has constant negative curvature. As such it is a solution of the vacuum Einstein equations with negative cosmological constant  $\Lambda < 0$

$$R_{\mu\nu} - \frac{1}{2}Rg_{\mu\nu} + \Lambda g_{\mu\nu} = 8\pi T_{\mu\nu}, \quad T_{\mu\nu} \equiv 0, \quad (2.3)$$

in the same way as Minkowski spacetime is a solution of the Einstein equations (2.3) for vanishing cosmological constant  $\Lambda = 0$ . A maximally symmetric spacetime with  $\Lambda > 0$  is called de Sitter space, or short  $dS$  space. Global  $AdS$  space with  $AdS$ -radius  $L$  is given by the metric

$$ds^2 = L^2 \left( -\cosh^2 \rho d\tau^2 + d\rho^2 + \sinh^2 \rho d\Omega_{S^{d-2}}^2 \right) \quad \rho \in \mathbb{R}_+, \tau \in [0, 2\pi]. \quad (2.4)$$

To avoid closed time-like curves one usually takes the universal cover where  $\tau \in \mathbb{R}$ . For two dimensions the spacetime ( $AdS_2$ ) can be embedded in flat 3-dimensional  $\mathbb{R}^{1,2}$  spacetime by defining

$$\begin{aligned} X^0 &= L \cosh \rho \cos \tau \\ X^1 &= L \sinh \rho \\ X^2 &= L \cosh \rho \sin \tau. \end{aligned} \quad (2.5)$$

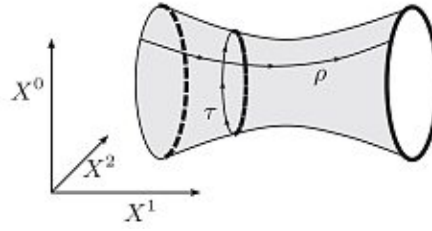
For a schematic picture see figure 2.1. The metric of  $\mathbb{R}^{1,2}$  is given by

$$ds^2 = - (dX^0)^2 + (dX^1)^2 - (dX^2)^2. \quad (2.6)$$

As one can easily check substituting (2.5) into (2.6) gives back the  $AdS$  metric of equation (2.4). Actually the situation is even more general. One can always embed an  $AdS$  spacetime in a Minkowski spacetime with one dimension higher in the same manner as in (2.6) for arbitrary dimensions, but it is of course only possible to draw it for three dimensions as in our example. Sometimes (in this thesis most of the time) the  $AdS_d$  metric in the coordinates of (2.4) is not the most useful one. Therefore we have to make a coordinate transformation. Here we just give a few examples of the  $AdS_d$  metric in different coordinates without explicitly deriving them. The coordinate transformation  $\tan \theta = \sinh \rho$  gives the metric of the Einstein static universe

$$ds^2 = \frac{L^2}{\cos^2 \theta} \left( -d\tau^2 + d\theta^2 + \sin^2 \theta d\Omega_{d-2}^2 \right). \quad (2.7)$$



Figure 2.1:  $AdS_2$  embedded in  $\mathbb{R}^{1,2}$  [29].

Also, there is the possibility of a completely different parameterization of the  $AdS_d$  spacetime embedded in  $\mathbb{R}^{d-1,2}$  given by

$$\begin{aligned} X^0 &= \frac{L^2}{2r} \left( 1 + \frac{r^2}{L^4} (\tilde{x}^2 - t^2 + L^2) \right) \\ X^i &= \frac{rx^i}{L} \quad \text{for } i \in \{1, \dots, d-2\} \\ X^{d-1} &= \frac{L^2}{2r} \left( 1 + \frac{r^2}{L^4} (\tilde{x}^2 - t^2 - L^2) \right) \\ X^d &= \frac{rt}{L}, \end{aligned} \tag{2.8}$$

resulting in the metric

$$ds^2 = \frac{L^2}{r^2} dr^2 + \frac{r^2}{L^2} (\eta_{\mu\nu} dx^\mu dx^\nu), \quad x^\mu \in \mathbb{R}^{d-2,1}, \quad r \in \mathbb{R}_+. \tag{2.9}$$

This metric is also called the Poincaré patch of AdS. Note that we only cover half of the  $AdS$  spacetime, because  $r > 0$ . The conformal boundary of this spacetime is located at  $r \rightarrow \infty$ . Making further the transformation  $z = \frac{L^2}{r}$  gives

$$ds^2 = \frac{L^2}{z^2} (dz^2 + \eta_{\mu\nu} dx^\mu dx^\nu), \tag{2.10}$$

with the conformal boundary at  $z \rightarrow 0$ . Note that it looks like this metric is singular at  $z = 0$ . This is however not a real singularity. The curvature of this metric is constant and negative for the whole spacetime. As a last transformation we can also make the substitution  $z = \exp(-\frac{r}{L})$  such that we obtain

$$ds^2 = dr^2 + L^2 e^{2r/L} \eta_{\mu\nu} dx^\mu dx^\nu, \tag{2.11}$$

with the conformal boundary again at  $r \rightarrow \infty$ . Each one of these  $AdS$  metrics might be useful in one or the other way. Note that here (and also in the following sections of this chapter) we have used the metric convention with negative temporal and positive spatial signs  $\eta_{\mu\nu} = \text{diag}(-1, 1, \dots, 1)$ , since most of the literature on general relativity uses this convention. Later, as for example in chapter 4, we will use mainly the other convention, which is more commonly used in particle physics. Which convention is used is always stated clearly when necessary to avoid confusion. Also in most of the calculations we do in this thesis it will not matter anyway.

## 2.3 Yang-Mills theory

Yang-Mills theory is a generalization of electromagnetism to a theory of interacting spin-1 fields. A Yang-Mills theory without additional matter is sometimes referred to as pure spin-1 Yang-Mills theory [30]. To generalize electromagnetism we alter the gauge potential  $A_\mu$  electromagnetic tensor  $F_{\mu\nu} = \partial_\mu A_\nu - \partial_\nu A_\mu$  by introducing Lie groups. We define the Lie-algebra valued gauge potential by

$$A_\mu = A_\mu^a T^a \quad (2.12)$$

and further the Lie-algebra valued field strength by

$$F_{\mu\nu} = \partial_\mu A_\nu - \partial_\nu A_\mu - i[A_\mu, A_\nu]. \quad (2.13)$$

$A_\mu^a$  describes a single spin 1 field with the index  $a = 1, \dots, \dim G$ , where  $\dim G$  is the dimension of the Lie group (the number of its generators  $T^a$ ). We choose the generators such that

$$\text{Tr} \{T^a T^b\} = \frac{1}{2} \delta^{ab} \quad \text{and} \quad [T^a, T^b] = i f^{abc} T^c. \quad (2.14)$$

Matter fields are represented by some spinor field  $\psi$  which couples to the gauge fields via the covariant derivative

$$\mathcal{D}_\mu \psi = \partial_\mu \psi - i A_\mu \psi. \quad (2.15)$$

In the adjoint representation, where the dimension of the group  $\dim G$  and the dimension of its representation  $\dim R$  are equal, the covariant derivative acting on  $\phi = \phi^a T^a$  can be written as

$$\mathcal{D}_\mu \phi = \partial_\mu \phi - i [A_\mu, \phi]. \quad (2.16)$$

Under gauge transformations with  $\Omega(x) \in G$  the gauge fields and the field strength transform according to

$$A_\mu \rightarrow \Omega(x) A_\mu \Omega^{-1}(x) + i \Omega(x) \partial_\mu \Omega^{-1}(x) \quad (2.17)$$

and

$$F_{\mu\nu} \rightarrow \Omega(x) F_{\mu\nu} \Omega^{-1}(x). \quad (2.18)$$

The action of the Yang-Mills theory without matter fields is given by

$$S_{\text{YM}} = -\frac{1}{2g_{\text{YM}}^2} \int d^4x \text{Tr} \{F^{\mu\nu} F_{\mu\nu}\} = -\frac{1}{4g_{\text{YM}}^2} \int d^4x F^{\mu\nu a} F_{\mu\nu}^a, \quad (2.19)$$

with the Yang-Mills coupling constant  $g_{\text{YM}}$ . The resulting equations of motion are the non-Abelian generalisations of the Maxwell equations given by

$$\begin{aligned} \mathcal{D}_\mu F^{\mu\nu} &= 0 \\ \mathcal{D}_\mu {}^* F^{\mu\nu} &= 0. \end{aligned} \quad (2.20)$$

The question arises whether one can generalize the action (2.19) in a way such that it is still gauge invariant as well as Lorentz invariant. If we also impose the restriction that the power of  $A_\mu$  in the action should not be higher than 4 (such that the action is quadratic in field strengths) there is only one possible candidate we can add, the so called theta term

$$S_\theta = \frac{\theta}{16\pi^2} \int d^4x \text{Tr} \{{}^* F^{\mu\nu} F_{\mu\nu}\}. \quad (2.21)$$

If  $\theta$  depends on the spacetime coordinates it has to be written inside the integral. It is then called the axion field. As mentioned one can alter the pure Yang-Mills theory by adding matter fields to the action. For scalar field this can be done by adding the term

$$S_{\text{scalar}} = \int d^4x \mathcal{D}_\mu \phi^\dagger \mathcal{D}^\mu \phi - V(\phi) \quad (2.22)$$

to the action. Here  $V(\phi)$  can include mass terms proportional to  $\phi^2$  as well as  $\phi^4$  interactions. Fermions can be added by an additional term of the form

$$S_{\text{fermion}} = \int d^4x i \bar{\psi} \not{D} \psi - m \bar{\psi} \psi. \quad (2.23)$$

If we take the action (2.19) with the symmetry group  $SU(3)$  and add six fermions (the quarks) with the correct charge coupling constant analogous to (2.23) we obtain the theory of QCD.

## 2.4 $\mathcal{N} = 4$ Super Yang-Mills theory in 3+1 dimensions

In this section we give an overview of the most important facts of  $\mathcal{N} = 4$  Super Yang-Mills (SYM) theory. Here  $\mathcal{N} = 4$  refers to the number of independent supersymmetries. A supersymmetry is a symmetry that transforms physical Bose fields into physical Fermi fields [31]. As the first part of this chapter, also this section is heavily based on [29]. To construct the Lagrangian for such a theory based on the previous section, we start by taking the pure Yang-Mills action terms (2.19) and (2.21) and add a term for four massless Weyl fermions  $\lambda_\alpha^a(x)$  with  $a = 1, 2, 3, 4$  to the Lagrangian.

$$\mathcal{L}_{\text{Weyl}} = -i \bar{\lambda}^a \bar{\sigma}^\mu D_\mu \lambda_a \quad (2.24)$$

Under the supersymmetry transformation these fermion fields should transform into bosonic fields and vice versa. Therefore also the degrees of freedom of the bosonic and fermionic fields in the theory have to match. Since so far the only bosonic field is the vector gauge field  $A_\mu$  we have to add further fields. In this case we add six real scalar fields  $\phi^i(x)$  with  $i = 1, \dots, 6$  to the Lagrangian by adding

$$\mathcal{L}_{\text{Scalar}} = - \sum_i D_\mu \phi^i D^\mu \phi^i. \quad (2.25)$$

Note that in this case we use the definition of the covariant derivative of the form  $D_\mu \bullet = \partial_\mu \bullet + i [A_\mu, \bullet]$  as described in the previous section. Also, we want all those fields to (self-)interact with the coupling strength  $g_{\text{YM}}$ . This can be realized by adding interaction terms (additionally to the naturally included interaction terms) in the Yang-Mills theory of the form

$$\mathcal{L}_{\text{int}} = g_{\text{YM}} \sum_{a,b,i} C_i^{ab} \lambda_a [\phi^i, \lambda_b] + g_{\text{YM}} \sum_{a,b,i} \bar{C}_{iab} \bar{\lambda}^a [\phi^i, \bar{\lambda}^b] + \frac{g_{\text{YM}}^2}{2} \sum_{i,j} [\phi^i, \phi^j]^2 \quad (2.26)$$

to the Lagrangian. Here  $C_i^{ab}$  are the Clebsch-Gordan coefficients that couple the Weyl fermions to the real scalars. So finally we can put together all the terms and obtain the full Lagrangian for the supersymmetric  $\mathcal{N} = 4$  Super Yang-Mills theory in 3+1 dimensions

$$\begin{aligned} \mathcal{L}_{\text{SYM}}^{\mathcal{N}=4} = \text{Tr} \left( -\frac{1}{2g_{\text{YM}}^2} F_{\mu\nu} F^{\mu\nu} + \frac{\theta}{16\pi^2} {}^* F_{\mu\nu} F^{\mu\nu} - i \bar{\lambda}^a \bar{\sigma}^\mu D_\mu \lambda_a - \sum_i D_\mu \phi^i D^\mu \phi^i \right. \\ \left. + g_{\text{YM}} \sum_{a,b,i} C_i^{ab} \lambda_a [\phi^i, \lambda_b] + g_{\text{YM}} \sum_{a,b,i} \bar{C}_{iab} \bar{\lambda}^a [\phi^i, \bar{\lambda}^b] + \frac{g_{\text{YM}}^2}{2} \sum_{i,j} [\phi^i, \phi^j]^2 \right). \end{aligned} \quad (2.27)$$

The variable  $\theta$  can be set to zero since the terms proportional to it are only boundary terms. This Lagrangian (2.27) is invariant under the supersymmetry transformations given by

$$\begin{aligned}\delta_\epsilon \phi^i &= \epsilon_a^\alpha C^{iab} \lambda_{\alpha b} \\ \delta_\epsilon \lambda_{\beta b} &= F_{\mu\nu}^+ \epsilon_{\alpha b} (\sigma^{\mu\nu})^\alpha_\beta + [\phi^i, \phi^j] \epsilon_{\beta a} (C_{ij})^a_b \\ \delta_\epsilon \bar{\lambda}^b_{\dot{\beta}} &= C_i^{ab} \epsilon_a^\alpha \bar{\sigma}^\mu_{\alpha\dot{\beta}} D_\mu \phi^i \\ \delta_\epsilon A_\mu &= \epsilon_a^\alpha (\sigma_\mu)_\alpha^\beta \lambda_{\dot{\beta}}^a,\end{aligned}\tag{2.28}$$

with  $F_{\mu\nu}^+ = \frac{1}{2}(F_{\mu\nu} + {}^*F_{\mu\nu})$ . This theory is renormalizable since the coupling constant is dimensionless and it is conformally invariant which means that its beta function vanishes to all orders of perturbation theory. The conformal symmetry group is given by  $SO(4,2)$ .

## 2.5 *AdS/CFT* correspondence

In this section we will motivate the *AdS/CFT* correspondence proposed by Maldacena [12] based on [32] and [29]. In its strongest form the conjecture states that  $\mathcal{N} = 4$   $SU(N)$  Super Yang-Mills theory in 3+1 dimensions with coupling  $g_{\text{YM}}$  is dynamically equivalent to type IIB superstring theory in 9+1 dimensions on  $AdS_5 \times S^5$  with string length  $l_s = \sqrt{\alpha'}$ , coupling  $g_s$ , curvature radius  $L$  and  $N$  units of  $F_{(5)}$  flux on  $S^5$ . As we will see the parameters of the two theories are identified such that

$$\begin{aligned}g_{\text{YM}}^2 &= 4\pi g_s \\ g_{\text{YM}}^2 N &= L^4/\alpha'^2.\end{aligned}\tag{2.29}$$

This conjecture is a concrete realization of the holographic principle described in section 2.1, since the degrees of freedom of the 5-dimensional theory in *AdS* are mapped to a four dimensional conformal field theory (*CFT*) living on its conformal boundary. Before we can understand this duality in more detail we have to understand D-branes.

### D-branes

D-branes, or often called  $Dp$ -branes with  $p$  the number of spatial dimensions it extends to, are objects where open strings with certain boundary conditions can end. The D in D-brane stands for Dirichlet. The strings attached to a Dirichlet brane have to satisfy Dirichlet boundary conditions in a certain number of directions. In the other directions they have to satisfy Neumann boundary conditions. For example in 3+1 spacetime dimensions strings ending on a D2-brane at  $x^3 = 0$  (a plane) fulfill Neumann boundary conditions in the directions  $x^1$  and  $x^2$  as well as in the time direction  $x^0$  and Dirichlet boundary condition in the  $x^3$  direction. Intuitively this is clear because a plane at  $x^3 = 0$  fixes the  $x^3$  coordinate of a string ending on it. It is straightforward to generalize this concept to arbitrary numbers of spacetime dimensions and values of  $p$ .

In the next subsection the most important branes are D3-branes embedded in  $(9+1)$ -dimensional spacetime. Here the open strings are constrained by Neumann boundary conditions in  $x^0, x^1, x^2$  and  $x^3$ . In the other directions  $x^4, x^5, x^6, x^7, x^8$  and  $x^9$  they have to fulfill Dirichlet boundary condition.

### Low energy limit and $g_s N \ll 1$

We consider type IIB superstring theory in  $(9+1)$ -dimensions with  $N$  D3-branes and take the low energy limit as well as the limit of small coupling  $g_s N \ll 1$ . In this limit the theory is appropriately described by massless open strings ending on the D3-branes. According to their transformation properties under worldvolume rotations of the D3-branes, the bosonic massless open string excitations longitudinal to the D3-branes give rise to a gauge field  $A_\mu$  and the bosonic massless open string excitations transversal to the D3-branes are described by six real scalar fields  $\phi^i$ . The action for the open strings and the interaction part of the action can be derived from the Dirac-Born-Infeld action

$$\mathcal{S}_{\text{DBI}} = -\frac{1}{(2\pi)^3 \alpha'^2 g_s} \text{Tr} \int d^4 x e^{-\phi} \sqrt{-\det(\mathcal{P}[g] + 2\pi\alpha' F)} + \text{fermions}, \quad (2.30)$$

where  $\mathcal{P}[g]_{\mu\nu} = g_{\mu\nu} + (2\pi\alpha') (g_{i+3\nu} \partial_\mu \phi^i + g_{\mu j+3} \partial_\nu \phi^j) + (2\pi\alpha')^2 g_{i+3j+3} \partial_\mu \phi^i \partial_\nu \phi^j$  is the pull-back with the coordinate directions of the Dirichlet boundary condition  $x^{i+3} = 2\pi\alpha' \phi^i$ . Expanding this action and taking the limit  $\alpha' \rightarrow 0$  ( $l_s = 0$ ) gives exactly the action of the  $SU(N)$   $\mathcal{N} = 4$  Super Yang-Mills theory of equation (2.27) if we identify the two different coupling constants by

$$4\pi g_s = g_{\text{YM}}^2. \quad (2.31)$$

The interaction part of the action, which would also follow from the Dirac-Born-Infeld action (2.30) vanishes in this limit. This means that open and closed strings decouple. The closed strings in this limit would be effectively described by flat supergravity.

### Low energy limit and $g_s N \gg 1$

In this case the  $N$  D3-branes are massive charged objects sourcing the supergravity fields in which the closed strings propagate. Here the open string description is not feasible because  $g_s N$  is related with the loop corrections and one has to deal with the strongly coupled open strings. An ansatz for the solution of the equations of motion of supergravity that preserves the  $SO(3,1) \times SO(6)$  symmetry of  $\mathbb{R}^{9,1}$  is

$$\begin{aligned} ds^2 &= H(r)^{-1/2} \eta_{\mu\nu} dx^\mu dx^\nu + H(r)^{1/2} \delta_{ij} dx^i dx^j \\ C_{(4)} &= (1 - H(r)^{-1}) dx^0 \wedge dx^1 \wedge dx^2 \wedge dx^3 + \dots \\ F_{(5)} &= dC_{(4)}. \end{aligned} \quad (2.32)$$

Plugging this into the equations of motion of  $(9+1)$ -dimensional type IIB supergravity  $\square_g H(r) = 0$  yields the solution

$$H(r) = 1 + \left(\frac{L}{r}\right)^4. \quad (2.33)$$

The constant  $L$  has to be determined from string theory

$$N = \frac{1}{2\kappa_{10}^2} \int_{S^5} *F_{(5)} \Rightarrow L^4 = 4\pi g_s N \alpha'^2. \quad (2.34)$$

In the limit  $r \rightarrow \infty$  the resulting metric is just flat  $(9+1)$ -dimensional Minkowski spacetime. If we take the limit  $r \rightarrow 0$ , which is the limit of low energies, we obtain the metric

$$ds^2 = \frac{r^2}{L^2} \eta_{\mu\nu} dx^\mu dx^\nu + \frac{L^2}{r^2} \delta_{ij} dx^i dx^j, \quad (2.35)$$

which is simply  $AdS_5 \times S^5$  spacetime. As we saw at the end of section 2.2 under the transformation  $z = \frac{L^2}{r}$  it can be written as

$$ds^2 = \frac{L^2}{z^2} (\eta_{\mu\nu} dx^\mu dx^\nu + dz^2) + L^2 ds_{S^5}^2. \quad (2.36)$$

### Maldacena's conjecture

We now summarize the results of the previous two sections. Starting with  $N$  D3-branes we took two different low energy limits. In the limit of  $g_s N \ll 1$  we find that the open strings are the dominant ones and that this theory describes  $\mathcal{N} = 4$  Super Yang-Mills theory in 3 + 1 dimensions and type IIB supergravity on  $\mathbb{R}^{9,1}$ . Taking on the other hand the limit  $g_s N \gg 1$  we find that the closed strings are the dominant ones. As shown in the previous section this leads either to type IIB supergravity on flat space for  $r \rightarrow \infty$  or to type IIB supergravity on  $AdS_5 \times S^5$ .

The conjecture is now the following: In both limits type IIB supergravity on flat  $\mathbb{R}^{9,1}$  spacetime is present and also both limits should be equivalent descriptions of the same physics. Therefore the other two theories should be equivalent. This means that  $\mathcal{N} = 4$  Super Yang-Mills theory in 3 + 1 dimension is equivalent to type IIB supergravity on  $AdS_5 \times S^5$ . If we further relax the condition of low energies we find the even stronger statement that  $\mathcal{N} = 4$  Super Yang-Mills theory in 3 + 1 dimension is equivalent to type IIB string theory on  $AdS_5 \times S^5$ . A sketch of the correspondence is shown in figure 2.2. A

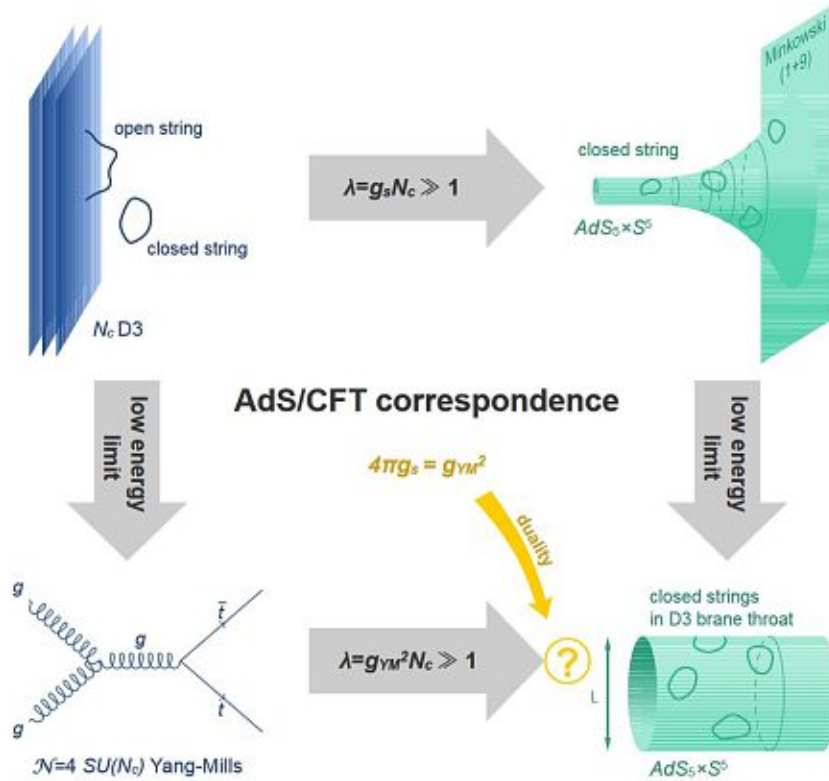


Figure 2.2: Sketch of the AdS/CFT correspondence [32].

hint that this conjecture is correct comes also from the symmetries of the two theories. The symmetry group of the  $\mathcal{N} = 4$  super Yang-Mills theory is  $PSU(2, 2|4)$ . The isometry group of  $AdS_5$  is  $SO(4, 2)$ , this follows from the embedding of  $AdS_d$  in  $\mathbb{R}^{d-1, 2}$  as discussed in section 2.2. The isometry group of  $S^5$  are the rotations in 6-dimensional Euclidean space also known as  $SO(6)$ . The symmetry groups of the spacetime coincide with the bosonic parts of the symmetry group  $PSU(2, 2|4)$ , which are  $SU(2, 2) \sim SO(4, 2)$  and  $SU(4) \sim SO(6)$ . Further string theory in  $AdS_5 \times S^5$  preserves the  $PSU(2, 2|4)$  symmetry and therefore the symmetries of the two theories are identical.

### Correlation functions

Having established the duality between two theories the question raises whether we can use it practically. As one might guess, the answer to this question is yes. But it is not trivial to do so. The idea is the following: Since both theories are invariant under the same symmetries it should be possible to relate the operators of the *CFT* side with fields of the *AdS* side, such that they transform in the same representation of the symmetry group. This can be realized by a one-to-one map between composite operators, which are invariant under symmetry transformations (gauge invariant) and classical fields in type IIB supergravity. An example for such an operator  $\mathcal{O}_\Delta(x)$  with conformal scaling dimension  $\Delta$  would be any symmetrized trace over  $\Delta$  elementary scalar fields  $\phi^i$

$$\mathcal{O}_\Delta(x) = \text{Str}(\phi^{i_1}(x)\phi^{i_2}(x)\dots\phi^{i_\Delta}(x)). \quad (2.37)$$

The dual fields on the *AdS* side can be found by calculating and solving the linearised equations of motion of the supergravity. Here we will not do this in detail, we will just state the main ideas and results. First of all we can decompose every field  $\varphi$  in a part living on the  $S^5$  and an other one living in  $AdS_5$ , analogous to separating radial and angular coordinate depending parts in a theory in  $\mathbb{R}^3$ , namely by introducing spherical harmonics. As for  $S^2$ , one can introduce spherical harmonics on the  $S^5$ , which satisfy the differential equation

$$\square_{S^5} Y^I = -\frac{1}{L^2}l(l+4)Y^I. \quad (2.38)$$

Using this we can write

$$\varphi(x, z, \Omega_5) = \sum_{I=0}^{\infty} \varphi^I(x, z)Y^I(\Omega_5). \quad (2.39)$$

One can now derive the equations of motion of the supergravity for small fluctuations of the metric and  $F_{(5)}$ , then expand them in the same manner as in equation (2.39) and further simplify the equation by defining fields  $s^I(z, x)$  as below. It turns out that these fields have to satisfy the equations of motion

$$\square_{AdS_5} s^I(z, x) = \frac{1}{L^2}l(l-4)s^I(z, x). \quad (2.40)$$

The idea is now that we can identify the field  $s^I(z, x)$  on the gravity side with the operators  $\mathcal{O}_\Delta(x)$  on the field theory side by setting  $l = \Delta$ . Similarly one can find the gravity dual of the stress energy tensor  $h_{\mu\nu} \leftrightarrow T_{\mu\nu}$  and, most importantly for this thesis, the four current  $A_\mu \leftrightarrow J_\mu$ . Using equation (2.40) we can also define the five-dimensional mass, since this is just a Klein-Gordon equation in five-dimensional *AdS* spacetime. For the simple case of scalar fields in equation (2.40) we find  $m^2L^2 = \Delta(\Delta - 4)$ . This means that the mass of

the gravity field is related to the dimension of the dual operator. In the general case of  $AdS_{d+1}$  the analog of equation (2.40) is

$$\square_{AdS_{d+1}} \phi = \frac{1}{L^2} \Delta(\Delta - d)\phi \implies m^2 L^2 = \Delta(\Delta - d). \quad (2.41)$$

Additionally for  $p$ -form fields (e.g. for vector mesons  $p = 1$ ) one can show that the five-dimensional mass is given by

$$m^2 L^2 = (\Delta - p)(\Delta + p - d). \quad (2.42)$$

The last thing left to do is to calculate the field theory correlation functions using the dual gravity theory. Exactly this possibility, to determine the correlation functions of the strongly coupled gauge theory by doing calculation within the weakly coupled dual theory, is what makes the *AdS/CFT* correspondence such a useful and interesting conjecture. As mentioned the field theory is defined on the boundary of the *AdS* space. Thus we have to expand a field  $\phi(z, x)$  (here without an index to distinguish it from the field theory operator) of the gravity side at the boundary  $z \rightarrow 0$

$$\phi(z, x)|_{z \rightarrow 0} \sim \phi_{(0)} z^{d-\Delta} + \langle \mathcal{O}_\Delta \rangle z^\Delta + \dots \quad (2.43)$$

Here  $\phi_{(0)}$  is the source of the operator  $\mathcal{O}_\Delta$  and  $\langle \mathcal{O}_\Delta \rangle$  its vacuum expectation value. As usually in QFT we can add the source terms to the action and calculate the partition function

$$\begin{aligned} \mathcal{S}' &= \mathcal{S} - \int d^d x \phi_{(0)}(x) \mathcal{O}_\Delta(x) \\ Z[\phi_{(0)}] &= e^{-W[\phi_{(0)}]} = \left\langle \exp \left( \int d^d x \phi_{(0)}(x) \mathcal{O}_\Delta(x) \right) \right\rangle_{\text{CFT}}. \end{aligned} \quad (2.44)$$

So the AdS/CFT correspondence stated in one single equation is

$$\boxed{W[\phi_{(0)}] = \mathcal{S}_{\text{sugra}}[\phi] \Big|_{\lim_{z \rightarrow 0} (\phi(z, x) z^{\Delta-d}) = \phi_{(0)}(x)}} \quad (2.45)$$

The correlation functions can be calculated as in QFT by calculating the variation of  $W[\phi_{(0)}]$  with respect to the sources. For an arbitrary number of sources  $\phi_{(0)}^i$  this means that the correlation function is given by

$$\langle \mathcal{O}_1(x_1) \mathcal{O}_2(x_2) \dots \mathcal{O}_n(x_n) \rangle_{\text{CFT}} = - \frac{\delta^n W}{\delta \phi_{(0)}^1(x_1) \delta \phi_{(0)}^2(x_2) \dots \delta \phi_{(0)}^n(x_n)} \Big|_{\phi_{(0)}^i=0}. \quad (2.46)$$

This conjecture will be generalized in the next section such that we can also apply it to QCD. However, the method for calculating the correlation function will stay the same. First we have to take the action of the dual gravity theory and derive the relevant equations of motion. The solution of this equation with appropriate boundary conditions at  $z \rightarrow 0$  can be plugged back into the action. Then we calculate the variation of the action in order to obtain the desired correlation function. In chapter 4 we will see how this works for concrete theories, where the dual gauge theory will be QCD rather than a *CFT*.



## 2.6 From *AdS/CFT* to *AdS/QCD*

The things discussed so far are all based on a conformal supersymmetric field theory. Our goal is however to apply the gauge/gravity duality to QCD, which is by no means conformal or supersymmetric. Nevertheless we can use the same formalism developed above and extend it to QCD. We "just" have to find a weakly coupled theory that is dual to QCD, or at least reproduces some of its most important features. One conjectures then that a theory I (in our case QCD) describes the same physical system as theory II. As in the case of the *AdS/CFT* correspondence we call such a relation a duality between two theories, see figure 2.3. Usually one of the two theories is strongly coupled and the other one weakly. In our case QCD is of course strongly coupled and its dual theory is supposed to be weakly coupled. The construction of such a theory is however by far not obvious and no

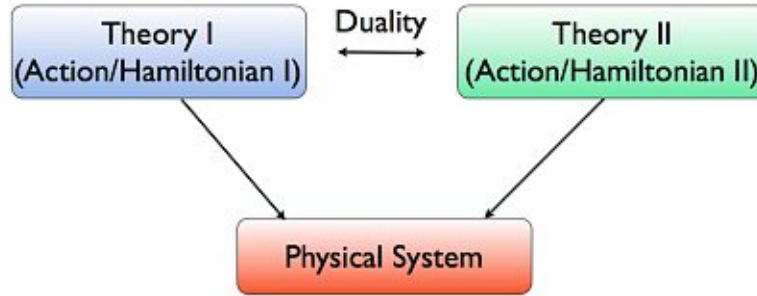


Figure 2.3: Two physical theories describing the same physical system are related by a duality [33].

theory that is exactly dual to QCD has been found yet. Nevertheless many theories which reproduce certain features have been proposed. The first attempts in this direction were made in [13] and [14]. Today there is a variety of different models, which are proposed to be dual to QCD in certain energy regimes, mainly low energy, and exhibit certain features in the same way as QCD does. For example, one such feature is chiral symmetry breaking.

It is straightforward to generalize our main formulas (2.44) and (2.45) for the evaluation of the correlation function in the *AdS/CFT* correspondence to *AdS/QCD* models. The partition function of QCD for a general source field  $\phi(z, x)$  of an operator  $\mathcal{O}_\Delta$  with scaling dimension  $\Delta$

$$Z[\phi_{(0)}] = e^{-W[\phi_{(0)}]} = \left\langle \exp \left( \int d^d x \phi_{(0)}(x) \mathcal{O}_\Delta(x) \right) \right\rangle_{\text{QCD}} \quad (2.47)$$

is identified with the exponential of the action of a dual weakly coupled 5-dimensional theory, such that

$$Z[\phi_{(0)}] = \left\langle \exp \left( \int d^d x \mathcal{O} \phi_{(0)} \right) \right\rangle_{\text{QCD}} = e^{-\mathcal{S}_{\text{dual}} \Big|_{\lim_{z \rightarrow 0} (\phi(z, x) z^{\Delta-d}) = \phi_{(0)}(x)}} \quad (2.48)$$

For the generating functional this means analogous to (2.45) that

$$\boxed{W[\phi_{(0)}] = \mathcal{S}_{\text{dual}}[\phi] \Big|_{\lim_{z \rightarrow 0} (\phi(z, x) z^{\Delta-d}) = \phi_{(0)}(x)}} \quad (2.49)$$

The  $n$ -point correlation functions are evaluated by calculating the  $n^{\text{th}}$  variation of both sides of equation (2.48) with respect to the source of the operator. Of particular interest

in this thesis is of course the two-point correlation function of the vector current  $J_V^{a\mu}(x)$

$$i \int d^4x e^{iqx} \langle 0 | T J_V^{a\mu}(x) J_V^{b\nu}(0) | 0 \rangle = \delta^{ab} (q^2 \eta^{\mu\nu} - q^\mu q^\nu) \Pi_V(-q^2). \quad (2.50)$$

This expression defines the hadronic vacuum polarization. It is calculated by taking the second derivative of the dual action  $S_{\text{dual}}[V_\mu]$  with respect to the source field  $V_\mu^a$  under certain conditions for the fields at the boundary of the  $AdS$  space

$$\frac{\delta^2 S_{\text{dual}}[V_\mu]}{\delta V_\mu^a(-q) \delta V_\nu^b(q)} = i \int d^4x e^{iqx} \langle 0 | T J_V^{a\mu}(x) J_V^{b\nu}(0) | 0 \rangle. \quad (2.51)$$

In practice the variation of the on shell action is calculated (this means under the assumption that the equations of motion are fulfilled). The generalization to the  $n$ -point correlation functions is straightforward. An important feature of the two-point function, which we will use a lot, is that we just need to calculate the linearized equations of motion (and therefore only take into account terms in the action which are quadratic in the fields). For all models we will discuss the procedure of calculating the hadronic vacuum polarization is in principle the same. We start by deriving the linearized equations of motion. Then we solve them either analytically or numerically. The solution is then plugged back into the dual action. After that we calculate the second variation of the action with respect to the field dual to the vector current. This gives us our final result for the vacuum polarization, which we will then further use to calculate the leading order HVP contributions to the anomalous magnetic moment of the muon  $a_\mu^{\text{HVP,LO}}$ .

As mentioned in section 1.2 there are roughly speaking two different types of models. The so called top-down models which are directly derived from string theory. The goal of such a theory would be to find the dual theory of QCD directly from string theory that reproduced the IR behavior of QCD at large- $N$  [15]. One example for such a model is the Sakai-Sugimoto model [16, 17]. As mentioned no theory that is exactly dual to QCD has been found yet. The other type of models are the bottom-up models. These models are most of the time only loosely based on string theory, only the main ideas are taken from it. Usually one constructs a five-dimensional action with the same symmetries as QCD and fixes various constants of the action by comparing results of the holographic model with gauge theory results. Examples for such models are the HW and SW model discussed in section 4.1 and 4.2. In both cases observable quantities are determined by calculating the correlation functions as described above. One key reason why it is interesting to study such models is that the low energy regime of QCD is not accessible by perturbation theory. So all our standard analytical techniques fail there. Finding a model which is exactly dual to QCD at all energy regimes would be equivalent to completely solving QCD. So far such a model is not within our reach.

## Chapter 3

# The anomalous magnetic moment of the muon

### 3.1 Current status of $a_\mu$

The anomalous magnetic moment for a general lepton is defined as  $a_l := \frac{1}{2}(g_l - 2)$ , with  $g_l$  being the gyromagnetic ratio of the lepton indicated by the index  $l$ . In this section we give a brief overview of the current theoretical and experimental values of  $a_\mu = \frac{1}{2}(g_\mu - 2)$  with a focus on the leading order HVP contribution. If not stated differently, all values are taken from the latest review of the status of the Standard Model calculation of the anomalous magnetic moment of the muon [25].

The best experimental result for  $a_\mu$  so far were achieved at the Brookhaven National Laboratory (BNL) at the beginning of this century providing the value

$$a_\mu^{\text{exp}} = 116592089(63) \times 10^{-11} \quad (3.1)$$

for the anomalous magnetic moment of the muon [34]. Currently there is an experiment running at Fermilab that aims to provide experimental data even more precise than that of the BNL experiment. The results of the experiment are expected to be released in the near future, but so far (3.1) is the best experimental value we have. An experiment with a different design than the ones at BNL and Fermilab, the J-PARC experiment, is under construction and aims to surpass everything previous in precision.

On the theoretical side the Standard Model predicts the value

$$\begin{aligned}
 a_\mu^{\text{SM}} &= a_\mu^{\text{QED}} + a_\mu^{\text{EW}} + a_\mu^{\text{HVP,LO}} + a_\mu^{\text{HVP,NLO}} + a_\mu^{\text{HVP,NNLO}} + a_\mu^{\text{HLbL}} + a_\mu^{\text{HLbL,NLO}} \\
 &= 116591810(43) \times 10^{-11},
 \end{aligned} \quad (3.2)$$

where all different contributions are listed in the first line of (3.2). Besides the QED terms there are also contributions from the electroweak interaction (EW) and the two types of hadronic contributions, the HVP and the light-by-light (LbL) terms. We will only discuss  $a_\mu^{\text{HVP,LO}}$  in this thesis. The difference between experimental and theoretical result is given by

$$\Delta a_\mu := a_\mu^{\text{exp}} - a_\mu^{\text{SM}} = 279(76) \times 10^{-11}, \quad (3.3)$$

corresponding to a  $3.7\sigma$  discrepancy.

As mentioned, in this thesis we are interested in the leading order HVP contributions to the anomalous magnetic moment of the muon  $a_\mu^{\text{HVP,LO}}$ . There are currently two more or less established ways of calculating this value. The first one is data-driven and uses experimental cross section data and dispersion relations to evaluate the leading order HVP contributions. The currently established value using this method is

$$a_\mu^{\text{HVP,LO}} = 693.1(4.0) \times 10^{-10}. \quad (3.4)$$

The second method is to use lattice QCD (LQCD) results. With LQCD one has the possibility of an ab initio determination of the HVP. However the uncertainty is quite high compared to the dispersive cross section data method. The LQCD calculations yield the value

$$a_\mu^{\text{HVP,LO}} = 711.6(18.4) \times 10^{-10}. \quad (3.5)$$

These are the values we have to compare to our results from holographic QCD calculations. Nevertheless we expect our values for  $a_\mu^{\text{HVP,LO}}$  to be lower than (3.4) and (3.5) as discussed in chapter 5. There we also give a complete discussion of the results obtained in this thesis and compare them to other data. Additionally the values for the dispersive approach structured by each contributing decay channel as well as the lattice data structured by the value of  $N_f$  can be found there.

### 3.2 Calculation of leading order HVP contribution to $a_\mu$

The aim of this section is to derive a formula for the calculation of the of the leading order (LO) HVP contributions to the anomalous magnetic moment of the muon  $a_\mu = \frac{1}{2}(g_\mu - 2)$ , where we just need the function  $\Pi_V(-q^2)$  for the vacuum polarization as an input plus some additional constants such as the muon mass. We are not going to give a full derivation with all details, since this would be a few pages of explicit calculations which are not really the main topic of this thesis. Instead we are just giving the main ideas of the derivation, such that one can use this section as a kind of manual for doing all the calculations explicitly.

The value for  $a_\mu$  is "hidden" inside the one-particle-irreducible (1PI) dressed vertex function with two external muon propagators and one photon propagator. We are of course

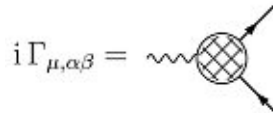


Figure 3.1: Pictorial representation of the dressed vertex function [24].

interested in the leading order HVP diagram of this vertex given in figure 3.2. Once we can write down the vertex function for the Feynman diagram in figure 3.2 it is straightforward to calculate  $a_\mu$  via projection techniques. However, writing down this vertex function (explicitly) is not so easy since the hadronic "blob" of the diagram includes QCD interactions and is therefore not accessible by perturbation theory. This is the reason why we

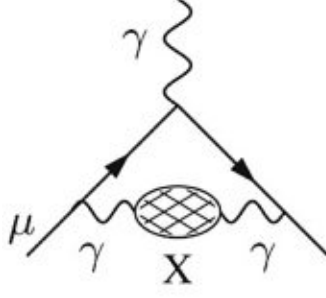


Figure 3.2: Leading order vertex diagram for the HVP [24].

use holographic QCD in order to describe the vertex. If we take the photon self energy function  $\Pi'_\gamma(k^2)$  as a known function (we can do so because this is exactly the two-point correlation function times a constant, which we are calculating using hQCD models), we can write down the vertex function by just using our basic QED knowledge. Expanding the full photon propagator in leading order gives

$$iD_{\gamma}^{\mu\nu'}(k^2) = \frac{-ig^{\mu\nu}}{k^2(1 + \Pi'_\gamma(k^2))} = \frac{-ig^{\mu\nu}}{k^2}(1 - \Pi'_\gamma(k^2) + \dots). \quad (3.6)$$

Clearly we are interested in the Feynman diagram where the photon propagator is denoted by  $ig^{\mu\nu}\Pi'_{\gamma\text{ren}}(k^2)/k^2$ . Here the renormalized self-energy function with  $\Pi'_{\gamma\text{ren}}(0) = 0$  is used. So we end up with the vertex corresponding to figure 3.2 given by

$$\Pi^\mu = -i^5 e^2 \int \frac{d^4k}{(2\pi)^4} \frac{\Pi'_{\gamma\text{ren}}(k^2)}{k^2} \frac{\gamma^\rho (\not{p}_2 - \not{k} + m) \gamma^\mu (\not{p}_1 - \not{k} + m) \gamma_\rho}{((p_2 - k)^2 - m^2)((p_1 - k)^2 - m^2)}. \quad (3.7)$$

Here  $p_1$  and  $p_2$  are the momenta of the two external fermions,  $k$  is the loop momentum. Note that compared to the previous definition of the vertex we now have  $\Pi^\mu = e\Gamma^\mu$ . It is well known, see e.g. [35], that given the vertex  $\Pi^\mu$ , one can project out  $a_\mu$  by using

$$a_\mu = -\lim_{q^2 \rightarrow 0} \text{Tr} \{ (\not{p}_1 + m) \Lambda_2^\mu (\not{p}_2 + m) \Pi_\mu \}, \quad (3.8)$$

where  $q = p_2 - p_1$  and  $(\not{p}_1 + m) \Lambda_2^\mu (\not{p}_2 + m)$  is the projection operator corresponding to the magnetic form factor. Explicitly performing this calculation using the vertex given in equation (3.7) one obtains

$$a_\mu^{\text{HVP,LO}} = -ie^2 \int \frac{d^4k}{(2\pi)^4} \frac{\Pi'_{\gamma\text{ren}}(k^2)}{k^2} \frac{[-4(pk) - \frac{4}{3}k^2 + \frac{16}{3m^2}(pk)^2]}{((p-k)^2 - m^2)^2}. \quad (3.9)$$

Now we can make a Wick rotation to Euclidean momentum space by substituting

$$\begin{aligned} k^0 &\rightarrow iK^4, & k^\mu k_\mu &\rightarrow -K^2 \\ \int d^4k \dots &\rightarrow i \int d^4K \dots \end{aligned} \quad (3.10)$$

After integrating out the angular part of the resulting integral we find

$$a_\mu^{\text{HVP,LO}} = \frac{\alpha}{\pi} \int_0^\infty dK^2 \underbrace{\Pi'_{\gamma\text{ren}}(K^2) \frac{m^2 K^2 Z^3 (1 - K^2 Z)}{1 + m^2 K^2 Z^2}}_{=: f(K^2)}, \quad Z = -\frac{K^2 - \sqrt{K^4 + 4m^2 K^2}}{2m^2 K^2}, \quad (3.11)$$

with the muon mass  $m = m_\mu$ . Now we have to use some QED/QCD arguments to manipulate this formula even further. We know that the electromagnetic current of the quarks is given by

$$J_{\text{em}}^\mu = \sum_f \bar{q}_f \gamma^\mu Q_{\text{em}} q_f, \quad (3.12)$$

where  $f$  represents the different flavors of the quarks. The charge matrix  $Q_{\text{em}}$  for two and three flavours are given by

$$Q_{\text{em}}^{N_f=2} = \frac{1}{3} \begin{pmatrix} 2 & 0 \\ 0 & -1 \end{pmatrix}, \quad Q_{\text{em}}^{N_f=3} = \frac{1}{3} \begin{pmatrix} 2 & 0 & 0 \\ 0 & -1 & 0 \\ 0 & 0 & -1 \end{pmatrix}. \quad (3.13)$$

We can write them in terms of the generators of  $SU(N_f)$  as

$$Q_{\text{em}}^{N_f=2} = \frac{1}{3} T_0 + T_3, \quad Q_{\text{em}}^{N_f=3} = T_3 + \frac{1}{\sqrt{3}} T_8. \quad (3.14)$$

In this fashion we can also decompose the electromagnetic current

$$J_{\text{em}}^{\mu N_f=2} = \frac{1}{3} J_V^{0\mu} + J_V^{3\mu}, \quad J_{\text{em}}^{\mu N_f=3} = J_V^{3\mu} + \frac{1}{\sqrt{3}} J_V^{8\mu}, \quad (3.15)$$

where the  $J_V^{a\mu}$ 's depend on the corresponding  $T^a$ 's. The hadronic electromagnetic current correlator is defined in the same way as the usual correlator by

$$ie^2 \int d^4x e^{iqx} \langle 0 | T J_{\text{em}}^\mu(x) J_{\text{em}}^\nu(0) | 0 \rangle = (q^2 \eta^{\mu\nu} - q^\mu q^\nu) \Pi_{\text{em}}^{\text{had}}(-q^2). \quad (3.16)$$

However, the vector current correlator we can calculate in hQCD,

$$i \int d^4x e^{iqx} \langle 0 | T J_V^{a\mu}(x) J_V^{b\nu}(0) | 0 \rangle = \delta^{ab} (q^2 \eta^{\mu\nu} - q^\mu q^\nu) \Pi_V(-q^2), \quad (3.17)$$

is not equal to the electromagnetic current correlator in the first place. It rather gives us exactly the current correlators we need to calculate  $\Pi_{\text{em}}^{\text{had}}(-q^2)$ , such as  $\langle J_V^{3\mu} J_V^{3\nu} \rangle$  for example. Working this out we find the following relations

$$\Pi_{\text{em}}^{N_f=2}(-q^2) = \frac{10}{9} e^2 \Pi_V(-q^2), \quad \Pi_{\text{em}}^{N_f=3}(-q^2) = \frac{4}{3} e^2 \Pi_V(-q^2). \quad (3.18)$$

This is equivalent to

$$\Pi_{\text{em}}^{\text{had}}(-q^2) = 2e^2 \text{Tr} Q_{\text{em}}^2 \Pi_V(-q^2). \quad (3.19)$$

We do not need to consider a higher number of flavours, because we are interested in observables in the low energy regime. All other quarks beside up, down and strange are too heavy to play a significant role in these processes. Sometimes it is not even possible to include the strange quark because its mass differs by more than one order of magnitude from the mass of the lighter two quarks. Despite this fact we can still use the  $N_f = 3$  result as an upper bound for a "real  $N_f = 3$ " holographic theory, as we will see in the case of the model of Kiritsis [20, 21, 22] in section 4.6. The reason why this gives an upper bound is that increasing the quark mass reduces its contribution, but SU(3) flavor symmetry ignores the fact that the strange quark is relatively heavy.

Now we are ready to substitute for  $\Pi'_{\gamma_{\text{ren}}}(K^2)$  in equation (3.11). With the definition  $\hat{\Pi}(K^2) := 4\pi^2 [\Pi_V(K^2) - \Pi_V(0)]$  we finally obtain

$$a_{\mu}^{\text{HVP,LO}} = \left(\frac{\alpha}{\pi}\right)^2 \int_0^{\infty} dK^2 f(K^2) \hat{\Pi}(K^2). \quad (3.20)$$

To emphasize the main statement of this section once more: If we can calculate  $\Pi_V(-q^2)$  in any theory or model, e.g. lattice QCD or in our case holographic QCD, we just have to plug it into the formula (3.20) and evaluate the integral to obtain the value of the leading order HVP contributions to the anomalous magnetic moment of the muon.

As we shall see in the next section, in holographic QCD we are essentially describing the hadronic blob of figure 3.2 as an exchange of neutral vector mesons. Pictorially this is illustrated in figure 3.3. In the large- $N$  limit of hQCD the leading order term is supposed to be this vector meson exchange. Therefore the dominant contributions to  $\Pi_V(-q^2)$  and further  $a_{\mu}^{\text{HVP,LO}}$  are from the vector mesons. The masses as well as the decay constants of these vector mesons can be explicitly calculated in the holographic QCD model. As we will discuss in chapter 5, considering only the first term in the large- $N$  expansion can lead to a significant error in the end.

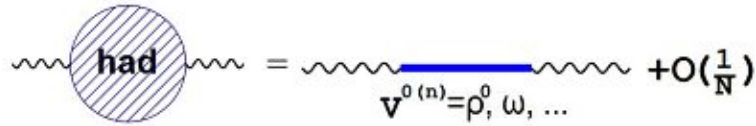


Figure 3.3: The hadronic blob as an exchange of a neutral vector meson [36].





## Chapter 4

# Holographic QCD models and their HVP

This chapter is the core of this thesis. Here we study the different holographic QCD models and calculate their associated hadronic vacuum polarization. For the first few models we will go into more detail for each of the steps to make things clearer. In the models after them the calculations are very similar and so we will not show all the steps explicitly but rather refer to the previous sections.

### 4.1 Hard-Wall Model (HW)

The hard-wall model [18] or short HW model is the simplest model discussed in this thesis. Based on this model the HVP was already calculated in [36] and applied to the problem of the anomalous magnetic moment of the muon. It is an example for a bottom-up model, since it is not constructed directly by deforming the super Yang-Mills theory, but rather a model constructed by hand such that the field content of the 5-dimensional theory reproduces holographically the dynamics of chiral symmetry breaking in QCD. The 5-dimensional action of the model is given by

$$S = \int d^5x \sqrt{g} \text{Tr} \left\{ |DX|^2 + 3|X|^2 - \frac{1}{4g_5^2} (F_L^2 + F_R^2) \right\}. \quad (4.1)$$

Here we made the following definitions for the fields, field strength tensor and covariant derivative

$$\begin{aligned} A_{L,R} &= A_{L,R}^a T^a \\ F_{MN} &= \partial_M A_N - \partial_N A_M - i[A_M, A_N] \\ D_M X &= \partial_M X - iA_{LM} X + iX A_{RM}. \end{aligned} \quad (4.2)$$

The indices  $M$  and  $N$  refer here to the 5-dimensional quantities. For the 4-dimensional part of them we will use Greek indices. The matrices  $T^a$ , with  $\text{Tr}[T^a T^b] = \frac{1}{2} \delta^{ab}$ , are the generators of the underlying symmetry group  $SU(N_f)$ , furthermore using the mostly minus convention the 5-dimensional metric is given by

$$ds^2 = \frac{1}{z^2} (-dz^2 + dx^\mu dx_\mu), \quad 0 < z \leq z_m. \quad (4.3)$$

Here we have set the  $AdS$  radius  $L$  to unity. Since the  $z$ -coordinate is bounded from above by a "hard boundary" at  $z = z_m$ , the model is called the hard-wall model. The introduction

of this boundary at  $z = z_m$  breaks the conformal symmetry. As mentioned above there is also a so called soft-wall model, where  $0 < z < \infty$ . In this case however one introduces a dilaton background in the action to break conformal symmetry. The fields  $A_{L\mu}$  and  $A_{R\mu}$  are referred to as left and right handed chiral gauge fields. Later it will be useful to use them in order to define the vector gauge field  $V_\mu$  and the axial vector gauge field  $A_\mu$  by

$$V = \frac{1}{2} (A_L + A_R), \quad A = \frac{1}{2} (A_L - A_R). \quad (4.4)$$

The field content of the 5-dimensional theory and their 4-dimensional dual quantities as well as the 5-dimensional mass  $m_5 = (\Delta - p)(\Delta + p - 4)$  for each operator pair are given in table 4.1. In the same way as described in equation (2.45) in section 2.5, we will relate

4D : $\mathcal{O}(x)$	5D : $\phi(x, z)$	$p$	$\Delta$	$m_5^2$
$\bar{q}_L \gamma^\mu T^a q_L$	$A_{L\mu}^a$	1	3	0
$\bar{q}_R \gamma^\mu T^a q_R$	$A_{R\mu}^a$	1	3	0
$\bar{q}_R^\alpha q_L^\beta$	$(2/z) X^{\alpha\beta}$	0	3	-3

Table 4.1: Field content of the hard-wall model [18].

the generating functional of the 4-dimensional theory (which is supposed to describe QCD)  $W_{4D}[\phi_0(x)]$  and the effective action of the 5-dimensional theory  $S_{5D, \text{eff}}[\phi(x, \epsilon)]$  evaluated under certain conditions at the boundary  $z = \epsilon$  with  $\epsilon \rightarrow 0$

$$W_{4D}[\phi_0(x)] = S_{5D, \text{eff}}[\phi(x, \epsilon)] \quad \text{at} \quad \phi(x, \epsilon) = \phi_0(x). \quad (4.5)$$

We now want to calculate the vacuum polarization function. In order to do so we first have to solve the equations of motion of the dual theory. Since we are interested in the correlation function of the vector currents  $\langle J_\mu^a(x) J_\nu^b(0) \rangle$ , we have to solve the equations of motion of the vector gauge potential  $V_\mu$  defined above. Using the gauge  $V_z = 0$  and  $\partial_\mu V^\mu = 0$  we find them to be given by

$$\partial_z \left( \frac{1}{z} \partial_z V_\mu^a(q, z) \right) + \frac{q^2}{z} V_\mu^a(q, z) = 0. \quad (4.6)$$

Here we already Fourier transformed with respect to the first four spacetime coordinates. Evaluating the relevant part of the action on shell (this means that the equations of motion are satisfied) gives the boundary term

$$S = - \frac{1}{2g_5^2} \int d^4x \left( \frac{1}{z} V_\mu^a \partial_z V^{\mu a} \right) \Big|_{z=\epsilon}. \quad (4.7)$$

An explicit derivation of this term is given in equation (4.43) and (4.44) for the case of the soft-wall model. To adapt the calculation for the case of the hard-wall model one just has to set  $\phi(z) = 0$ , such that  $e^{-\phi(z)} = 1$ .  $V_\mu$  can be decomposed as

$$V^\mu(q, z) = V(q, z) V_0^\mu(q), \quad (4.8)$$

where  $V_0^{\mu a}(q)$  is the Fourier transform of the source of the vector current  $J_\mu^a = \bar{q} \gamma_\mu t^a q$  we are interested in. From equation (2.46) we know that in order to obtain a  $n$ -point correlation function on the field theory side we have to calculate the  $n^{\text{th}}$  variation of the

5-dimensional action. Doing so we can calculate the two-point correlation function of the vector current

$$i \int dx e^{iqx} \langle J_\mu^a(x) J_\nu^b(0) \rangle = \delta^{ab} (q_\mu q_\nu - q^2 \eta_{\mu\nu}) \Pi_V(-q^2) \quad (4.9)$$

by calculating the second variation of (4.7) with respect to  $V_0^\mu$ . We find that

$$\Pi_V(-q^2) = - \frac{1}{g_5^2 q^2} \frac{\partial_z V(q, z)}{z} \Big|_{z=\epsilon}. \quad (4.10)$$

Luckily the equations of motion can be solved analytically. Using the boundary conditions  $V(q, \epsilon) = 1$  and  $\partial_z V(q, z)|_{z=z_m} = 0$  yields

$$V(q, z) = \frac{z J_1(qz) Y_0(qz_m) - z Y_1(qz) J_0(qz_m)}{\epsilon J_1(q\epsilon) Y_0(qz_m) - \epsilon Y_1(q\epsilon) J_0(qz_m)} \Big|_{\epsilon \rightarrow 0}. \quad (4.11)$$

Taking explicitly the limit  $\epsilon \rightarrow 0$  gives

$$V(q, z) = \frac{1}{2} \pi q z \left( \frac{J_1(qz) Y_0(qz_m)}{J_0(qz_m)} - Y_1(qz) \right). \quad (4.12)$$

Plugging this result into equation (4.10) yields

$$\Pi_V(-q^2) = - \frac{1}{g_5^2} \frac{1}{q\epsilon} \frac{J_0(qz_m) Y_0(q\epsilon) - Y_0(qz_m) J_0(q\epsilon)}{J_0(qz_m) Y_1(q\epsilon) - Y_0(qz_m) J_1(q\epsilon)}, \quad (4.13)$$

expanding this at  $\epsilon \rightarrow 0$  gives

$$\Pi_V(-q^2) = \frac{1}{g_5^2} \left[ - \frac{\pi Y_0(qz_m)}{2 J_0(qz_m)} + \gamma - \log 2 + \log q\epsilon + \mathcal{O}(\epsilon^2) \right]. \quad (4.14)$$

There are two parameters in this model which have to be fitted, the coupling constant  $g_5$  and the parameter  $z_m$ . Fixing them is possible in many different way. Below we are going to discuss three different values, where one is coming from the HW1 model and the other two from two different fits in the HW2 model.

Before we tackle this problem we have to deal with another issue. The expression (4.14) obviously diverges like  $\log(\epsilon)$  for  $\epsilon \rightarrow 0$ . This means we have to somehow get rid of the  $\log(\epsilon)$  term in (4.14). This can be done by renormalizing  $\Pi_V(-q^2)$ , i.e. that we add a counter term  $S_c(\mu)$  to the action resulting in an additional term

$$\Pi_V^c(Q^2) = - \frac{1}{g_5^2} \log(\mu\epsilon), \quad (4.15)$$

which exactly cancels the divergent term in (4.14). How this works precisely is described in more detail for the case of the soft-wall model in section 4.2. The corresponding renormalized vacuum polarization is

$$\Pi_V^{\text{ren}}(-q^2) = \lim_{\epsilon \rightarrow 0} [\Pi_V(-q^2) + \Pi_V^c(-q^2)] = \frac{1}{g_5^2} \left[ - \frac{\pi Y_0(qz_m)}{2 J_0(qz_m)} + \gamma - \log 2 + \log \frac{q}{\mu} \right]. \quad (4.16)$$

For the calculation of  $a_\mu$  we have to subtract  $\Pi_V^{\text{ren}}(0)$  from this expression in order to plug it into the integral (3.20). We do this because the coupling constant  $\alpha$  is defined in the

low energy limit. This is equivalent to a minimal subtraction followed by the addition of a finite counterterm. Using the relations [37]

$$Y_0(z) = \frac{2}{\pi} \left[ \gamma + \log\left(\frac{1}{2}z\right) \right] J_0(z) - \frac{4}{\pi} \sum_{n=1}^{\infty} \frac{(-1)^n}{n} J_{2n}(z) \quad \text{and} \quad J_n(0) = 0 \quad \text{for } n > 0, \quad (4.17)$$

we find

$$\Pi_V^{\text{ren}}(0) = \frac{1}{g_5^2} \left[ -\log(z_m) + \log\left(\frac{1}{\mu}\right) \right], \quad (4.18)$$

and thus

$$\Pi_V^{\text{ren}}(-q^2) - \Pi_V^{\text{ren}}(0) = \frac{1}{g_5^2} \left[ -\frac{\pi}{2} \frac{Y_0(qz_m)}{J_0(qz_m)} + \gamma + \log\left(\frac{qz_m}{2}\right) \right]. \quad (4.19)$$

Next we discuss an alternative method to the one above. We can also derive an expression for the vacuum polarization by using Green's function for the differential equation (4.6). As shown in [38] the Green's function of the differential equation

$$\hat{L}G(q; z, z') = z\delta(z - z'), \quad \hat{L} = z\partial_z \left( \frac{1}{z}\partial_z \right) + q^2 \quad (4.20)$$

can be written as the spectral sum of the product of the eigenfunctions divided by their eigenvalues i.e.

$$G(q; z, z') = \sum_n \frac{\psi_{V_n}(z)\psi_{V_n}(z')}{q^2 - m_{V_n}^2 + i\varepsilon}. \quad (4.21)$$

The eigenfunctions  $\psi_{V_n}(z)$  of the differential equation (4.6) can be obtained by replacing  $V_\mu^a(q, z) \rightarrow \psi_{V_n}(z)$  and  $q^2 \rightarrow m_{V_n}^2$  under the boundary conditions  $\psi_{V_n}(\epsilon \rightarrow 0) = 0$  and  $\partial_z \psi_{V_n}(z_m) = 0$ . The eigenfunctions are normalized such that

$$\int_\epsilon^{z_m} \frac{dz}{z} (\psi_{V_n}(z))^2 = 1. \quad (4.22)$$

In the following we will drop the  $i\varepsilon$  prescription to simplify our notation. Explicitly the eigenfunctions are given by

$$\psi_{V_n}(z) = \frac{\sqrt{2}z J_1(zm_{V_n})}{z_m J_1(z_m m_{V_n})}. \quad (4.23)$$

For a plot of the normalized eigenfunctions  $\psi_{V_n}(z)$  see figure 4.1.

We now show that  $V(q, z') = \lim_{z \rightarrow \epsilon} (-(1/z)\partial_z G(q; z, z'))$  by using Green's second identity. In its general form it states

$$\int_U (\psi \nabla^2 \varphi - \varphi \nabla^2 \psi) dV = \oint_{\partial U} \left( \psi \frac{\partial \varphi}{\partial \mathbf{n}} - \varphi \frac{\partial \psi}{\partial \mathbf{n}} \right) dS, \quad (4.24)$$

with  $\varphi$  and  $\psi$  twice continuously differentiable in a region  $U$ . Here  $\nabla$  stands for a general differential operator. In our case  $U$  is the one-dimensional region  $z \in [0, z_m]$  and  $\nabla^2 = \hat{L}$ . The directional derivative is given as  $\frac{\partial}{\partial \mathbf{n}} = \frac{1}{z}\partial_z$ . Applying (4.24) to our problem, we identify  $\psi = V(q, z)$  and  $\varphi = G(q; z, z')$ , which gives

$$\begin{aligned} \int_0^{z_m} \frac{dz}{z} (V(q, z)\hat{L}G(q; z, z') - G(q; z, z')\hat{L}V(q, z)) &= \\ &= V(q, z) \frac{1}{z} \frac{\partial G(q; z, z')}{\partial z} - G(q; z, z') \frac{1}{z} \frac{\partial V(q, z)}{\partial z} \Bigg|_{z=\epsilon}^{z_m}. \end{aligned} \quad (4.25)$$

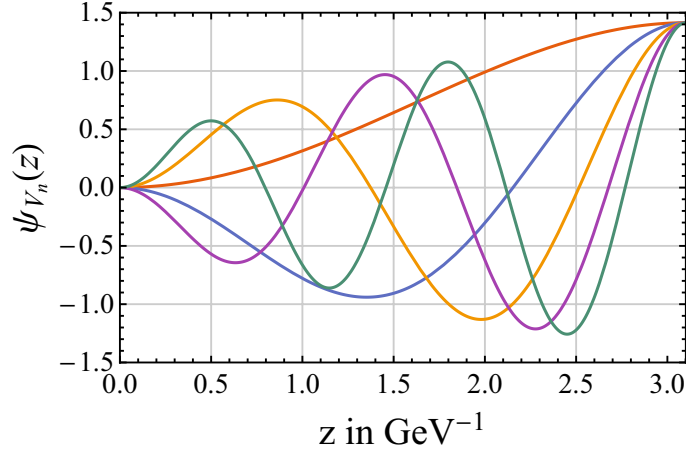


Figure 4.1: Plot of the first five eigenstates for the hard-wall model.

Using (4.20) as well as  $\hat{L}V(q, z) = 0$  and all the boundary conditions we imposed on  $\psi_{V_n}$  and  $V(q, z)$  we find

$$\int_0^{z_m} \frac{dz}{z} V(q, z) z \delta(z - z') = \lim_{z \rightarrow \epsilon} \left( V(q, z) \frac{1}{z} \frac{\partial G(q; z, z')}{\partial z} \right). \quad (4.26)$$

Carrying out the integral on the left-hand side we find the desired formula stated above

$$V(q, z') = \lim_{z \rightarrow \epsilon} \left( -(1/z) \partial_z G(q; z, z') \right). \quad (4.27)$$

Plugging this now into equation (4.10) yields the vacuum polarization

$$\Pi_V(-q^2) = \frac{1}{g_5^2} \sum_n \frac{[\psi'_{V_n}(\epsilon)/\epsilon]^2}{(q^2 - m_{V_n}^2 + i\epsilon) m_{V_n}^2}. \quad (4.28)$$

From this expression we can read off the decay constants  $F_{V_n}$  defined by  $\langle 0 | J_V^{\mu a}(0) | V_n^b \rangle = F_{V_n} \delta^{ab} \epsilon^\mu$  as

$$F_{V_n}^2 = \lim_{\epsilon \rightarrow 0} \frac{1}{g_5^2} [\psi'_{V_n}(\epsilon)/\epsilon]^2 = \frac{1}{g_5^2} [\psi''_{V_n}(0)]^2. \quad (4.29)$$

For the calculation of  $a_\mu$  we of course need  $\Pi_V^{\text{ren}}(-q^2) - \Pi_V^{\text{ren}}(0)$ . From (4.28) it is straightforward to see that

$$\Pi_V^{\text{ren}}(-q^2) - \Pi_V^{\text{ren}}(0) = \sum_{n=1}^m \frac{q^2 F_{V_n}^2}{(q^2 - m_{V_n}^2) m_{V_n}^4} + \mathcal{O}\left(\frac{q^2}{m_{V_m}^2}\right). \quad (4.30)$$

Here we also indicated the error if we truncate the sum at a certain value  $n = m$ . The equation (4.30) is equal to equation (4.19) in the case of  $m \rightarrow \infty$ . However usually it is simpler to use expression (4.30), since solving for eigenfunctions is simpler in problems not solvable analytically. Also, by solving for the eigenfunctions one obtains the mass spectrum "for free", which is also an advantage compared to searching for all poles of a non-analytical function.

For this simple model we can perform calculations analytically for both cases. Also more importantly, they both provide the same results. The calculated values for the masses of the vector mesons as well as the corresponding decay constants can be found in table 4.2. The results obtained by applying the HW model to the anomalous magnetic moment of the muon can be found in table 4.3.

#### 4.1.1 HW1 model

Now we are ready to fix the parameters. We can do this by switching to Euclidean momentum  $Q^2 = -q^2$  and expanding  $\Pi_V(Q^2)$  for large  $Q^2$ . The result can then be compared with the operator product expansion OPE of  $\Pi_V(Q^2)$ . The constant  $g_5$  is fitted such that the leading term of the OPE and the holographic result for  $\Pi_V(Q^2)$  have the same prefactor. At large  $Q^2$  the holographic result in leading order is given by

$$\Pi_V(Q^2) = \frac{1}{2g_5^2} \log Q^2, \quad (4.31)$$

which can be seen directly from equation (4.14). The OPE is given by [39, 40]

$$\Pi_V(Q^2) = \frac{N_c}{24\pi^2} \left(1 + \frac{\alpha_s}{\pi}\right) \log\left(\frac{Q^2}{\mu^2}\right) - \frac{\alpha_s}{24\pi} \frac{N_c}{3} \frac{\langle G^2 \rangle}{Q^4} + \frac{14N_c}{27} \frac{\pi\alpha_s \langle q\bar{q} \rangle^2}{Q^6}. \quad (4.32)$$

By comparing equation (4.32) and (4.31) we find

$$\frac{1}{g_5^2} = \frac{N_c}{12\pi^2}. \quad (4.33)$$

After Wick rotation (4.19) to Euclidean space this is exactly the expression we need in the integral (3.20). However there is still one parameter left to fix, namely the upper bound of the  $z$ -coordinate  $z_m$ . It is fixed such that the mass of the lightest eigenmode equals the mass of the first rho meson  $\rho(770)$ ,  $m_\rho = 775.5$  MeV. This can be done by analyzing the poles of  $\Pi_V^{\text{ren}}(-q^2)$ . It has poles exactly at  $q^2 = m_{V_n}^2$ , where  $m_{V_1} = m_\rho$  (the mass of the lightest rho meson). So we have to solve the equation  $J_0(qz_m) = 0$  for  $q$ . Doing so gives

$$z_m = 3.101 \text{ GeV}^{-1}. \quad (4.34)$$

The masses of the other meson states are also determined by the poles of  $\Pi_V^{\text{ren}}(-q^2)$ . As we will see later, this is of course consistent with the other method of calculating the vacuum polarization given below.

#### 4.1.2 HW2 model

The model discussed so far is usually referred to as HW1 model. However, there is also another HW model called HW2 (or Hirn-Sanz model) [41] with 2 different sets of parameters. The usual set is obtained by fitting the rho meson mass (HW2) and the other by fitting the UV asymptotic (UV-fit). For our application the only difference between the HW1 and HW2 model are the values of the parameters  $g_5$  and  $z_m$ . The fit for the "standard" hard-wall model - HW1 - is the one discussed above. We will not go into too much detail about how the fit in the HW2 works, but rather just state the main arguments. The HW2

model imposes different boundary conditions on the eigenfunctions for the axial vector sector than the HW1 model

$$\psi_n^A(0) = \psi_n^A(z_m) = 0. \quad (4.35)$$

This raises the need of either modifying  $g_5$  or  $z_m$ . The value of  $g_5$  is changed in the HW2 model, whereas in the HW2 (UV-fit) model the value for  $z_m$  is changed compared to the HW1 model. Summarizing the values of the parameters we have

$$\begin{aligned} \text{HW1} &: g_5 = 2\pi \quad z_m = 3.101 \text{ GeV}^{-1}, \\ \text{HW2} &: g_5 = 4.932 \quad z_m = 3.101 \text{ GeV}^{-1}, \\ \text{HW2 (UV-fit)} &: g_5 = 2\pi \quad z_m = 2.4359 \text{ GeV}^{-1}. \end{aligned} \quad (4.36)$$

The resulting numerical values are given in table 4.2 and 4.3.

	HW1		HW2		HW2 (UV-fit)	
n	$M_{V_n}$	$F_{V_n}^{1/2}$	$M_{V_n}$	$F_{V_n}^{1/2}$	$M_{V_n}$	$F_{V_n}^{1/2}$
1	775.5	329.3	775.5	371.7	987.2	419.2
2	1780	616.2	1780	695.5	2266	784.5
3	2791	863.8	2791	975.0	3553	1100
4	3802	1090	3802	1230	4841	1387
5	4815	1301	4815	1468	6130	1656
6	5827	1501	5827	1694	7419	1911
7	6840	1693	6840	1911	8708	2155
8	7853	1878	7853	2119	9997	2390

Table 4.2: Vector meson masses  $M_{V_n}$  and decay constants  $F_{V_n}^{1/2}$  in MeV.

	values for $a_\mu^{\text{HVP,LO}} (10^{-10})$	
	$N_f = 2$	$N_f = 3$
HW1	476.3	571.6
HW2	773.1	927.7
HW2 (UV-fit)	303.9	364.7

Table 4.3: Calculated values for  $a_\mu^{\text{HVP,LO}} [\times 10^{-10}]$  for different parameter fits of the HW model.

## 4.2 Soft-Wall Model (SW)

For the so called soft-wall model the action of the full 5-dimensional dual gravity theory is given by [19, 42]

$$S = \int d^5x e^{-\Phi(z)} \sqrt{g} \text{Tr} \left\{ |DX|^2 + 3|X|^2 - \frac{1}{2g_5^2} (F_V^2 + F_A^2) \right\}, \quad (4.37)$$

with  $d^5x = d^4x dz$  where  $d^4x$  denotes the usual 3 + 1 spacetime components. The metric is given by the *AdS* metric  $ds^2 = g_{MN} dx^M dx^N = \frac{1}{z^2} (\eta_{\mu\nu} dx^\mu dx^\nu - dz^2)$ , therefore  $\sqrt{g} = \frac{1}{z^5}$ .

The dilaton coupling  $e^{-\Phi(z)}$  will be discussed in more detail later. Here the covariant derivative of the scalar field  $X$  is defined via

$$D^M X = \partial^M X - i[V^M, X] - i\{A^M, X\}, \quad (4.38)$$

the field strength tensor for the vector field is given by

$$F_V^{MN} := \partial^M V^N - \partial^N V^M - i([V^M, V^N] + [A^M, A^N]), \quad (4.39)$$

whereas for the axial vector field it is given by

$$F_A^{MN} := \partial^M A^N - \partial^N A^M - i([V^M, A^N] + [A^M, V^N]). \quad (4.40)$$

We also note that  $V_M := V_{Ma}T^a$  and  $A_M := A_{Ma}T^a$ , where the  $T^a$ 's are the generators of the gauged isospin symmetry. Varying the action with respect to the vector gauge field  $V^M$  gives the following equations of motion

$$\partial_M \left( e^{-\Phi(z)} \sqrt{g} F^{MNa} \right) + e^{-\Phi(z)} \sqrt{g} f^{abc} F^{MNa} V_M^b F^{MNc} = 0, \quad (4.41)$$

where  $F_{MN}^a$  is understood to be the  $a$ -th coefficient in  $F_V^{MN} = F_V^{MNa} T^a$ . Note that we use capital Latin letters as the summation index for the five spacetime components and lower case letters for the summation index contracted with the generators  $T^a$  of the symmetry group. As usual upper spacetime indices can only be contracted with lower once and vice versa. For the indices of the 4-dimensional part of the spacetime we will use Greek letters in the following. The coefficients  $f^{abc}$  are the structure coefficients of the corresponding symmetry group. We can linearize the equations of motion, since we are here only interested in the two-point correlator as pointed out for the case of the HW model in [18]. We can use an axial-like gauge  $V_z = 0$  as well as the condition for isospin conservation  $\partial^\mu V_\mu = 0$ . Further we can Fourier transform the 4-dimensional spacetime coordinates such that  $\int d^4x e^{iqx} V_\mu^a(x^\mu, z) = V_\mu^a(q, z)$  to obtain

$$\partial_z \left( \frac{e^{-\Phi}}{z} \partial_z V_\mu^a \right) + \frac{q^2 e^{-\Phi}}{z} V_\mu^a = 0. \quad (4.42)$$

Here  $z^2 \partial_z = -\partial^z$  was used. We need to solve this equation in order to calculate the two-point correlation function. There are again two possible ways to calculate the correlation function. Either by straightforward solving (4.42) or by expanding the correlator in an infinite tower of vector mesons. But before we discuss these two methods we first have a closer look at the relation between  $V_\mu^a$  and the correlator itself.

### 4.2.1 The SW two-point correlation function

The holographic duality states that there is a one-to-one correspondence between the fields in the 5-dimensional gravity theory and the field theory operators. At the boundary the value of the gravity fields can be directly interpreted as the source of the field theory operator [29]. In our specific case this means that we can take the vector gauge field  $V_\mu^a$  and use it to deduce the correlation function of the sources  $\langle J_\mu^a(x) J_\nu^b(0) \rangle$ . In order to do so we first split the field into two parts  $V_\mu^a(q, z) = V(q, z) \tilde{V}_\mu^a(q)$ . The latter one  $\tilde{V}_\mu^a(q)$  is interpreted as the source of the vector current  $J_\mu^a$ .  $V(q, z)$  is normalized to  $V(q, \epsilon) = 1$ , where  $z = \epsilon$  means that we take the limit  $\epsilon \rightarrow 0$  as  $z$  approaches the boundary. The



correlator can now be calculated as usually in QFT by taking the second variation of the partition function (which is related to the 5-dimensional action). In order to do that it is best to first isolate the part of the action which does not vanish by validity of the equations of motion. Again, since we are only interested in the two-point correlation function, linear equations of motions are sufficient. This means that we can drop all the terms in the action which are of degree four or higher. Partially integrating the relevant part of the equations of motion gives

$$\begin{aligned}
S &= \int d^5x e^{-\Phi(z)} \sqrt{g} \text{Tr} \left\{ -\frac{1}{2g_5^2} F_V^2 \right\} \\
&= -\frac{1}{4g_5^2} \int d^5x e^{-\Phi(z)} \sqrt{g} (\partial_M V_N^a - \partial_N V_M^a) F_V^{MNa} \\
&= -\frac{1}{2g_5^2} \int d^5x e^{-\Phi(z)} \sqrt{g} (\partial_M V_N^a) F_V^{MNa} \\
&= -\frac{1}{2g_5^2} \int d^5x \left[ \partial_M \left( e^{-\Phi(z)} \sqrt{g} V_N^a F_V^{MNa} \right) - V_N^a \partial_M \left( e^{-\Phi(z)} \sqrt{g} F_V^{MNa} \right) \right].
\end{aligned} \tag{4.43}$$

We used the fact that  $\text{Tr} [T^a T^b] = \frac{1}{2} \delta^{ab}$ . The second term in the brackets is equal to zero, since it fulfills the linearised equations of motion. For the first term we can use Stokes' theorem to get rid of the integration over  $z$ .

$$\begin{aligned}
S &= -\frac{1}{2g_5^2} \int d^5x \partial_M \left( e^{-\Phi(z)} \sqrt{g} V_N^a F_V^{MNa} \right) \\
&= -\frac{1}{2g_5^2} \int d^4x z^2 e^{-\Phi(z)} \sqrt{g} \left( V_\mu^a F_V^{z\mu a} \right) \Big|_{z=\epsilon} \\
&= -\frac{1}{2g_5^2} \int d^4x \frac{e^{-\Phi(z)}}{z^3} \left( V_\mu^a F_V^{z\mu a} \right) \Big|_{z=\epsilon} \\
&= -\frac{1}{2g_5^2} \int d^4x \left( \frac{e^{-\Phi(z)}}{z} V_\mu^a \partial_z V^{\mu a} \right) \Big|_{z=\epsilon}
\end{aligned} \tag{4.44}$$

In the last line the gauge condition  $V_z = 0$  has been used. With the help of (4.44) we can now calculate the two-point correlator of the source by taking the second variation. Using the previously mentioned isospin conservation constraint  $\partial^\mu V_\mu = 0$  ( $q^\mu V_\mu = 0$ ), and therefore  $\tilde{V}_\mu^a \tilde{V}^{\mu a} = \tilde{V}_\mu^a \tilde{V}_\nu^b \Pi^{\mu\nu} \delta^{ab}$  with  $\Pi^{\mu\nu} \equiv \eta^{\mu\nu} - q^\mu q^\nu / q^2$ , we find

$$i \int d^4x e^{iqx} \langle J_\mu^a(x) J_\nu^b(0) \rangle = -\frac{e^{-\Phi}}{g_5^2} \delta^{ab} (q^2 \eta_{\mu\nu} - q_\mu q_\nu) \frac{\partial_z V(q, z)}{q^2 z} \Big|_{z=\epsilon}. \tag{4.45}$$

This makes it possible for us to isolate the self energy function

$$\Pi_V(-q^2) = -\frac{e^{-\Phi}}{g_5^2} \frac{\partial_z V(q, z)}{q^2 z} \Big|_{z=\epsilon}. \tag{4.46}$$

#### 4.2.2 Calculating the self energy function for the SW Model

For the SW model we choose a non-trivial background dilaton function  $\Phi(z) = \kappa^2 z^2$ . This achieves a Regge-type spectrum of mesons of the form  $M_{V_n}^2 = 4\kappa^2(n+1)$  [43], as we will show later.

### Variant A

The first method to calculate the self energy function is to solve equation (4.42) for  $V_\mu^a(q, z)$  with the boundary conditions  $V(q, \epsilon) = 1$  in the limit  $\epsilon \rightarrow 0$  and  $\lim_{z \rightarrow \infty} V(q, z) = 0$ . The general analytical solution to this equation is given by [43]

$$V(q, z) = A {}_1F_1\left(-\frac{q^2}{4\kappa^2}, 0, (\kappa z)^2\right) + BU\left(-\frac{q^2}{4\kappa^2}, 0, (\kappa z)^2\right), \quad (4.47)$$

with the confluent hypergeometric function of first kind  ${}_1F_1$  and one of second kind  $U$ . Imposing the boundary conditions we find that the solution is

$$V(q, z) = \Gamma\left(1 - \frac{q^2}{4\kappa^2}\right) U\left(\frac{-q^2}{4\kappa^2}, 0, (\kappa z)^2\right). \quad (4.48)$$

Plugging this into equation (4.46), switching to the Euclidean momentum  $Q^2 = -q^2$  and expanding in a series for small  $\epsilon$  gives

$$\Pi_V(Q^2) = \frac{1}{2g_5^2} \left( \psi^{(0)}\left(\frac{Q^2}{4\kappa^2} + 1\right) + \log(\kappa^2) + 2\log(\epsilon) + 2\gamma \right) + \mathcal{O}(\epsilon). \quad (4.49)$$

Here  $\gamma = 0.577\dots$  is the Euler-Mascheroni constant,  $\psi^{(0)}$  is the polygamma function, which is in general given as the derivative of logarithm of the gamma function by  $\psi^{(n)}(z) = \frac{d^{n+1}}{dz^{n+1}} \log \Gamma(z)$ . In our special case we have  $\psi^{(0)}(z) = \psi(z) = \frac{\Gamma'(z)}{\Gamma(z)}$ . All terms of higher order in  $\epsilon$  denoted by  $\mathcal{O}(\epsilon)$  vanish as  $\epsilon \rightarrow 0$ . However the term proportional to  $\log(\epsilon)$  does not. To get rid of it we have to introduce a counterterm analogous to [44] by

$$S_c(\mu) = \int d^4x \left( \frac{e^{-\Phi(\epsilon)}}{2g_5^2} \log(\epsilon\mu) \right) \text{Tr} \{F_V(x, \epsilon)\}^2, \quad (4.50)$$

which leads to a counterterm in the self energy function according to

$$\Pi_V^c(Q^2) = -\frac{1}{g_5^2} \log(\mu\epsilon). \quad (4.51)$$

Here  $\mu$  is the renormalization scale. Together this yields

$$\Pi_V^{\text{ren}}(Q^2) = \lim_{\epsilon \rightarrow 0} [\Pi_V(q^2) + \Pi_V^c(q^2)] = \frac{1}{2g_5^2} \left( \psi^{(0)}\left(\frac{Q^2}{4\kappa^2} + 1\right) + \log\left(\frac{\kappa^2}{\mu}\right) + 2\gamma \right). \quad (4.52)$$

We can use the fact that  $\psi^{(0)}(n) = -\gamma + \sum_{k=1}^{n-1} \frac{1}{k}$  and the  $n$ -th harmonic number  $H_n = 1 + \frac{1}{2} + \frac{1}{3} + \dots + \frac{1}{n} = \sum_{k=1}^n \frac{1}{k}$  to simplify this even more

$$\Pi_V^{\text{ren}}(Q^2) = \frac{1}{2g_5^2} \left( H_{\frac{Q^2}{4\kappa^2}} + \log\left(\frac{\kappa^2}{\mu}\right) + \gamma \right). \quad (4.53)$$

Note that here we actually use the analytic continuation of the harmonic number to the complex plane  $H_x = \int_0^1 \frac{1-t^x}{1-t} dt = -\sum_{k=1}^{\infty} \binom{x}{k} \frac{(-1)^k}{k}$ , since  $\frac{Q^2}{4\kappa^2}$  can (and in our application will) be a real number. For the calculation of the observable quantity  $a_\mu$  we need  $\bar{\Pi}_V(Q^2) = \Pi_V^{\text{ren}}(Q^2) - \Pi_V^{\text{ren}}(0)$ , which we find is given by

$$\bar{\Pi}_V(Q^2) = \frac{1}{2g_5^2} H_{\frac{Q^2}{4\kappa^2}}. \quad (4.54)$$

### Variante B expansion in an infinite tower of vector mesons

The second way to calculate the hadronic vacuum polarization is to expand the self energy function in terms of the infinite tower of vector mesons. For Minkowski momentum  $q^2 = -Q^2$  the exact self energy function has poles at  $q^2 = M_{V_n}^2$ . The vector gauge field can be expanded in the following way [45]

$$V_\mu^a(x, z) = \sum_{n=0}^{\infty} V_\mu^{a,(n)}(x) \psi_{V_n}(z). \quad (4.55)$$

After Fourier transformation and replacing  $q^2$  in equation (4.42) by  $M_{V_n}^2$  we can solve for a normalizable function  $\psi_{V_n}(z)$  for each value of  $M_{V_n}^2 = M_n^2$ .  $\psi_{V_n}(z) = \psi_n(z)$  has to be normalizable (and therefore vanishes at  $z \rightarrow \infty$ ) and also has to fulfill  $\psi_n(\epsilon) = 0$ . In order to solve the resulting equation (still with the dilaton function  $\Phi(z) = \kappa^2 z^2$ )

$$\partial_z \left( \frac{e^{-\kappa^2 z^2}}{z} \partial_z \psi_n \right) + \frac{M_n^2 e^{-\kappa^2 z^2}}{z} \psi_n = 0, \quad (4.56)$$

we can make simplifications analogous to [43] and [19] by substituting

$$\psi_n(z) = e^{\kappa^2 z^2/2} \sqrt{z} \Psi_n(z). \quad (4.57)$$

This is essentially the same as described in appendix A with  $u = z$ . The resulting differential equation is then

$$-\Psi_n'' + \left( \kappa^4 z^2 + \frac{3}{4z^2} \right) \Psi_n = M_n^2 \Psi_n. \quad (4.58)$$

Solving this equation with the mentioned conditions gives

$$\Psi_n(z) = \kappa^2 z^2 \sqrt{\frac{2}{n+1}} e^{-\kappa^2 z^2/2} \frac{L_n^1(\kappa^2 z^2)}{\sqrt{z}}, \quad (4.59)$$

which directly leads us to the solution of equation (4.56)

$$\psi_n(z) = \kappa^2 z^2 \sqrt{\frac{2}{n+1}} L_n^1(\kappa^2 z^2). \quad (4.60)$$

The first four eigenfunctions  $\Psi_n(z)$  are given in figure 4.2. The eigenvalues (squared meson masses) provide a linear spectrum

$$M_{V_n}^2 = 4\kappa(n+1). \quad (4.61)$$

Here  $n$  starts with  $n = 0$  for the lightest vector meson. As we have shown for the case of the hard-wall model explicitly in section 4.1, one can derive the current correlator by using basic knowledge about the Green's function in terms of the eigenstates of a differential operator. The generalization to the soft-wall model is straightforward and the resulting current correlator is given by

$$\Pi_V(-q^2) = \frac{1}{g_5^2} \sum_{n=0}^{\infty} \frac{F_{V_n}^2}{(q^2 - M_{V_n}^2) M_{V_n}^2}, \quad (4.62)$$

where

$$F_{V_n} = \frac{1}{g_5 z} e^{-\kappa^2 z^2} \partial_z \psi_n(z) \Big|_{z=\epsilon \rightarrow 0}. \quad (4.63)$$

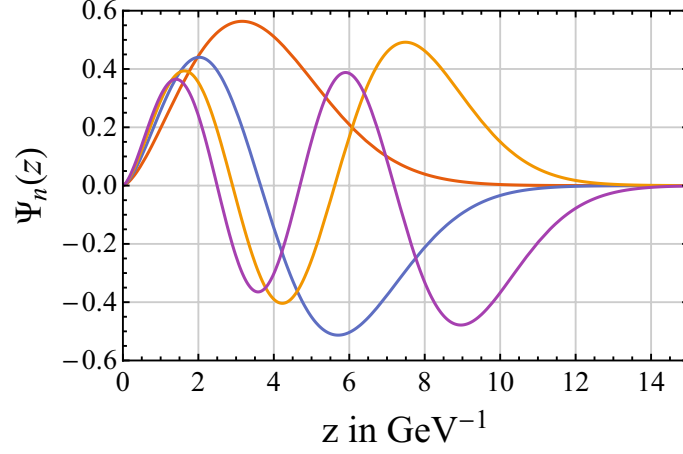


Figure 4.2: Plot of the first four eigenstates  $\Psi_n(z)$  for the standard soft-wall model.

One can show by using (4.60) that the decay constant  $F_{V_n}$  is given by the simple form

$$F_{V_n} = \frac{1}{g_5} \kappa^2 \sqrt{8(n+1)}. \quad (4.64)$$

For the subtracted and renormalized current correlator in Euclidean momentum  $Q^2$  this finally leads to

$$\bar{\Pi}_{V_n}(Q^2) = \Pi_V^{\text{ren}}(Q^2) - \Pi_V^{\text{ren}}(0) = \sum_{n=0}^{\infty} \frac{Q^2 F_{V_n}^2}{(Q^2 + M_{V_n}^2) M_{V_n}^4}. \quad (4.65)$$

The results for the mass spectrum of the SW model as well as the decay constants can be found in table 4.4. The result for the calculated leading order HVP contribution to the anomalous magnetic moment of the muon  $a_\mu$  is given in table 4.5 at the end of the next section 4.3.

n	$M_{V_n}$	$F_{V_n}^{1/2}$
1	775.0	260.0
2	1096	309.2
3	1342	342.2
4	1550	367.7
5	1733	388.8
6	1898	406.9
7	2050	422.9
8	2192	437.2

Table 4.4: Vector meson masses  $M_{V_n}$  and decay constants  $F_{V_n}^{1/2}$  of the standard SW model in MeV.

### 4.3 Generalized SW Model

Following [45] we can generalize the action of the 5-dimensional gravity theory in a way such that we can shift our meson mass spectrum by an arbitrary constant  $M_{V_n}^2 = 4\kappa^2(n+1+b)$ .

We again use the  $AdS$  metric for the 5-dimensional space and work with the general ansatz

$$S = \int d^4x dz f^2 \left( -\frac{1}{4g_5^2} F_{MN}^2 \right), \quad (4.66)$$

for the relevant part of the holographic action. We do not trace over any indices therefore we have a factor  $\frac{1}{4g_5^2}$  in front, also the indices are all lower ones. Our task is now to determine a function  $f(z)$  which provides a differential equation for the meson states and the desired mass spectrum. The differential equation corresponding to the action (4.66) is  $\partial_z (f^2 \partial_z \psi_{V_n}) + f^2 M_{V_n}^2 \psi_{V_n} = 0$ . After some manipulation ( $\psi_{V_n} = \frac{\Psi_n}{f}$ ) this gives

$$-\Psi_n'' + \frac{f''}{f} \Psi_n = M_n^2 \Psi_n. \quad (4.67)$$

For  $\frac{f''}{f} = \kappa^4 z^2 + \frac{3}{4z^2}$  we know from (4.61) above that we would obtain the mass spectrum  $M_{V_n}^2 = 4\kappa^2(n+1)$ . To get our desired spectrum we find

$$\frac{f''}{f} = \kappa^4 z^2 + \frac{3}{4z^2} + 4\kappa^2 b, \quad (4.68)$$

and therefore

$$f(z) = \Gamma(1+b) \frac{e^{-\kappa^2 z^2/2}}{\sqrt{z}} U(b, 0, \kappa^2 z^2). \quad (4.69)$$

This generalizes the action to

$$S = \int d^4x dz \sqrt{g} e^{-\kappa^2 z^2} U^2(b, 0, \kappa^2 z^2) \left( -\frac{1}{4g_5^2} F_{MN} F^{MN} \right). \quad (4.70)$$

With this action we will now calculate the HVP for some specific choices of the parameters  $\kappa$  and  $b$ . For  $V(q, z)$  and the condition  $\lim_{z \rightarrow \infty} V(q, z) = 0$  we find

$$V(q, z) = \frac{\Gamma\left(-\frac{q^2}{4\kappa^2} + b + 1\right) U\left(b - \frac{q^2}{4\kappa^2}, 0, \kappa^2 z^2\right)}{\Gamma(b+1) U(b, 0, \kappa^2 z^2)}. \quad (4.71)$$

Furthermore, for the self energy function, by using (4.46) as well as subtracting the self-energy function for  $q^2 = 0$  as in (4.52), we find

$$\bar{\Pi}_V(q^2) = -\frac{1}{2g_5^2} \left( \frac{(q^2 - 4\kappa^2 b) \left( H_b - H_{b - \frac{q^2}{4\kappa^2}} \right)}{q^2} + b\psi^{(1)}(b+1) \right). \quad (4.72)$$

The last thing left to determine before calculating the HVP are the parameters  $\kappa$  and  $b$ . In [45] this is done by comparing the expansion of (4.72) for large  $q^2$  (or equivalently large Euclidean  $Q^2$ ) with the operator product expansion (OPE). There the following values have been chosen

$$\begin{aligned} \kappa &= 0.4525 \text{ GeV} & b &= 0.046 \\ \kappa &= 0.55 \text{ GeV} & |b| &= 0.3, \end{aligned} \quad (4.73)$$

where the first set of values are simple numerical fits of the OPE, whereas the latter ones are for  $\kappa$  the correct value to match the  $\mathcal{O}(Q^{-4})$  term (for the  $b = 0$  case) and for  $b$  the

correct value to obtain a realistic value for the gluon condensate. The calculated value for the leading order HVP effects on the anomalous magnetic moment of the muon can be found in table 4.5. Here we used  $b = -0.3$  since this gives the more realistic result.

Another idea is to use the decay width for the estimation of the parameters. In the paper [45] they found

$$\kappa = 0.524 \text{ GeV} \quad b = -0.3, \quad (4.74)$$

where the predicted value for  $b$  is the same as above. This fit does provide an even higher result for  $a_\mu^{\text{HVP,LO}}$  as can be seen in table 4.5. The mass spectra for each case can easily be calculated via  $M_{V_n}^2 = 4\kappa^2(n+1+b)$ . We did not explicitly calculate the decay constants here, since we used the analytical result (4.72) for the calculation of  $a_\mu^{\text{HVP,LO}}$ .

Another approach to generalize the SW model is taken in [46], here a 5-dimensional mass is introduced in the action. In the simplest form (linearised form) it is given by

$$S_{5\text{D}} = \frac{1}{2g_5^2} \int d^4x dz \sqrt{g} e^{\phi(z)} \left( -\partial^M V^N \partial_M V_N + m_5^2 V^N V_N \right). \quad (4.75)$$

The goal is to completely leave out the dilaton background  $e^{\phi(z)} = 1$  and obtain the correct mass spectrum due to the ansatz

$$m_5^2(z) = bz^2 + c^2z^4 \quad (4.76)$$

for the 5-dimensional mass. The corresponding equations of motion are

$$\left[ q^2 + z\partial_z \left( \frac{1}{z} \partial_z \right) - \frac{m_5^2(z)}{z^2} \right] V_\mu(q, z) = 0. \quad (4.77)$$

Proceeding as usual by solving the equations of motion under the conditions  $V(q, 0) = 1$  and  $\lim_{z \rightarrow \infty} V(q, z) = 0$  we find

$$V(q, z) = e^{-\frac{1}{2}(cz^2)} \Gamma \left( \frac{-q^2 + b + 4c}{4c} \right) U \left( \frac{b - q^2}{4c}, 0, cz^2 \right). \quad (4.78)$$

Passing to Euclidean momentum  $Q^2 = -q^2$  gives

$$V(q, z) = e^{-\frac{1}{2}(cz^2)} \Gamma \left( 1 + \frac{Q^2 + b}{4c} \right) U \left( \frac{Q^2 + b}{4c}, 0, cz^2 \right). \quad (4.79)$$

Before proceeding further we would like to determine the mass spectrum provided by equation (4.77). We can do this by making a very similar substitution to (4.57),

$$V(q, z) \rightarrow \sqrt{z} \psi_{V_n}(z), \quad (4.80)$$

which yields

$$-\psi_{V_n}'' + \left( c^2 z^2 + \frac{3}{4z^2} \right) \psi_{V_n} = (M_{V_n}^2 - b) \psi_{V_n}. \quad (4.81)$$

Comparing this with our result from section 4.2.2, especially equation (4.61), we immediately notice that

$$M_{V_n}^2 = 4c(1+n) + b. \quad (4.82)$$

Because of the obvious analogy to the standard SW model from now on we write  $\kappa^2 = c$ . Now we can continue with the calculation of the HVP. Expanding (4.79) in powers of  $z$  yields

$$V(q, z) = 1 + \frac{1}{4}z^2 \left( (b + q^2) \left( H_{\frac{q^2+b}{4\kappa^2}} + \log(\kappa^2) + 2\log(z) \right) + (\gamma - 1)b - 2\kappa^2 + (\gamma - 1)q^2 \right) + \mathcal{O}(z^3) \quad (4.83)$$

in the limit  $z \rightarrow 0$ . Here a different renormalization than above (see equation (4.51)) is used. We simply drop the logarithmically divergent term  $\log(\frac{z^2}{\kappa^2})$  in equation (4.83) instead of renormalizing the current correlator afterwards. (The results for both methods are equal, but since we are following [46] we use this method.) Doing so we find

$$\Pi_V(Q^2) = -\frac{(b - Q^2) H_{\frac{b-Q^2}{4\kappa^2}} + (\gamma - 1)b - 2\kappa^2 - \gamma Q^2 + Q^2}{2\kappa^2 Q^2}. \quad (4.84)$$

This expression has a serious problem for the calculation of the HVP. It does diverge at  $Q^2 \rightarrow 0$ . We solve this problem by simply subtracting the divergent part. However this is not an acceptable solution since this is not equivalent to a renormalization with a local counterterm. Further we again subtract  $\Pi_V(0)$  to obtain

$$\bar{\Pi}_V(Q^2) = \frac{4\kappa^2(b - Q^2) H_{\frac{b}{4\kappa^2}} - 4\kappa^2(b - Q^2) H_{\frac{b-Q^2}{4\kappa^2}} - bQ^2\psi^{(1)}\left(\frac{b}{4\kappa^2} + 1\right)}{8\kappa^4 Q^2}. \quad (4.85)$$

The parameters  $\kappa$  and  $b$  are again fitted using the OPE. The values found for the parameters are

$$\kappa = 0.5477 \text{ GeV} \quad |b| = 0.36 \text{ GeV}^2. \quad (4.86)$$

The resulting value for  $a_\mu^{\text{HVP,LO}}$  can be found in Table 4.5.

values for $a_\mu^{\text{HVP,LO}}$ ( $10^{-10}$ )			
model	parameters	$N_f = 2$	$N_f = 3$
standard SW	$\kappa = 387.5 \text{ GeV}$	276.4	331.7
generalized SW [45]	$\kappa = 0.4525 \text{ GeV}, b = 0.046$	188.1	225.8
	$\kappa = 0.55 \text{ GeV}, b = -0.3$	320.9	385.0
generalized SW [46]	$\kappa = 0.524 \text{ GeV}, b = -0.3$	350.8	421.0
	$\kappa = 0.5477 \text{ GeV}, b = 0.36 \text{ GeV}^2$	304.5	365.4

Table 4.5: Calculated values of  $a_\mu^{\text{HVP,LO}}$  from the standard SW model and two generalizations of it. Note that for the model in the last line the definition of  $b$  is different than for the one above. Therefore it has dimension of energy squared.

#### 4.4 Interpolating between HW and SW model

In this section we discuss two models that interpolate between the previously discussed hard-wall and soft-wall models. The idea is to combine some features of the HW and the SW model into one single model.

#### 4.4.1 Dilaton background for the HW model

The idea here is to introduce a dilaton background in the hard-wall model. This is of course equivalent to introducing an upper bound to the  $z$ -coordinate in the soft-wall model. By doing so we have got an additional parameter that needs to be fixed (in total we have to fix the three constants  $g_5$ ,  $z_m$  and  $\kappa$ ). How we are going to fix them in detail is shown below. But before we do so, we have to calculate  $\Pi_V(-q^2)$  explicitly.

Since we only introduce an upper bound in the  $z$ -coordinate the differential equations for the dual fields are the same as in the soft-wall model

$$\partial_z \left( \frac{e^{-\Phi}}{z} \partial_z V_\mu^a \right) + \frac{q^2 e^{-\Phi}}{z} V_\mu^a = 0. \quad (4.87)$$

However the boundary conditions need to be adapted such that we have

$$V(q, \epsilon) = 1, \quad \partial_z V(q, z)|_{z=z_m} = 0, \quad (4.88)$$

which for the eigenfunctions would mean the same as in the HW model

$$\psi_{V_n}(\epsilon) = 0, \quad \partial_z \psi_{V_n}(z_m) = 0. \quad (4.89)$$

The general solution of (4.87) is of course the same as in equation (4.47). Determining the constants gives

$$V(q, z) = - \frac{q^4 \Gamma\left(-\frac{q^2}{4\kappa^2}\right) L_{\frac{q^2}{4\kappa^2}}^{-1}(\kappa^2 z^2) U\left(1 - \frac{q^2}{4\kappa^2}, 1, \kappa^2 z_m^2\right)}{16\kappa^4 L_{\frac{q^2}{4\kappa^2}-1}(\kappa^2 z_m^2)} - \frac{q^2 \Gamma\left(-\frac{q^2}{4\kappa^2}\right) U\left(-\frac{q^2}{4\kappa^2}, 0, z^2 \kappa^2\right)}{4\kappa^2}. \quad (4.90)$$

Using, as in the soft-wall model, that  $\Pi_V(-q^2) = - \frac{e^{-\Phi}}{g_5^2} \frac{\partial_z V(q, z)}{q^2 z} \Big|_{z=\epsilon}$  we find by taking the limit  $\epsilon \rightarrow 0$  and renormalizing in the same way as in section 4.2

$$\Pi_V^{\text{ren}}(-q^2) = \frac{1}{2g_5^2} \left( H_{-\frac{q^2}{4\kappa^2}} + \frac{\Gamma\left(1 - \frac{q^2}{4\kappa^2}\right) U\left(1 - \frac{q^2}{4\kappa^2}, 1, \kappa^2 z_m^2\right)}{L_{\frac{q^2}{4\kappa^2}-1}(\kappa^2 z_m^2)} + \gamma \right). \quad (4.91)$$

As we know, the poles of this function are located at the values of the meson masses. This can be seen by expanding it in a sum over normalizable eigenstates as we did previously in section 4.1 and 4.2. For later convenience let us also calculate the subtracted self-energy function  $\bar{\Pi}_V(q^2) = \Pi_V^{\text{ren}}(-q^2) - \Pi_V^{\text{ren}}(0)$

$$\bar{\Pi}_V(q^2) = \frac{1}{2g_5^2} \left( \text{Chi}(\kappa^2 z_m^2) + H_{-\frac{q^2}{4\kappa^2}} + \frac{\Gamma\left(1 - \frac{q^2}{4\kappa^2}\right) U\left(1 - \frac{q^2}{4\kappa^2}, 1, \kappa^2 z_m^2\right)}{L_{\frac{q^2}{4\kappa^2}-1}(\kappa^2 z_m^2)} - \text{Shi}(\kappa^2 z_m^2) \right), \quad (4.92)$$

with  $\text{Shi}(z) = \int_0^z \sinh(t)/t dt$  and  $\text{Chi}(z) = \gamma + \log(z) + \int_0^z (\cosh(t) - 1)/t dt$ . To fix the parameters  $g_5$ ,  $z_m$  and  $\kappa$  we are going to do the following. First we fix  $g_5^2$  and  $\kappa$  by matching the first two terms of the OPE. Then  $z_m$  is determined such that the mass of the first vector meson is  $m_\rho = 775 \text{MeV}$ . As mentioned we do this by looking at the poles



of equation (4.91) (one can also use (4.92), since it has the same poles). Again switching to Euclidean momentum  $Q^2 = -q^2$  and expanding (4.91) at large  $Q^2$  we find

$$\Pi_V^{\text{ren}}(Q^2) = \frac{1}{g_5^2} \left( \gamma + \frac{1}{2} \log \left( \frac{Q^2}{4\kappa^2} \right) + \frac{\kappa^2}{Q^2} - \frac{2\kappa^4}{3Q^4} + \frac{16\kappa^8}{15Q^8} + \mathcal{O} \left( \frac{1}{Q^{10}} \right) \right). \quad (4.93)$$

Comparing this to the OPE (also used before in equation (4.32))

$$\Pi_V(Q^2) = \frac{N_c}{24\pi^2} \left( 1 + \frac{\alpha_s}{\pi} \right) \log \left( \frac{Q^2}{\mu^2} \right) - \frac{\alpha_s}{24\pi} \frac{N_c}{3} \frac{\langle G^2 \rangle}{Q^4} + \frac{14N_c}{27} \frac{\pi\alpha_s \langle q\bar{q} \rangle^2}{Q^6}, \quad (4.94)$$

we find first of all that  $g_5^2 = 4\pi^2$  as it is the case in the SW and the standard HW model. Secondly we see that

$$\kappa = \left( \frac{\langle \frac{\alpha}{\pi} G^2 \rangle}{24} 6\pi^2 \right)^{\frac{1}{4}}, \quad (4.95)$$

where  $\langle \frac{\alpha}{\pi} G^2 \rangle$  can be calculated as in [39]. However this is where we encounter a problem. It is supposed that  $\langle \frac{\alpha}{\pi} G^2 \rangle = 0.012 \text{ GeV}^4$ , which yields  $\kappa \approx 0.415 \text{ GeV}$ . But this value for  $\kappa$  would make it impossible to fit  $z_m$  to match the mass of the first vector meson. The reason for this is that we cannot have a meson mass in this model being lower than the lowest meson mass of the soft-wall model with the same value for  $\kappa$ . This is something not completely obvious to see, but intuitively it is clear when we think about the expansion of the vector gauge field in its eigenfunctions. Since we have the same differential equation in both models, just the upper  $z$  boundary is finite in our current case, we expect the eigenvalues to get higher with a lower boundary in the same way as the energy eigenvalues of a particle in an infinite square well get higher when the walls come closer together.

Anyway, we still have the problem of the "too high" value for  $\langle \frac{\alpha}{\pi} G^2 \rangle$  in our model. However, this quantity is not known that precisely and so we will choose it in the following simply by hand loosely based on its value given in [39] by  $\langle \frac{\alpha}{\pi} G^2 \rangle = 0.012 \text{ GeV}^4$ . To be more precise, we are going to do calculations for different values of the gluon condensate. These values together with their associated values for  $\kappa$  and  $z_m$  are given in table 4.6. Given now

$\langle \frac{\alpha}{\pi} G^2 \rangle (\text{GeV}^4)$	$\kappa (\text{GeV})$	$z_m (\text{GeV}^{-1})$
0.003	0.2933	3.775
0.005	0.3333	4.169
0.007	0.3625	4.743
0.008	0.3748	5.237
0.009	0.3860	6.642

Table 4.6: Parameters  $\kappa$  and  $z_m$  corresponding to the chosen value of  $\langle \frac{\alpha}{\pi} G^2 \rangle$ .

these parameters, we can calculate the mass spectrum for each set of them by solving the eigenvalue equation with the boundary conditions (4.89). Doing so we obtain the mass spectra given in table 4.7. The results for  $a_\mu^{\text{HVP,LO}}$  using this model for the five parameter fits described above are given in table 4.8 for  $N_f = 2$  and  $N_f = 3$ .

$\langle \frac{\alpha}{\pi} G^2 \rangle$ (GeV <sup>4</sup> )	0.003	0.005	0.007	0.008	0.009
$M_{V_1}$ (MeV)	775	775	775	775	775
$M_{V_2}$ (MeV)	1531	1429	1319	1250	1140
$M_{V_3}$ (MeV)	2337	2145	1929	1786	1524
$M_{V_4}$ (MeV)	3156	2879	2564	2352	1944
$M_{V_5}$ (MeV)	3981	3622	3210	2931	2383
$M_{V_6}$ (MeV)	4808	4368	3861	3517	2834

Table 4.7: Masses of the first six vector meson state for each value of  $\langle \frac{\alpha}{\pi} G^2 \rangle$ .

	values for $a_\mu^{\text{HVP,LO}}$ ( $10^{-10}$ )				
$\langle \frac{\alpha}{\pi} G^2 \rangle$ (GeV <sup>4</sup> )	0.003	0.005	0.007	0.008	0.009
$N_f = 2$	366.2	332.6	304.3	291.1	278.3
$N_f = 3$	439.5	399.1	365.1	349.4	333.9

Table 4.8: Results for  $a_\mu^{\text{HVP,LO}}$  for each value of  $\langle \frac{\alpha}{\pi} G^2 \rangle$  and  $N_f = 2, 3$ .

#### 4.4.2 Improved holographic QCD background

In this subsection we discuss the model proposed in [47]. The idea there is to replace the dilaton background of the soft-wall model  $e^{-\Phi} = e^{-\kappa^2 z^2}$  with a background that interpolates between HW and SW model. This background is given by

$$e^{-\Phi(z)} = \frac{e^{\lambda^2 z_0^2} - 1}{e^{\lambda^2 z_0^2} + e^{\lambda^2 z^2} - 2}. \quad (4.96)$$

This background has one parameter more than the HW and SW model and exhibits certain features as we can see in figure 4.3. For  $z \rightarrow 0$  we find that  $\lim_{z \rightarrow 0} e^{-\Phi(z)} = 1$  as in the case

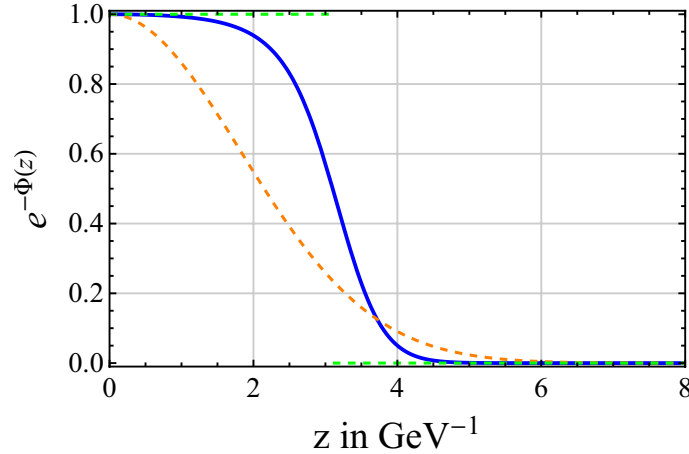


Figure 4.3: Plot of the dilaton background  $e^{-\Phi(z)}$  for the HW model (dashed green), the SW model (dashed orange) and the model interpolating between these two (blue). The latter one is given in equation (4.96). As we can see, the proposed background has features of both of the other two models.

of the soft-wall model. At  $z = z_0$ , the usual upper bound of the hard-wall model we find

that  $e^{-\Phi(z)}|_{z=z_0} = \frac{1}{2}$ . Formally we can recover the hard-wall model in the limit  $\lambda z_0 \rightarrow \infty$ , the soft-wall model is given by the limit  $\lambda z \gg \lambda z_0$ . For  $\lambda z_0$  we stick to the fit of [47], for  $z_0$  we use the same value as in the case of the HW model which is slightly different compared to the value in the reference paper. So the parameters we use are

$$\lambda z_0 = 2.1, \quad z_0 = 3.101 \text{ GeV}. \quad (4.97)$$

The value  $\lambda z_0 = 2.1$  provides a very good fit of the pion electromagnetic form factor  $F_\pi(Q^2)$ , whereas the pion decay constant is poorly fitted by the value  $f_\pi = 88.0 \text{ MeV}$ .

For the calculation of the mass spectrum, the decay constant and further the leading order HVP contribution to  $a_\mu$  pretty much nothing changes compared to the soft-wall model in section 4.2. We simply can substitute our expression for  $e^{-\Phi(z)}$  in all the equations given there. Therefore we will not write down all the terms and equations explicitly here, but rather refer to the section on the soft-wall model for them. It is clearly not possible to solve our equations analytically, so we have to rely on numerical calculations of the eigenvalues and eigenfunctions. As in the case of the pure soft-wall model we obtain the eigenvalue equation

$$\partial_z \left( \frac{e^{-\Phi(z)}}{z} \partial_z \psi_n \right) + \frac{M_{V_n}^2 e^{-\Phi(z)}}{z} \psi_n = 0. \quad (4.98)$$

Applying the same transformation as in the SW model,  $\psi_n(z) = e^{\Phi(z)/2} \sqrt{z} \Psi_n(z)$ , yields

$$-\Psi_n'' + V_v(z) \Psi_n = M_{V_n}^2 \Psi_n, \quad (4.99)$$

with the potential

$$V_v(z) = \frac{4e^{\lambda^2 z^2} (4\lambda^4 z^4 - 3) + e^{2\lambda^2 z^2} (4\lambda^4 z^4 + 3) + (6 - 8\lambda^4 z^4) e^{\lambda^2(z^2+z_0^2)} - 12e^{\lambda^2 z_0^2} + 3e^{2\lambda^2 z_0^2} + 12}{4z^2 (e^{\lambda^2 z^2} + e^{\lambda^2 z_0^2} - 2)^2}. \quad (4.100)$$

Solving equation (4.99) for the mass spectrum as well as calculating the decay constants

$$F_{V_n} = \frac{1}{g_5 z} e^{-\Phi(z)} \partial_z \psi_n(z) \Big|_{z=\epsilon \rightarrow 0} \quad (4.101)$$

is straightforward. The 5-dimensional coupling constant  $g_5$  has also the same value as in the SW model, because in the limit  $g_5$  is fitted both models yield the same result. The resulting values of  $M_{V_n}$  and  $F_{V_n}$  for the first eight meson states can be found in table 4.9.

Given them and as usually

$$\Pi_V^{\text{ren}}(Q^2) - \Pi_V^{\text{ren}}(0) = \sum_{n=0}^{\infty} \frac{Q^2 F_{V_n}^2}{(Q^2 + M_{V_n}^2) M_{V_n}^4}, \quad (4.102)$$

we can calculate  $a_\mu^{\text{HVP,LO}}$ . The resulting values using the first sixteen vector meson states can be found in table 4.10.

n	$M_{V_n}$	$F_{V_n}^{1/2}$
1	769.4	319.8
2	1590	521.9
3	2202	602.4
4	2608	636.2
5	2953	675.4
6	3256	709.3
7	3531	736.6
8	3786	761.8

Table 4.9: Vector meson masses  $M_{V_n}$  and decay constants  $F_{V_n}^{1/2}$  of the model interpolating between HW and SW model in MeV.

	values for $a_\mu^{\text{HVP,LO}} (10^{-10})$	
	$N_f = 2$	$N_f = 3$
Interpolating model [47]	452.6	543.1

Table 4.10: Calculated values for  $a_\mu^{\text{HLO}}$  within a model interpolating between HW and SW model.

## 4.5 Li and Huang dilaton model

The so far discussed models have been giving a quite good description of the meson spectra and their decay constants. However they have also some very big shortcomings. As we have seen, the hard-wall model of section 4.1 provides a meson mass spectrum  $m_{V_n}^2 \sim n^2$ , different from the expected linear Regge behavior  $m_{V_n}^2 \sim n$ . The soft-wall model of section 4.2 on the other hand shows exactly this linear Regge behavior. When it comes to the description of chiral symmetry breaking only the HW model can provide a consistent realization of it. The question is now whether one can find a model that provides the correct Regge trajectory as well as a consistent realization of chiral symmetry breaking. The model proposed by Li and Huang in [48] and [49] does provide exactly these features.

The self-consistent hQCD model developed by them is formulated in the framework of graviton-dilaton systems, such that the dilaton field is dual to the dimension-2 gluon condensate responsible for the linear confinement. The scalar field corresponding to the quark anti-quark condensate can explain chiral symmetry breaking. The 5-dimensional action of the graviton-dilaton system is given by

$$S_G = \frac{1}{16\pi G_5} \int d^5x \sqrt{g_s} e^{-2\Phi} (R + 4\partial_M \Phi \partial^M \Phi - V_G(\Phi)). \quad (4.103)$$

In the pure soft-wall model the quadratic dilaton factor was introduced by hand in order for the model to yield a linear spectrum for the vector mesons. The metric was still  $AdS$  and in the action the factor  $e^{-\Phi}$  was multiplied, which altered the equations of motion compared to the HW model. Here the dilaton field is introduced dynamically. Solving the equations of motion (the Einstein equations and additional field equations in this case) selfconsistently, automatically gives a deformation of the  $AdS$  metric. As we will see, the

resulting metric will be of the form

$$ds^2 = b_s^2(z) (\eta_{\mu\nu} dx^\mu dx^\nu - dz^2), \quad b_s(z) \equiv e^{A_s(z)}. \quad (4.104)$$

Note that for  $A_s(z) = -\log(z/L)$  we would again obtain the pure  $AdS$  metric  $ds^2 = g_{MN} dx^M dx^N = \frac{L^2}{z^2} (\eta_{\mu\nu} dx^\mu dx^\nu - dz^2)$ . Previously we left out (set to unity) the factor  $L^2$ , as it does not alter our results in any way, but in order to stick to the notation of [49] we include it here. The 5-dimensional action for the mesons propagating in the dilaton background is basically the same as for the soft-wall model

$$S_M = - \int d^5x \sqrt{g_s} e^{-\Phi} \text{Tr} \left\{ |DX|^2 + V_X(X^+ X, \Phi) + \frac{1}{4g_5^2} (F_L^2 + F_R^2) \right\}. \quad (4.105)$$

The only difference here is that we left the scalar potential  $V_X$  arbitrary for now, such that it can also contain terms where the scalar field and the dilaton field mix. The complete action is then given by

$$S = S_G + \frac{N_f}{N_c} S_M, \quad (4.106)$$

where we also have a different prefactor in front of the field strength tensor compared to section 4.2. This does not matter in the end, but as mentioned we keep it here to stick to the notation of the paper of Li and Huang. In [49] it is shown that two different dilaton backgrounds can reproduce the glueball spectra of lattice calculations. We call the two resulting models Model I and Model II with the corresponding background fields

$$\begin{aligned} \text{Model I: } \quad \Phi(z) &= \mu_G^2 z^2 \\ \text{Model II: } \quad \Phi(z) &= \mu_G^2 z^2 \tanh(\mu_G^2 z^2). \end{aligned} \quad (4.107)$$

The scalar field  $X$  is expected to have a nonzero VEV  $\chi(z)$ , which yields the vacuum action to be given by

$$\begin{aligned} S_{vac} &= S_{G,vac} + \frac{N_f}{N_c} S_{M,vac} \\ S_{G,vac} &= \frac{1}{16\pi G_5} \int d^5x \sqrt{g_s} e^{-2\Phi} (R + 4\partial_M \Phi \partial^M \Phi - V_G(\Phi)) \\ S_{M,vac} &= - \int d^5x \sqrt{g_s} e^{-\Phi} \left( \frac{1}{2} \partial_M \chi \partial^M \chi + V_C(\chi, \Phi) \right). \end{aligned} \quad (4.108)$$

The variation of the action (4.108) with respect to the metric and the scalar field yields (after a lengthy calculation, which we skip here)

$$\begin{aligned} -A_s'' + A_s'^2 + \frac{2}{3} \Phi'' - \frac{4}{3} A_s' \Phi' - \frac{\lambda}{6} e^\Phi \chi'^2 &= 0, \\ \Phi'' + (3A_s' - 2\Phi') \Phi' - \frac{3\lambda}{16} e^\Phi \chi'^2 - \frac{3}{8} e^{2A_s - \frac{4}{3}\Phi} \partial_\Phi \left( V_G(\Phi) + \lambda e^{\frac{7}{3}\Phi} V_C(\chi, \Phi) \right) &= 0, \\ \chi'' + (3A_s' - \Phi') \chi' - e^{2A_s} V_{C,\chi}(\chi, \Phi) &= 0, \end{aligned} \quad (4.109)$$

where  $V_{C,\chi}$  is the derivative of  $V_C$  with respect to  $\chi$ . We also defined  $\lambda = \frac{16\pi G_5 N_f}{L^3 N_c}$  in order to simplify our notation. The idea is now the following: Given one of the dilaton fields  $\Phi(z)$  of (4.107) and the scalar field  $\chi$ , we can solve self-consistently the equations in (4.109) for the metric deformation  $A_s(z)$ , the dilaton potential  $V_G(\Phi)$  and the scalar

potential  $V_C(\chi, \Phi)$ . In our case most important is of course the field  $A_s(z)$ , since we will need it to calculate the meson spectrum and the associated HVP. To solve for  $A_s(z)$  it is actually sufficient to know  $\chi'(z)$ . The field  $\chi(z)$  itself is constrained in the UV region by the condition

$$\chi(z) \xrightarrow{z \rightarrow 0} m_q \zeta z + \frac{\sigma}{\zeta} z^3, \quad (4.110)$$

with  $\zeta^2 = \frac{N_c^2}{4\pi^2 N_f}$ . In the IR we demand the following conditions for  $A_s(z)$  to hold

$$A'_s(z) \xrightarrow{z \rightarrow \infty} 0, A_s(z) \xrightarrow{z \rightarrow \infty} \text{const.} \quad (4.111)$$

Using (4.111) together with the first equation of (4.109), we see that  $\chi(z)$  at  $z \rightarrow \infty$  has to fulfill the equation

$$\frac{2}{3}\Phi'' - \frac{\lambda}{6}e^\Phi \chi'^2 = 0. \quad (4.112)$$

This means that in the IR we have

$$\chi(z) \xrightarrow{z \rightarrow \infty} \sqrt{\frac{8}{\lambda}} \mu_G e^{-\Phi/2}. \quad (4.113)$$

Using the UV and IR behavior, we can parameterize  $\chi'(z)$  for our two different dilaton backgrounds of equation (4.107).

$$\text{Model I: } \chi'(z) = \sqrt{\frac{8}{\lambda}} \mu_G e^{-\Phi/2} (1 + c_1 e^{-\Phi} + c_2 e^{-2\Phi}) \quad (4.114)$$

$$\text{Model II: } \chi'(z) = \sqrt{\frac{8}{\lambda}} \mu_G e^{-\Phi/2} \left(1 + d_1 e^{-\Phi} + d_2 z^2 e^{-2\Phi} - \frac{1}{2} e^{-3\Phi}\right)$$

The various constants that appear here are defined by

$$\begin{aligned} c_1 &= -2 + \frac{5\sqrt{2\lambda}m_q\zeta}{8\mu_G} + \frac{3\sqrt{2\lambda}\sigma}{4\zeta\mu_G^3}, & c_2 &= 1 - \frac{3\sqrt{2\lambda}m_q\zeta}{8\mu_G} - \frac{3\sqrt{2\lambda}\sigma}{4\zeta\mu_G^3}, \\ d_1 &= -\frac{1}{2} + \frac{\sqrt{\lambda}m_q\zeta}{2\sqrt{2}\mu_G}, & d_2 &= \frac{3\sqrt{\lambda}\sigma}{2\sqrt{2}\zeta\mu_G}. \end{aligned} \quad (4.115)$$

By integrating (4.114) we can easily calculate  $\chi(z)$ , but for our purpose it is not necessary to do so. Our focus is now rather on solving the first equation in (4.109) for  $A_s(z)$ . Keep in mind that we have to impose the boundary conditions (4.111) on  $A_s$ . As we expect  $A_s(z)$  to approach  $-\log(z)$  at  $z \rightarrow 0$  in order to obtain the pure *AdS* background, we define

$$A(z) = A_s(z) + \log(z). \quad (4.116)$$

So we get rid of the divergence of  $A_s(z)$  at  $z = 0$  and can impose the boundary conditions

$$A(0) = 0, \quad A'(0) = 0. \quad (4.117)$$

These conditions automatically yield a solution for  $A_s(z)$  that satisfies (4.111). The resulting differential equation for  $A(z)$  reads

$$-A''(z) - \frac{4}{3}\left(A'(z) - \frac{1}{z}\right)\Phi'(z) + \left(A'(z) - \frac{1}{z}\right)^2 - \frac{1}{z^2} - \frac{1}{6}\lambda\chi'^2 e^{\Phi(z)} + \frac{2\Phi''(z)}{3} = 0. \quad (4.118)$$

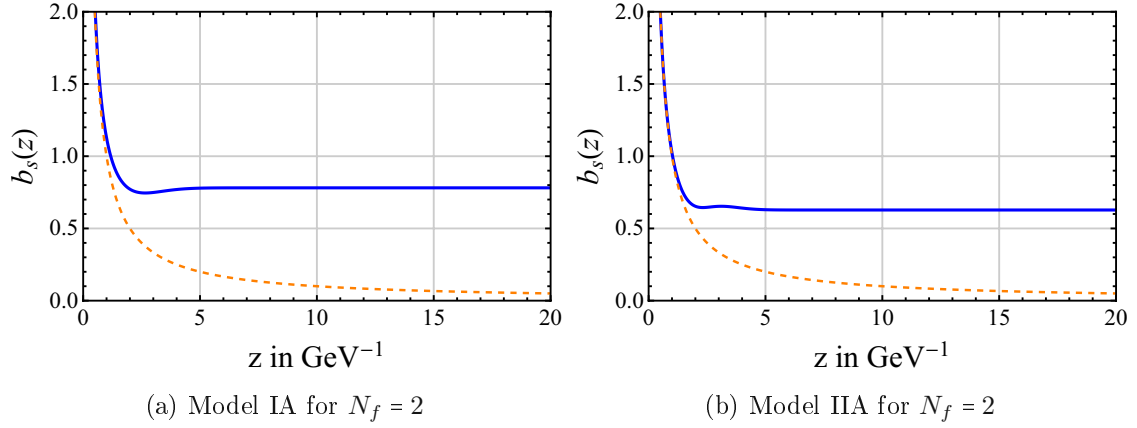


Figure 4.4: Plot of the metric function  $b_s(z) = e^{A_s(z)}$  for the Li-Huang model in blue compared to  $b_s(z)$  for the standard SW model (dashed orange line). Here we only plot the two cases Model IA and IIA with  $N_f = 2$ . For the other ones the plots are very similar.

	Model IA	Model IB	Model IIA	Model IIB
$G_5/L^3$	0.75	0.75	0.75	0.75
$m_q(\text{MeV})$	5.8	5.0	8.4	6.2
$\sigma^{1/3}(\text{MeV})$	180	240	165	226
$\mu_G$	0.43	0.43	0.43	0.43

Table 4.11: Parameters for the different Li-Huang models.

Equation (4.118) can be solved by choosing a suitable UV cutoff. Using equation (4.116) we can then determine  $A_s(z)$  and therefore also  $b_s(z) = e^{A_s(z)}$ . In fig 4.4 we plot  $b_s(z)$  and compare it to the corresponding expression from the standard SW model, where we simply have  $A_s(z) = -\log(z)$ . The various parameters and constants appearing in our equations so far are fixed in table 4.11. These values have been found in [49] to produce meson spectra in good agreement with the experimental data. The difference between parameter set A and B has to do with the pion states. Set A gives better values for the pion form factor, the results for the decay constants are worse. For the set B it is exactly the other way round.

#### 4.5.1 Vector meson states and the HVP

Having determined the metric deforming function  $A_s(z)$ , we are ready to calculate the vector meson states and their contribution to the hadronic vacuum polarization. The way this is done is very similar to the previous sections. Up to quadratic order in the fields the action for the vector mesons can be written as

$$S_V^{(2)} = -\frac{N_f}{2g_5^2 N_c L^3} \int d^5x e^{-\Phi} b_s^5 \left( \partial_z V_\mu^\perp \partial^z V^{\perp\mu} + \partial_\mu V_\nu^\perp \partial^\mu V^{\perp\nu} \right). \quad (4.119)$$

Deriving the equations of motion is straightforward and analogous to the SW and HW model. Also the expansion in a tower of vector mesons works in completely the same way. The resulting differential equation for the vector meson states after making the substitution

$\psi_{V_n} \rightarrow e^{\frac{1}{2}(\Phi - A_s)} \Psi_n$  is

$$-\Psi_n'' + V_v \Psi_n = m_n^2 \Psi_n, \quad (4.120)$$

with the potential  $V_v$  given by <sup>1</sup>

$$V_v = \frac{A_s'' - \Phi''}{2} + \frac{(A_s' - \Phi')^2}{4}. \quad (4.121)$$

In figure 4.5 we plot this potential for two sets of parameters and compare it to the potential resulting from the standard soft-wall model. We have performed the numerical calculations

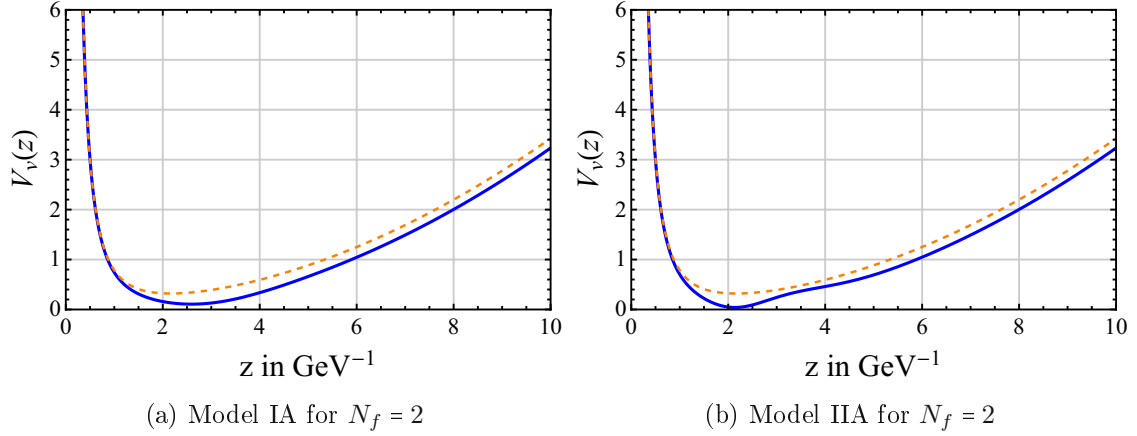


Figure 4.5: Plot of the potential  $V_v(z)$  for the Li-Huang model in blue compared to the potential for the standard SW model (dashed orange line). The potential for the Li-Huang model is plotted for Model IA and IIA with  $N_f = 2$ . For the other models the plots are very similar.

for all four models. In figure 4.6 one can see the first few eigenfunctions for Model IA.

Vector meson masses $M_{V_n}$ (MeV)								
$N_f = 2$					$N_f = 3$			
n	Mod IA	Mod IB	Mod IIA	Mod IIB	Mod IA	Mod IB	Mod IIA	Mod IIB
1	719.9	744.0	747.6	771.6	727.6	771.5	754.4	796.6
2	1133	1138	1133	1136	1135	1143	1134	1139
3	1424	1427	1428	1430	1425	1431	1429	1432
4	1664	1666	1667	1670	1665	1670	1668	1672
5	1873	1875	1875	1878	1874	1878	1876	1880
6	2061	2063	2063	2065	2062	2065	2063	2067
7	2233	2235	2235	2236	2234	2237	2235	2238
8	2393	2395	2395	2396	2394	2396	2395	2397

Table 4.12: Calculated masses for the first eight vector mesons.

The masses of the eight lightest vector mesons are given in table 4.12 <sup>2</sup>. As in the models

<sup>1</sup>In [49] they made a typo by only writing down first derivatives in the first term of  $V_v$ . The same error has been made there for all other hadronic states too, however their calculation seems to be correct in the end.

<sup>2</sup>Note that in [49] the values for  $N_f = 3$  are falsely stated to belong to  $N_f = 2$ . The same is the case for the decay constant of the vector meson with the lowest mass.



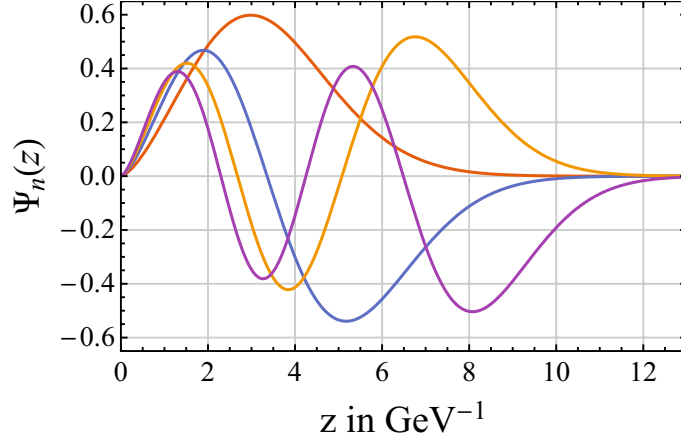


Figure 4.6: Plot of the first four eigenstates for the Li-Huang model (Model IA and  $N_f = 2$ ). The number of nodes determines the value  $n$ . For example the ground state has zero nodes. Also here the plots of other sets of parameters are very similar.

discussed before, we are again interested in the decay constants  $\langle 0 | J_V^{\mu a}(0) | V_n^b \rangle = F_{V_n} \delta^{ab} \epsilon^\mu$ . In the same manner as we did for the soft-wall model in equation (4.43), (4.44) and the following lines we can derive an expression for the decay constant. Doing the calculation explicitly one finds

$$F_{V_n} = \sqrt{\frac{N_f}{g_5^2 N_c}} e^{A_s - \Phi} \partial_z \psi_{V_n}(z) \Big|_{z \rightarrow 0}. \quad (4.122)$$

It should be immediately clear that we would obtain the result for the decay constants of the hard-wall model (4.29) for  $A_s(z) = -\log(z)$  and  $\Phi(z) = 0$ . To obtain the result for the soft-wall model (4.63) one would have to set  $A_s(z) = -\log(z)$  and  $\Phi(z) = \kappa^2 z^2$ . The prefactor  $\sqrt{\frac{N_f}{g_5^2 N_c}}$  is in fact independent of  $N_f$  and  $N_c$  in the following sense. As we know from the previous sections, the coupling constant  $g_5$  is fitted such that the leading order term in the OPE is matched. Doing so for the model here, we find

$$\frac{N_f}{g_5^2 N_c} = \frac{1}{4\pi^2}. \quad (4.123)$$

This means that  $g_5$  then depends on  $N_f$  and  $N_c$ , but no longer the prefactor  $\sqrt{\frac{N_f}{g_5^2 N_c}}$  itself. However the theory itself is of course different for each value of  $N_f$  and  $N_c$ . We performed calculations with  $N_c = 3$  for  $N_f = 2$  as well as  $N_f = 3$ . In table 4.13 we summarize the values of the decay constants squared  $F_{V_n}^2$  for the first eight vector mesons of each of the four different models. The expansion of the hadronic vacuum polarization in terms of the meson eigenfunctions (and therefore the decay constants) works in the same way as shown explicitly in section 4.1. Hence the Euclidean HVP reads

$$\Pi_V^{\text{ren}}(Q^2) - \Pi_V^{\text{ren}}(0) = \sum_{n=1}^m \frac{Q^2 F_{V_n}^2}{(Q^2 + m_{V_n}^2) m_{V_n}^4} + \mathcal{O}\left(\frac{Q^2}{m_{V_m}^2}\right). \quad (4.124)$$

The resulting values for the LO HVP contributions to the anomalous magnetic moment of the muon  $a_\mu$  are given in table 4.14. For the latter calculation we included all vector

Vector meson decay constants $F_{V_n}^{1/2}$ (MeV)								
n	$N_f = 2$				$N_f = 3$			
	Mod IA	Mod IB	Mod IIA	Mod IIB	Mod IA	Mod IB	Mod IIA	Mod IIB
1	268.7	275.4	288.2	293.8	270.9	282.4	289.9	298.8
2	331.0	331.4	329.2	332.3	331.0	332.8	329.9	336.7
3	371.4	370.8	367.7	366.5	371.2	370.1	367.3	365.7
4	401.4	401.2	400.8	399.1	401.4	400.7	400.3	397.2
5	425.8	425.8	426.5	425.6	425.9	425.7	426.3	424.2
6	446.7	446.7	447.4	447.2	446.7	446.8	447.4	446.7
7	465.0	465.0	465.4	465.6	465.0	465.1	465.5	465.6
8	481.3	481.4	481.5	481.8	481.3	481.5	481.6	482.1

Table 4.13: Calculated values for the decay constants of the first eight vector mesons.

values for $a_\mu^{\text{HVP,LO}}$ ( $10^{-10}$ )				
	Model IA	Model IB	Model IIA	Model IIB
$N_f = 2$	386.8	359.7	402.3	371.6
$N_f = 3$	453.5	397.5	472.1	410.7

Table 4.14: Results for  $a_\mu^{\text{HVP,LO}}$  using the Li-Huang model. The calculation includes states up to  $n = 16$ .

meson states up to  $n = 16$ . Therefore the error we make in the calculation of the Euclidean vacuum polarization is  $\mathcal{O}(\frac{Q^2}{M_{V_{17}}^2})$ .

## 4.6 Holographic QCD model from Sen's tachyon action

In this section we are going to work with a model proposed by Kiritsis et al. [20, 21, 22], which has several string theory ingredients. Most prominently is tachyon condensation, which is still to be considered a main mechanism of chiral symmetry breaking in this model. This model is still considered to be a bottom-up model even though it contains a lot of input from string theory. However a full derivation from string theory is far out of reach. In several ways this model is an improvement of the above discussed hard-wall and soft-wall model (see section 4.1 and 4.2). Therefore it is very interesting to see what the model of Kiritsis et al. predicts for the hadronic vacuum polarization compared to these other models.

From string theory we suppose that the meson physics, and therefore also the physics of vector mesons we are mainly interested in, is described by the dynamics of a D4- $\overline{\text{D4}}$ -brane systems in a background of closed strings. The corresponding gravity action (we choose it in the following to be 6-dimensional) reads

$$S = \int d^6x \sqrt{g_{(6)}} \left[ e^{-2\phi} \left( \mathcal{R} + 4(\partial\phi)^2 + \frac{c}{\alpha'} \right) - \frac{1}{2 \cdot 6!} F_{(6)}^2 \right], \quad (4.125)$$

where  $c$  is just a constant and  $\alpha' = l_s^2$ . We will not go into more detail about this action.

The solution of the equations of motion resulting from the action (4.125) relevant for us is

$$ds_6^2 = -g_{tt}dt^2 + g_{zz}dz^2 + g_{xx}dx_3^2 + g_{\eta\eta}d\eta^2 = \frac{R^2}{z^2} [dx_{1,3}^2 + f_\Lambda^{-1}dz^2 + f_\Lambda d\eta^2], \quad (4.126)$$

where  $R^2$  is just a constant we could already set to unity at this point (in the same manner as we did for the HW model) and

$$f_\Lambda = 1 - \frac{z^5}{z_\Lambda^5}. \quad (4.127)$$

With the constant  $Q_c$  we have

$$F_{(6)} = \frac{Q_c}{\sqrt{\alpha'}} \sqrt{-g_{(6)}} d^6x, \quad (4.128)$$

the dilaton is constant and given by

$$e^\phi = \frac{1}{Q_c} \sqrt{\frac{2c}{3}}. \quad (4.129)$$

The  $\eta$ -coordinate is compactified and identified periodically. The  $z$ -coordinate runs from 0 to  $z_\Lambda$ . In this background we place our D4- $\overline{\text{D4}}$ -brane pair. However, we are placing the branes not arbitrary, but rather in such a way that it makes our life easier. The pair is placed at a fixed value of  $\eta$  with zero distance. So what we have here is a 5-dimensions quark model embedded in a 6-dimensional glue model. We describe this by an effective DBI-like action for the dynamics of the tachyon on the brane pair given by [50]

$$S = - \int d^4x dz V(|T|) \left( \sqrt{-\det \mathbf{A}_L} + \sqrt{-\det \mathbf{A}_R} \right). \quad (4.130)$$

This is not that different from what we will use for the formulation of the Sakai-Sugimoto model in section 4.7. The relevant quantities in the action (4.130) are

$$\mathbf{A}_{(i)MN} = g_{MN} + \frac{2\pi\alpha'}{g_V^2} F_{MN}^{(i)} + \pi\alpha'\lambda \left( (D_M T)^* (D_N T) + (D_N T)^* (D_M T) \right), \quad (4.131)$$

$$D_M T = \left( \partial_M + iA_M^L - iA_M^R \right) T, \quad T = \tau e^{i\theta}, \quad (4.132)$$

and the tachyon potential

$$V = \mathcal{K} e^{-\frac{1}{2}\mu^2\tau^2}. \quad (4.133)$$

We included two constants  $g_V$  and  $\lambda$ , which we will fix later. The metric here is induced from (4.126)

$$ds_5^2 = -g_{tt}dt^2 + g_{zz}dz^2 + g_{xx}dx_3^2 = \frac{R^2}{z^2} [dx_{1,3}^2 + f_\Lambda^{-1}dz^2]. \quad (4.134)$$

The constants in the definitions above should not bother us here. As we will see, most of them will drop out anyway.

The plan to "solve" the model for the (vector) meson states is now the following. First we are going to solve for the vacuum solution, where we set all the fields to zero except the tachyon field  $\tau(z)$ . The vacuum solution for  $\tau(z)$  is then plugged back into the action (4.130). After that we expand the resulting action in quadratic order in the fields dual to the vector current. In principle we could also do that for the other fields, but here

we are just interested in the two-point correlation function of the vector current. Having the quadratic action we proceed as for all the other models discussed before in this thesis, namely by deriving the equations of motion, solving them, calculating the second variation of the (on shell) action with respect to the dual fields at the boundary and finally evaluating the vacuum polarization.

The vacuum action with  $\theta, A_L, A_R \equiv 0$  reads

$$S = -2\mathcal{K} \int d^4x dz e^{-\frac{1}{2}\mu^2\tau^2} g_{tt}^{\frac{1}{2}} g_{xx}^{\frac{3}{2}} \sqrt{g_{zz} + 2\pi\alpha'\lambda (\partial_z\tau)^2}. \quad (4.135)$$

The variation with respect to the tachyon field  $\tau(z)$  yields the differential equation

$$\tau'' - \frac{4\mu^2 z f_\Lambda}{3} \tau'^3 + \left(-\frac{3}{z} + \frac{f'_\Lambda}{2f_\Lambda}\right) \tau' + \left(\frac{3}{z^2 f_\Lambda} + \mu^2 \tau'^2\right) \tau = 0. \quad (4.136)$$

This equation has two important features we will use in the following. The first is its UV asymptotic given by two constants  $c_1$  and  $c_3$

$$\tau = c_1 z + \frac{\mu^2}{6} c_1^3 z^3 \log z + c_3 z^3 + \mathcal{O}(z^5). \quad (4.137)$$

The second one is that it is invariant under the a rescaling of  $z$

$$z \rightarrow \tilde{z} = z/z_\Lambda, \quad (4.138)$$

and also under the rescaling of the tachyon function  $\tau(z)$  itself by a constant. The latter means in fact that we can choose  $\mu$  freely. Here we will always use  $\mu^2 = \pi$ . The solution of equation (4.136) does diverge at some point. As described in [21], we need to find the solution which diverges exactly at  $z = z_\Lambda$ . This is by far not easy, since one encounters numerous numerical issues. We solve the equation using the shooting technique. We know that in the UV the solution of the equation has to behave as in (4.137). So we fix the value for  $c_1$  and then adapt the value  $c_3$  such that the divergence occurs in the IR at  $z = z_\Lambda$ . For the numerical calculations one also has to choose an UV as well as an IR cutoff additional to the physical IR cutoff. In [22] it is suggested to use the values

$$z_\Lambda^{-1} = 522 \text{MeV}, \quad c_1 = 0.0125, \quad (4.139)$$

in order to obtain the best fit of the meson spectrum in the end. So we will stick to this choice of the values for the whole section. The function  $\tau(z)$  we obtain as the solution of equation (4.136) is plotted in figure 4.7. The value we obtain for the other constant is

$$c_3 \approx 0.37. \quad (4.140)$$

We now have  $\tau(z)$  of the vacuum. In case of the full theory this is then equivalent to its vacuum expectation value  $\langle \tau \rangle(z)$ . Now we can proceed by expanding the action (4.130) up to quadratic order in the fields. As for all the other models discussed before we also define the vector and axial vector gauge fields here by

$$V_M = \frac{A_M^L + A_M^R}{2}, \quad A_M = \frac{A_M^L - A_M^R}{2}, \quad (4.141)$$

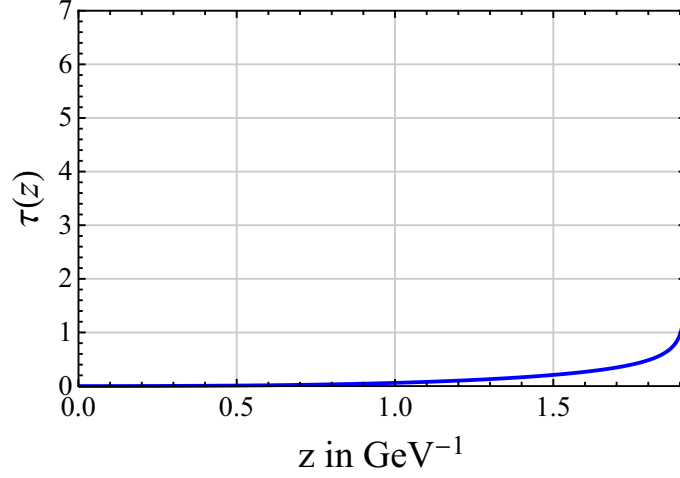


Figure 4.7: The resulting tachyon field  $\tau(z)$  for the values of (4.139). As we can see, it diverges exactly at  $z = z_\Lambda$ .

with their associated field strength tensors  $V_{MN}$  and  $A_{MN}$  and work in the gauge  $A_z = V_z = 0$ ,  $\partial^\mu V_\mu = \partial^\mu A_\mu = 0$ . For convenience let us also define  $\tilde{g}_{zz} = g_{zz} + 2\pi\alpha'\lambda (\partial_z \langle \tau \rangle)^2$ , as it will simplify our notation a bit. The vector part of the action up to quadratic order then reads

$$S_V = -\frac{(2\pi\alpha')^2}{g_V^4} \mathcal{K} \int d^4 x dz e^{-\frac{1}{2}\mu^2 \tau^2} \left[ \frac{1}{2} \tilde{g}_{zz}^{-\frac{1}{2}} V_{\mu\nu} V^{\mu\nu} + g_{xx} \tilde{g}_{zz}^{-\frac{1}{2}} \partial_z V_\mu \partial_z V^\mu \right]. \quad (4.142)$$

Using the Euler-Lagrange equations, expanding in a tower of vector meson states and replacing as usual  $q^2 = -M_{V_n}^2$  (note our metric convention here, see (4.134)) we find the eigenvalue equation for the meson states

$$-\frac{1}{e^{-\frac{1}{2}\mu^2 \tau^2} \tilde{g}_{zz}^{-\frac{1}{2}}} \partial_z \left( e^{-\frac{1}{2}\mu^2 \tau^2} g_{xx} \tilde{g}_{zz}^{-\frac{1}{2}} \partial_z \psi_{V_n}(z) \right) = M_{V_n}^2 \psi_{V_n}(z). \quad (4.143)$$

To make things a little bit clearer we substitute for all the metric coefficients and set  $\mu^2 = \pi$ . The latter one is allowed as argued above.

$$-\frac{e^{\frac{\pi\tau(z)^2}{2}}}{\sqrt{\frac{1}{z^2 \left(1 - \frac{z^5}{z_\Lambda^5}\right)} + \frac{1}{3}\pi (\tau'(z))^2}} \partial_z \left( \frac{1}{z^2} \frac{e^{-\frac{\pi\tau(z)^2}{2}}}{\sqrt{\frac{1}{z^2 \left(1 - \frac{z^5}{z_\Lambda^5}\right)} + \frac{1}{3}\pi (\tau'(z))^2}} \partial_z \psi_{V_n}(z) \right) = M_{V_n}^2 \psi_{V_n}(z) \quad (4.144)$$

As we see the constant  $R^2$  drops out completely of the equation, the only constant left is  $z_\Lambda$ . The factor  $\frac{1}{3}\pi$  in the square root of the denominators is obtained after imposing

$$\frac{R^2 \mu^2}{2\pi\alpha'\lambda} = 3. \quad (4.145)$$

This choice is explained in [21]. To solve this equation we would like to first transform it to a form such that only a single second derivative is left. This can be done analogously

to appendix A. The variable transformation is given by

$$u(z) = \int_0^z \sqrt{\left(1 - \frac{z'^5}{z_\Lambda^5}\right)^{-1} + \frac{\pi z'^2}{3} (\tau'(z'))^2} dz'. \quad (4.146)$$

This transformation maps the values of  $z \in [0, z_\Lambda]$  to  $u \in [0, \infty)$  as we can see in figure 4.8. For the transformed differential equation in the Liouville normal form we find

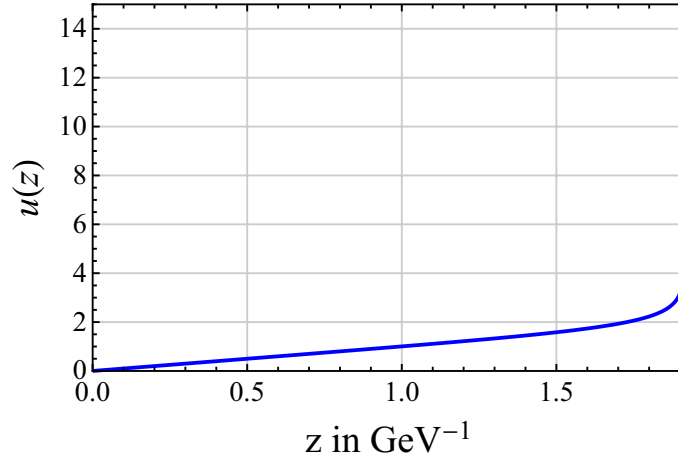


Figure 4.8: Dependence of the new coordinate  $u$  of the old one  $z$ . The compact coordinate  $z$  is mapped on the non compact coordinate  $u(z)$ .

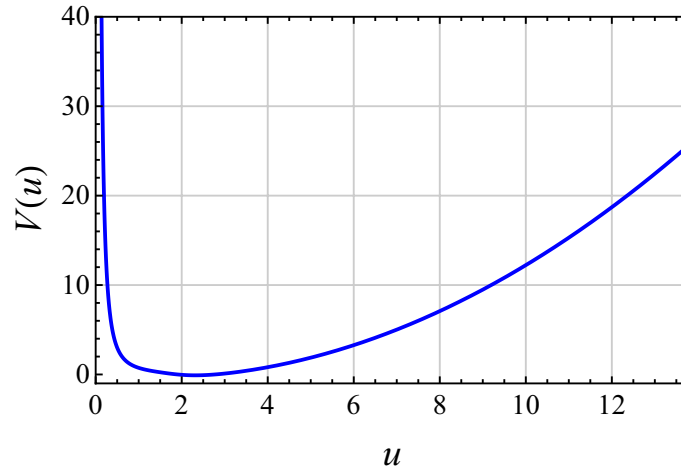


Figure 4.9: Plot of the potential  $V(u)$ . Note that this already looks very similar to the potential obtained for the soft-wall model.

$$-\frac{d^2 \alpha_n(u)}{du^2} + V(u) \alpha_n(u) = M_{V_n}^2 \alpha_n(u), \quad (4.147)$$

where

$$\Xi(u) = \frac{e^{-\frac{\pi}{4} \tau(z(u))^2}}{\sqrt{z(u)}}, \quad V(u) = \frac{1}{\Xi} \frac{d^2 \Xi}{du^2}, \quad \alpha_n(u) = \Xi(u) \psi_{V_n}(z(u)). \quad (4.148)$$

Clearly, neither the potential  $V(u)$  nor the function  $\Xi(u)$  are given by analytical expressions. Here we have to completely rely on numerical calculations from the beginning. The potential  $V(u)$  as well as the first few eigenfunctions  $\alpha_n(u)$  are plotted in figure 4.9 and 4.10. After solving (4.147) we are ready to start calculating the hadronic vacuum polar-

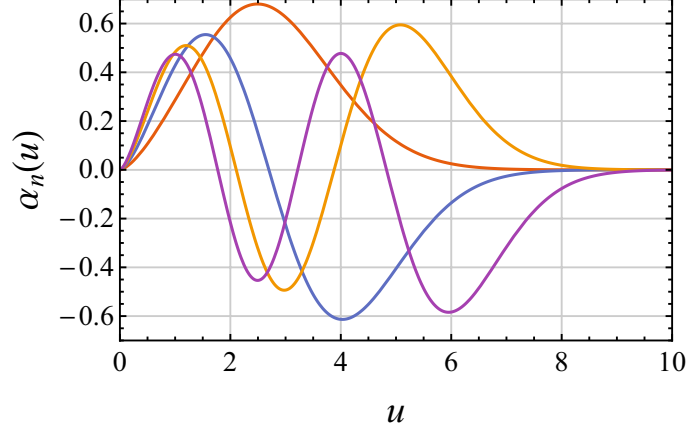


Figure 4.10: Plot of the first four eigenstates  $\alpha_n(u)$  for the tachyon condensation model.

ization. The steps here are not completely obvious from what we know from the soft-wall model of section 4.2, so we are trying to write down most things explicitly. From (4.142) we find the on shell action

$$\begin{aligned}
S_V &= -\frac{(2\pi\alpha')^2}{g_V^4} \mathcal{K} \int d^4x dz e^{-\frac{1}{2}\mu^2\tau^2} \left[ \frac{1}{2} \tilde{g}_{zz}^{\frac{1}{2}} V_{\mu\nu} V^{\mu\nu} + g_{xx} \tilde{g}_{zz}^{-\frac{1}{2}} \partial_z V_\mu \partial_z V^\mu \right] \\
&= -\frac{(2\pi\alpha')^2}{g_V^4} \mathcal{K} \int d^4x dz [\partial_z (\alpha_1(z) V_\mu \partial_z V^\nu) + \alpha_2(z) (\partial_\mu (V_\nu \partial^\mu V^\nu) - \partial_\nu (V_\mu \partial^\mu V^\nu))] \\
&= -\frac{(2\pi\alpha')^2}{g_V^4} \mathcal{K} \int d^4x [\alpha_1(z) V_\mu \partial_z V^\nu]_{z=0}^{z=z_\Lambda} \\
&= \frac{(2\pi\alpha')^2}{g_V^4} \mathcal{K} \int d^4x \alpha_1(z) V_\mu \partial_z V^\nu \Big|_{z \rightarrow 0} \\
&= \frac{(2\pi\alpha')^2}{g_V^4} \mathcal{K} \int \frac{d^4q}{(2\pi)^4} \alpha_1(z) V_\mu(q, z) \partial_z V^\mu(-q, z) \Big|_{z=\epsilon},
\end{aligned} \tag{4.149}$$

where from top to bottom we first partially integrated, then defined

$$\alpha_1(z) = e^{-\frac{1}{2}\mu^2\tau^2} g_{xx} \tilde{g}_{zz}^{-\frac{1}{2}}, \quad \alpha_2(z) = e^{-\frac{1}{2}\mu^2\tau^2} \tilde{g}_{zz}^{\frac{1}{2}}, \tag{4.150}$$

threw away the boundary terms proportional to  $\alpha_2(z)$ , evaluated the  $z$  integral and finally performed a Fourier transformation for all spacetime coordinates except  $z$ . In our usual expansion  $V_\mu(q, z) = V(q, z) \tilde{V}_\mu(q)$  we then have to take the second variation with respect to  $\tilde{V}_\mu(q)$  using the boundary condition  $V(q, 0) = 1$ . Thus we find

$$\Pi_V(-q^2) = -2 \frac{(2\pi\alpha')^2 \mathcal{K}}{g_V^4} \frac{\partial_z V(q, z)}{q^2} \Big|_{z \rightarrow \epsilon}. \tag{4.151}$$

Expanding  $\alpha_1(z)$  in the limit  $z \rightarrow 0$  yields

$$\begin{aligned}
\alpha_1(z)|_{z \rightarrow 0} &= e^{-\frac{1}{2}\mu^2\tau^2} g_{xx} \tilde{g}_{zz}^{-\frac{1}{2}} \Big|_{z \rightarrow 0} \\
&= e^{-\frac{1}{2}\mu^2\tau^2} \frac{R^2}{z^2} \frac{1}{\sqrt{\frac{R^2}{z^2 \left(1 - \frac{z^5}{z^5 \Lambda}\right)} + 2\pi\alpha'\lambda (\tau'(z))^2}} \Big|_{z \rightarrow 0} \\
&\approx R^2 \frac{1}{\sqrt{\frac{R^2 z^4}{z^2} + 2\pi\alpha' z^4 \lambda (\tau'(z))^2}} \\
&\approx \frac{R}{z} \frac{1}{\sqrt{1 + \frac{2\pi\alpha'\lambda}{R^2} z^2 (\tau'(z))^2}} \rightarrow \frac{R}{z}.
\end{aligned} \tag{4.152}$$

So we now have to fit the constant left over in the self energy function

$$\Pi_V(-q^2) = -2 \frac{(2\pi\alpha')^2 \mathcal{K} R \partial_z V(q, z)}{g_V^4 q^2 z} \Big|_{z=\epsilon} \tag{4.153}$$

using the OPE expansion. Luckily one can show that in the UV as well as in the IR our model is equal to the soft-wall model. This means that at least in these limits we know how  $V(q, z)$  does look like from section 4.2. Therefore fitting the prefactor for  $N_c = 3$  yields

$$2 \frac{(2\pi\alpha')^2 \mathcal{K} R}{g_V^4} = \frac{1}{4\pi^2}. \tag{4.154}$$

In the same manner as for all the previous models we can then find the decay constants expressed in terms of the eigenfunctions of equation (4.144), by using Green's function as described explicitly for the case of the hard-wall model in section 4.1. So in the end we obtain

$$F_{V_n}^2 = \lim_{\epsilon \rightarrow 0} \frac{1}{4\pi^2} \left[ \frac{\psi'_{V_n}(\epsilon)}{\epsilon} \right]^2 = \frac{1}{4\pi^2} [\psi''_{V_n}(0)]^2, \tag{4.155}$$

with the full subtracted self energy function as usually given by

$$\Pi_V^{\text{ren}}(-q^2) - \Pi_V^{\text{ren}}(0) = \sum_{n=1}^m \frac{q^2 F_{V_n}^2}{(q^2 - m_{V_n}^2) m_{V_n}^4} + \mathcal{O}\left(\frac{q^2}{m_{V_m}^2}\right). \tag{4.156}$$

Note that the eigenfunctions  $\psi_{V_n}(u)$  are normalized as

$$\int_0^{z_\Lambda} dz \left( e^{-\frac{\pi\tau(z)^2}{2}} \sqrt{\frac{1}{z^2 \left(1 - \frac{z^5}{z^5 \Lambda}\right)} + \frac{1}{3}\pi (\tau'(z))^2} \psi_{V_n}(z) \psi_{V_m}(z) \right) = \delta_{mn}, \tag{4.157}$$

whereas the transformed eigenfunctions are normalized canonically as

$$\int_0^\infty du \alpha_n(u) \alpha_m(u) = \delta_{mn}. \tag{4.158}$$

The eigenfunctions, the mass spectrum and further the decay constants can be calculated numerically. The results for the first eight vector mesons can be found in table 4.15. The



n	$M_{V_n}$	$F_{V_n}^{1/2}$
1	765.4	313.2
2	1382	418.0
3	1806	488.7
4	2158	538.4
5	2466	577.3
6	2744	610.4
7	2999	639.4
8	3236	665.5

Table 4.15: Vector meson masses  $M_{V_n}$  and decay constants  $F_{V_n}^{1/2}$  of the tachyon condensation model in MeV.

	values for $a_\mu^{\text{HVP,LO}} (10^{-10})$	
	$N_f = 2$	$N_f = 3$
tachyon condensation model	442.3	530.8 <sup>3</sup>

Table 4.16: Calculated values for  $a_\mu^{\text{HVP,LO}}$  within the tachyon condensation model including the contributions from the first 16 meson states.

leading order HVP contributions to  $a_\mu$  calculated in this model can be found in table 4.16.

Note, however, that the value for  $N_f = 3$  can just be viewed as an upper bound for the value of  $a_\mu^{\text{HVP,LO}}$ . The cause of this is hidden in the construction of the model. The approximate mass symmetry of the quark masses is an essential ingredient there. Adding a third quark, in this case the strange quark, with a mass more than ten times as high as the mass of the other quarks leads to a violation of this symmetry and therefore cannot give a correct value. The reason why we expect it to be the upper bound is pretty simple. Including the third quark and assuming the symmetry still holds implies that the mass of the additional quark should not be of the same order as the other two. However, this means that its production in decay processes as an example would become much more likely than it would be for a higher quark mass. A more likely production of the quark results in an higher contribution to  $a_\mu^{\text{HVP,LO}}$  and so we conclude that this approximation can just give us an upper bound.

## 4.7 Sakai-Sugimoto model

The Sakai-Sugimoto model [16, 17] is a top-down hQCD model, which can be derived from type IIA superstring theory by introducing  $N_f$  D8- $\overline{\text{D8}}$ -brane pairs and  $N_c$  D4-branes. Sakai and Sugimoto constructed their model similar to [23], which is supposed to be the dual theory of 4-dimensional Yang-Mills theory. The difference is that Sakai and Sugimoto used D8- $\overline{\text{D8}}$ -brane pairs instead of D6- $\overline{\text{D6}}$ -brane pairs in the D4-brane background.

The D4/D8/ $\overline{\text{D8}}$  configuration is given in the following way. The D4-brane background is embedded such that the 4<sup>th</sup> spatial coordinate is compactified on a  $S^1$  with radius  $M_{KK}^{-1}$ .

<sup>3</sup>As discussed above this value can just be viewed as an upper bound

This compact direction is used to break supersymmetry by imposing appropriate boundary conditions. The D8- $\overline{\text{D8}}$  probe brane pairs are added such that in the UV they are transverse to the  $S^1$ . We obtain the boundary conditions for the strings as shown in table 4.17. There

	0	1	2	3	(4)	5	6	7	8	9
D4	N	N	N	N	N	D	D	D	D	D
D8- $\overline{\text{D8}}$	N	N	N	N	D	N	N	N	N	N

Table 4.17: Boundary conditions defined by the brane configuration of the Sakai-Sugimoto model. N stands for Neumann- and D for Dirichlet boundary condition. The 4<sup>th</sup> spatial coordinate is in brackets, since it is compactified.

are now basically six different ways in which open strings can end at the different branes. In [16] it is argued that strings stretching between the D8- and  $\overline{\text{D8}}$ -brane do not influence the theory in the low energy regime and are therefore irrelevant. The strings between either D4- and D8- or D4- and  $\overline{\text{D8}}$ -brane are  $N_f$  flavors of massless fermions interpreted as the quarks of QCD with different chirality. Further the  $U(N_f)_{\text{D8}} \times U(N_f)_{\overline{\text{D8}}}$  gauge symmetry of the  $N_f$  D8- $\overline{\text{D8}}$  pairs is interpreted as the  $U(N_f)_L \times U(N_f)_R$  chiral symmetry of QCD. The three missing types of strings are the ones starting and ending at the same brane. For the 4-4 case their low-energy excitations are described by the gauge field  $A_\mu^{(\text{D4})}$  ( $\mu = 0, 1, 2, 3$ ) and the scalar fields  $A_4^{(\text{D4})}$  and  $\Phi^i$  ( $i = 5, \dots, 9$ ). For the 8-8 case and its anti-counterpart there exists a 9-dimensional gauge field  $A_\mu$  for each. The latter ones are interpreted as the dual fields of the mesons and are important in the following. But before we can calculate the mesons states we have to discuss the background metric as well as the induced metric on the D8-branes.

#### 4.7.1 Background and induced metric

The background without the probe D8-branes consists just of the  $N_c$  D4-branes with the compactified coordinate  $x^4$  as given in the first line of table 4.17. As first noticed by Witten in 1998 [51], this gives the dual of four dimensional Yang-Mill theory in the low energy regime. The solution for the metric is given by

$$ds^2 = \left(\frac{U}{R}\right)^{3/2} (\eta_{\mu\nu} dx^\mu dx^\nu + f(U) d\tau^2) + \left(\frac{R}{U}\right)^{3/2} \left(\frac{dU^2}{f(U)} + U^2 d\Omega_4^2\right), \quad (4.159)$$

with the function  $f(U) = 1 - \frac{U_{\text{KK}}^3}{U^3}$ . The Greek indices  $\mu, \nu = 0, 1, 2, 3$  refer to the first four spacetime coordinates.  $\tau \sim \tau + \frac{4\pi}{3} \frac{R^{3/2}}{U_{\text{KK}}^{1/2}}$  is the periodic coordinate of the compactified dimension and  $U$  is a radial coordinate with the holographic boundary at  $U \rightarrow \infty$ .  $U_{\text{KK}}$  is the lower bound of  $U$  and  $R$  a constant related to string theory parameters by  $R^3 = \pi g_s N_c l_s^3$ . The later very useful Kaluza-Klein mass is given by

$$M_{\text{KK}} = \frac{2\pi}{\delta\tau} = \frac{3}{2} \frac{U_{\text{KK}}^{1/2}}{R^{3/2}}. \quad (4.160)$$

From the background metric (4.159) we can calculate the induced metric on the D8-brane transverse to the 4<sup>th</sup> space direction as in table 4.17 by making  $U = U(\tau)$  dependent of  $\tau$

$$ds_{\text{D8}}^2 = \left(\frac{U}{R}\right)^{3/2} \eta_{\mu\nu} dx^\mu dx^\nu + \left(\left(\frac{U}{R}\right)^{3/2} f(U) + \left(\frac{R}{U}\right)^{3/2} \frac{U'^2}{f(U)}\right) d\tau^2 + \left(\frac{R}{U}\right)^{3/2} U^2 d\Omega_4^2, \quad (4.161)$$

For later convenience let us also introduce new coordinates for  $U$  and  $\tau$  given by

$$\begin{aligned} y &= r \cos \theta, & z &= r \sin \theta \\ U^3 &= U_{\text{KK}}^3 + U_{\text{KK}} r^2, & \theta &\equiv \frac{2\pi}{\delta\tau} \tau = \frac{3}{2} \frac{U_{\text{KK}}^{1/2}}{R^{3/2}} \tau. \end{aligned} \quad (4.162)$$

#### 4.7.2 Meson states

Now we are ready to derive the equations of motion for the fields dual to the mesons. As mentioned before we have a 9-dimensional gauge field on the D8-brane with the components  $A_\mu$ ,  $A_z$  and  $A_\alpha$  with  $\mu = 0, 1, 2, 3$  and  $\alpha = 5, 6, 7, 8$ . We are only interested in the 5-dimensional states  $A_\mu$ ,  $A_z$ , so we assume that they are independent of the other four and set  $A_\alpha = 0$ . Note that the index  $z$  of  $A_z$  refers to the coordinate defined in (4.162). The dynamics of the fields is described by the DBI action plus additional Chern-Simons (CS) terms

$$S_{D8} \propto \int d^9 x e^{-\phi} \sqrt{-\det(g_{MN} + 2\pi\alpha' F_{MN})} + S_{CS}, \quad (4.163)$$

with  $e^\phi = g_s \left(\frac{U}{R}\right)^{3/4}$ . Integrating over the 4-dimensional sphere parametrized by  $x^\alpha$ , requiring that all fields do not depend on them, and expanding up to second order in the gauge field yields

$$S_{D8} \propto \int d^4 x dz \text{Tr} \left[ \frac{R^3}{4U_z} \eta^{\mu\nu} \eta^{\rho\sigma} F_{\mu\rho} F_{\nu\sigma} + \frac{9}{8} \frac{U_z^3}{U_{\text{KK}}} \eta^{\mu\nu} F_{\mu z} F_{\nu z} \right] + \mathcal{O}(F^3). \quad (4.164)$$

We can now expand the gauge field in complete sets of orthonormal functions  $\psi_n(z)$  and  $\phi_n(z)$ . Additionally we can add external gauge fields  $A_{L\mu}(x^\mu)$  and  $A_{R\mu}(x^\mu)$  to the expansion of  $A_\mu(x^\mu, z)$ , such that we have

$$\begin{aligned} A_\mu(x^\mu, z) &= A_{L\mu}(x^\mu) \psi_+(z) + A_{R\mu}(x^\mu) \psi_-(z) + \sum_{n=1}^{\infty} B_\mu^{(n)}(x^\mu) \psi_n(z) \\ A_z(x^\mu, z) &= \varphi^{(0)}(x^\mu) \phi_0(z) + \sum_{n=1}^{\infty} \varphi^{(n)}(x^\mu) \phi_n(z). \end{aligned} \quad (4.165)$$

Here we used  $\psi_\pm(z) \equiv \frac{1}{2}(1 \pm \psi_0(z))$  with  $\psi_0(z) \equiv \frac{2}{\pi} \arctan z$ , which is the non-normalizable zero mode of the differential equation (4.169) given below. For now we set the external gauge field to  $A_{L\mu} = A_{R\mu} = 0$  to simplify our notation. Before we substitute (4.165) into equation (4.164) let us make the very useful coordinate transformation

$$Z \equiv \frac{z}{U_{\text{KK}}}, \quad K(Z) \equiv 1 + Z^2 = \left(\frac{U_z}{U_{\text{KK}}}\right)^3. \quad (4.166)$$

First substituting only  $A_\mu(x^\mu, z) = \sum_{n=1}^{\infty} B_\mu^{(n)}(x^\mu) \psi_n(z)$  and ignoring all other terms gives

$$S_{D8} = \kappa \int d^4 x dZ \sum_{n,m} \text{Tr} \left[ \frac{1}{4} K^{-1/3} F_{\mu\nu}^{(n)} F^{(m)\mu\nu} \psi_n \psi_m + \frac{1}{2} M_{\text{KK}}^2 K B_\mu^{(n)} B^{(m)\mu} \partial_Z \psi_n \partial_Z \psi_m \right] + \dots \quad (4.167)$$

In order to obtain the action for a massive vector gauge field with canonical normalization, we impose the normalization condition

$$\kappa \int dZ K^{-1/3} \psi_n \psi_m = \delta_{nm} \quad (4.168)$$

for the orthonormal fields  $\psi_n$  given as solutions of the eigenvalue equation

$$-K^{1/3}\partial_Z(K\partial_Z\psi_n) = \lambda_n\psi_n, \quad m_{V_n}^2 \equiv \lambda_n M_{\text{KK}}^2. \quad (4.169)$$

Integrating over the  $Z$  coordinate as well as imposing an analogous condition for the fields  $\phi_n$ ,

$$(\phi_m, \phi_n) \equiv \frac{9}{4}\kappa U_{\text{KK}}^3 \int dZ K \phi_m \phi_n = \delta_{mn}, \quad (4.170)$$

we obtain for the DBI action (now also including the expansion of  $A_z$ )

$$S_{\text{DS}}^{\text{DBI}} \propto \int d^4x \text{Tr} \left[ \left( \partial_\mu \varphi^{(0)} \right)^2 + \sum_{n=1}^{\infty} \left( \frac{1}{2} \left( \partial_\mu B_\nu^{(n)} - \partial_\nu B_\mu^{(n)} \right)^2 + \lambda_n \left( B_\mu^{(n)} - \lambda_n^{-1/2} \partial_\mu \varphi^{(n)} \right)^2 \right) \right], \quad (4.171)$$

up to interaction terms. The scalar fields  $\varphi^{(n)}$  are eaten by the gauge field, such that we have no mixing between vector mesons and pions. Now we are ready to also include the external gauge fields as in the expansion of equation (4.165). We can manipulate the first two terms a little bit

$$\begin{aligned} A_{L\mu}(x^\mu)\psi_+(z) + A_{R\mu}(x^\mu)\psi_-(z) &= A_{L\mu}(x^\mu)\frac{1}{2}(1+\psi_0(z)) + A_{R\mu}(x^\mu)\frac{1}{2}(1-\psi_0(z)) \\ &= \frac{1}{2}(A_{L\mu}(x^\mu) + A_{R\mu}(x^\mu)) + \frac{1}{2}(A_{L\mu}(x^\mu) - A_{R\mu}(x^\mu))\psi_0(z) \\ &= \mathcal{V}_\mu + \mathcal{A}_\mu\psi_0(z), \end{aligned} \quad (4.172)$$

where we have defined  $\mathcal{V}_\mu \equiv \frac{1}{2}(A_{L\mu} + A_{R\mu})$  and  $\mathcal{A}_\mu \equiv \frac{1}{2}(A_{L\mu} - A_{R\mu})$  for the vector and axial part of the external gauge field. As we will see, solutions of equation (4.169)  $\psi_n(z)$  with odd number  $n$  are even function and will be interpreted as vector meson states. The ones with even  $n$  are odd functions and will therefore be interpreted as axial-vector mesons. It is reasonable to redefine the coefficients  $B_\mu^{(n)}$  by

$$v_\mu^n \equiv B_\mu^{(2n-1)}, \quad a_\mu^n \equiv B_\mu^{(2n)}. \quad (4.173)$$

So we obtain for the gauge field from equation (4.165) with our new defined coefficients

$$A_\mu = \mathcal{V}_\mu + \mathcal{A}_\mu\psi_0(z) + \sum_{n=1}^{\infty} v_\mu^n \psi_{2n-1} + \sum_{n=1}^{\infty} a_\mu^n \psi_{2n}. \quad (4.174)$$

The multiplet of fields contained in  $A_z$  represents the Goldstone bosons according to spontaneously broken  $U_A(N_f)$  symmetry

$$U(x^\mu) = \mathbf{P} \exp \left\{ i \int_{-\infty}^{\infty} dz' A_z(x^\mu, z') \right\} \equiv \exp \{ 2i\Pi(x^\mu)/f_\pi \} \in U(N_f). \quad (4.175)$$

But since the analysis of the pion field  $\Pi(x^\mu)$  is not the main interest of this study we will not go into detail about this too much and continue with our study of the vector meson states.

Continuing our study of the vector meson states we plug the gauge field expansion (4.174) back into the DBI action (4.164) to obtain an effective action up to quadratic order of the

form

$$S_{D8} = \int d^4x \left[ \frac{1}{2} \text{Tr} (\partial_\mu v_\nu^n - \partial_\nu v_\mu^n)^2 + \frac{1}{2} \text{Tr} (\partial_\mu a_\nu^n - \partial_\nu a_\mu^n)^2 \right. \\ \left. + a_{\mathcal{V}v^n} \text{Tr} (\partial^\mu \mathcal{V}^\nu - \partial^\nu \mathcal{V}^\mu) (\partial_\mu v_\nu^n - \partial_\nu v_\mu^n) + a_{\mathcal{A}a^n} \text{Tr} (\partial^\mu \mathcal{A}^\nu - \partial^\nu \mathcal{A}^\mu) (\partial_\mu a_\nu^n - \partial_\nu a_\mu^n) \right. \\ \left. + \lambda_{v^n} \text{Tr} (v_\mu^n)^2 + \lambda_{a^n} \text{Tr} (a_\mu^n)^2 \right]. \quad (4.176)$$

Here we used the following definitions

$$\lambda_{v^n} \equiv \lambda_{2n-1}, \quad \lambda_{a^n} \equiv \lambda_{2n} \\ a_{\mathcal{V}v^n} \equiv \kappa \int dz K^{-1/3} \psi_{2n-1}, \quad a_{\mathcal{A}a^n} \equiv \kappa \int dz K^{-1/3} \psi_{2n} \psi_0. \quad (4.177)$$

Diagonalizing the kinetic term by redefining

$$\tilde{v}_\mu^n \equiv v_\mu^n + a_{\mathcal{V}v^n} \mathcal{V}_\mu, \quad \tilde{a}_\mu^n \equiv a_\mu^n + a_{\mathcal{A}a^n} \mathcal{A}_\mu \quad (4.178)$$

yields

$$S_{D8} = \int d^4x \left[ \frac{1}{2} \text{Tr} (\partial_\mu \tilde{v}_\nu^n - \partial_\nu \tilde{v}_\mu^n)^2 + \frac{1}{2} \text{Tr} (\partial_\mu \tilde{a}_\nu^n - \partial_\nu \tilde{a}_\mu^n)^2 + \lambda_{a^n} \text{Tr} (\tilde{a}_\mu^n)^2 + \lambda_{v^n} \text{Tr} (\tilde{v}_\mu^n)^2 \right. \\ \left. - 2F_{a^n} \text{Tr} (\tilde{a}_\mu^n \mathcal{A}^\mu) + \lambda_{a^n} a_{\mathcal{A}a^n}^2 \text{Tr} (\mathcal{A}_\mu)^2 - 2F_{v^n} \text{Tr} (\tilde{v}_\mu^n \mathcal{V}^\mu) + \lambda_{v^n} a_{\mathcal{V}v^n}^2 \text{Tr} (\mathcal{V}_\mu)^2 \right], \quad (4.179)$$

where we already identified the decay constants by making the substitution

$$F_{A_n} \equiv \lambda_{a^n} a_{\mathcal{A}a^n}, \quad F_{V_n} \equiv \lambda_{v^n} a_{\mathcal{V}v^n}. \quad (4.180)$$

A complete derivation of this action and also for higher order terms is given in the appendix

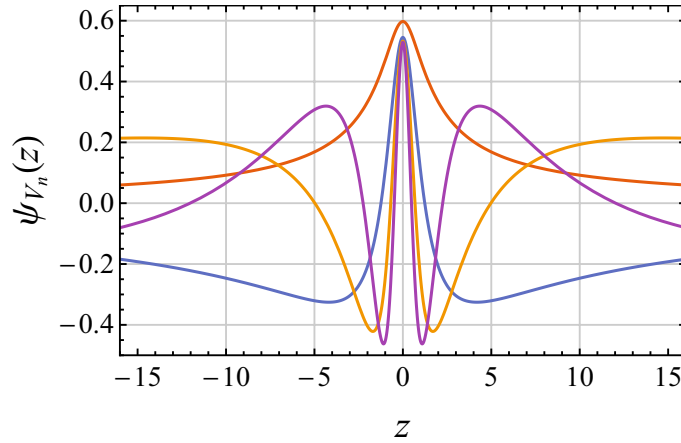


Figure 4.11: Plot of the first four eigenstates  $\psi_{V_n}(z)$  for the Sakai-Sugimoto model. As mentioned those are the symmetric eigenstates, which are interpreted as the vector meson states.

of [17]. From this form of the action (4.179) we can easily read off the decay constants for the vector and axial vector mesons

$$\langle 0 | J_\mu^{(V)a}(0) | v^{nb} \rangle = F_{V_n} \delta^{ab} \epsilon_\mu, \quad \langle 0 | J_\mu^{(A)a}(0) | a^{nb} \rangle = F_{A_n} \delta^{ab} \epsilon_\mu. \quad (4.181)$$

Using equation (4.177),  $F_{V_n}$  is given by

$$F_{V_n} = \lambda_{v^n} \kappa \int dz K^{-1/3} \psi_{2n-1}. \quad (4.182)$$

Using the equations of motion for  $\psi_{2n-1}$  (4.169) this equates to

$$F_{V_n} = -\kappa \int dz \partial_z (K \partial_z \psi_{2n-1}) = -\kappa (K \partial_z \psi_{2n-1})|_{-\infty}^{+\infty} = -2\kappa (K \partial_z \psi_{2n-1})|_{z=+\infty}, \quad (4.183)$$

where in the last step we have used that  $\psi_{2n-1}$  and also its derivative are the same at  $z \rightarrow \pm\infty$ . Note that in order to be consistent with the notation of the previous section, the eigenfunctions of the meson states are denoted by  $\psi_{V_n} = \psi_{2n-1}$ . The first four functions  $\psi_{V_n}$  are plotted in figure 4.11.

To summarize, we have to solve the equation of motion (4.169) with the boundary conditions  $\psi_n(\pm\infty) = 0$  and then plug the results into equation (4.183) to calculate  $F_{V_n}$ . Once we have  $F_{V_n}$  it is straightforward to calculate the hadronic vacuum polarization by expanding the self-energy function in terms of the meson states, as shown extensively for the case of the hard-wall model in section 4.1. The masses and decay constants calculated for the Sakai-Sugimoto model can be found in table 4.18. The resulting contributions to  $a_\mu$  to leading order from the HVP are given for the case of two and three flavors of quarks in table 4.19.

n	$M_{V_n}$	$F_{V_n}^{1/2}$
1	776.4	428.1
2	1609	889.7
3	2436	1344
4	3259	1796
5	4081	2247
6	4901	2696
7	5721	3144
8	6540	3592

Table 4.18: Vector meson masses  $M_{V_n}$  and decay constants  $F_{V_n}^{1/2}$  of the Sakai-Sugimoto model in MeV.

	values for $a_\mu^{\text{HVP,LO}} (10^{-10})$	
	$N_f = 2$	$N_f = 3$
Sakai-Sugimoto	1890	2268

Table 4.19: Values for  $a_\mu^{\text{HVP,LO}}$  within the Sakai-Sugimoto model including the contributions from the first 16 meson states.

## Chapter 5

# Conclusion and Outlook

In this chapter we summarize our results for the leading order HVP contributions to the anomalous magnetic moment of the muon  $a_\mu^{\text{HVP,LO}}$ . We also discuss the results of the other two commonly used techniques - dispersion relation and lattice QCD - and compare them with the hQCD predictions. All values for the results of other techniques are taken from [25] if no other source is cited.

### 5.1 Results from holographic QCD

#### 5.1.1 Anomalous magnetic moment

The numerous models presented in chapter 4 give a broad range of predictions for  $a_\mu^{\text{HVP,LO}}$ . All the values we calculated are summarized in table 5.1. To assess all the values we have to compare them with results obtained from other techniques. Those are given in section 5.2.

As we can see, nearly all our values lie below the ones calculated using other techniques. This could have several reasons. One might be simply that the models we used are not accurate enough for the description of QCD. In some sense this might be true, however since other quantities such as the mass spectrum are predicted quite well, it could also have other reasons. One of them has already been pointed out for the hard-wall model by Hong et al. [36]. It seems that we are missing higher order contributions of meson loops in the large- $N_c$  expansion, which are not accessible to calculations in current holographic frameworks established only in the large- $N_c$  limit. Despite this fact it should still be possible to compare our results to the dispersive result when we consider the  $e^+e^- \rightarrow \pi^+\pi^-$  processes (in regards to the dispersion relation calculations) only, since for example four pion processes are expected to be described by higher order terms in the large- $N_c$  expansion. Comparing our  $N_f = 2$  results from table 5.1 to the  $e^+e^- \rightarrow \pi^+\pi^-$  contributions of table 5.3 we see that at least for some models these values fit quite well (within 20% or less). Unfortunately not even the more advanced models such as the tachyon condensation model and the interpolating model do match the data well enough. Additionally it is interesting that most of the models underestimate the leading order HVP contribution to  $a_\mu$  except the Sakai-Sugimoto model, which yields by far to high values.

Values for $a_\mu^{\text{HVP,LO}}$ in units of $10^{-10}$		
Model	$N_f = 2$	$N_f = 3$
HW1	476.3	571.6
HW2	773.1	927.7
HW2 (UV-fit)	303.9	364.7
standard SW	276.4	331.7
generalized SW [45]	188.1	225.8
	320.9	385.0
generalized SW [46]	350.8	421.0
	304.5	365.4
Interpolating model	366.2	439.5
	332.6	399.1
	304.3	365.1
	291.1	349.4
	278.3	333.9
Interpolating model [47]	452.6	543.1
Sakai-Sugimoto model	1890	2268
tachyon condensation model [20, 21, 22]	442.3	530.8
	386.8	453.5
Li and Huang dilaton model [48, 49]	359.7	397.5
	402.3	472.1
	371.6	410.7

Table 5.1: Summary of all the calculated values for the leading order HVP contributions to the anomalous magnetic moment of the muon  $a_\mu^{\text{HVP,LO}}$  in units of  $10^{-10}$ . For details of the calculations for each model consider chapter 4. The citations are just to clarify about which model we are talking. The values given are the ones calculated in chapter 4 and not from any of the cited papers.



### 5.1.2 Mass spectrum

In chapter 4 we have also calculated the mass spectrum for each of the models. In each section the masses of the first eight vector mesons are given. It is useful to compare them to the experimental masses given in table 5.4. Even though the experimental results have quite some uncertainties (except for  $\rho(770)$ ) we should find a very similar prediction for the spectrum in the holographic models. Some of the models of chapter 4 indeed match the experimental values, but many do not as we will discuss in the following.

The hard-wall model masses of table 4.2 are far away from the experimental values. However the soft-wall model with its linear  $M_{V_n}^2$  spectrum (see table 4.4) does fit the experimental masses quite well, even better than all the models interpolating between HW and SW model. This is surprising since the latter ones are supposed to provide a more accurate description of QCD.

The more advanced models do match the mass spectrum reasonably well. The best fit is obtained from the model of Kiritsis et al. (see table 4.15), but also the predictions of the Li Huang dilaton model and the Sakai-Sugimoto model of table 4.12 and 4.18 are not too far away from the experimental data.

## 5.2 Other results

### 5.2.1 Results from lattice QCD

To compare with the lattice QCD results is a little bit simpler than for the dispersive results, because this kind of calculations give a separated value for each quark flavor in the first place. The values in this case are given in table 5.2. The value considering only the up and down quark is the  $N_f = 2$  value. Adding also the strange quark contribution gives the  $N_f = 3$  value. In total the result from the lattice calculations (including all six quarks) is

$$a_\mu^{\text{HVP,LO}} = 711.6(18.4) \times 10^{-10}, \quad (5.1)$$

which differs from the dispersion relation result. For more details see section 3.1.

$a_\mu^{\text{HVP,LO}}(ud)$	$a_\mu^{\text{HVP,LO}}(s)$
650.2	53.2

Table 5.2: Contributions of the different quarks to  $a_\mu^{\text{HVP,LO}}$  up to  $N_f = 3$  from lattice QCD in units of  $10^{-10}$  [25].

### 5.2.2 Results from dispersive calculations

In the dispersive approach the hadronic vacuum polarization is calculated from cross section data of a virtual photon decaying into hadrons. From the contributions of the different decay channels it is possible to isolate the  $N_f = 2, 3$  contributions. This is important in order to compare them with our holographic QCD results. The contributions to  $a_\mu^{\text{HVP,LO}}$  found by two different groups are listed by decay channel in table 5.3. Both groups used slightly different methods, so the results differ from each other. The contributions from

the heavier quarks are not listed in this table. As mentioned in chapter 3 the best total leading order prediction from this method is given by

$$a_\mu^{\text{HVP,LO}} = 693.1(4.0) \times 10^{-10}. \quad (5.2)$$

The total values in table 5.3 are the ones we want to compare with.

Contribution up to $N_f = 3$		
	DHMZ19 [52]	KNT19 [53]
$\pi^+ \pi^-$	507.85	504.23
$\pi^+ \pi^- \pi^0$	46.21	46.63
$\pi^+ \pi^- \pi^+ \pi^-$	13.68	13.99
$\pi^+ \pi^- \pi^0 \pi^0$	18.03	18.15
$K^+ K^-$	23.08	23.00
$K_S K_L$	12.82	13.04
$\pi^0 \gamma$	4.41	4.58
Total $N_f = 2$	590.18	587.58
Total $N_f = 3$	626.08	623.62

Table 5.3: Contributions of the different decay channels to  $a_\mu^{\text{HVP,LO}}$  up to  $N_f = 3$  in units of  $10^{-10}$  [25].

### 5.2.3 Experimental vector meson masses

Experimental vector meson masses $M_{V_n}$ in units of MeV		
$n$	Meson	Measured mass in MeV
1	$\rho(770)$	775.3
2	$\rho(1450)$	1465
(*)	$\rho(1570)^{(*)}$	1570
3	$\rho(1700)$	1720
4	$\rho(1900)$	1909
(*)	$\rho(2000)^{(*)}$	2000
5	$\rho(2150)$	2201
6	$\rho(2270)$	2265

Table 5.4: Experimentally measured vector meson masses  $M_{V_n}$  in units of MeV [54]. The values with a star (\*) are not very well confirmed experimentally, so we only consider the values for the states without the stars in our discussion. The  $\rho(1570)$  state seems to be a resonance of the vector meson with higher and lower mass, which we refer to as  $n = 2, 3$ .

The experimentally obtained vector meson masses can be found in table 5.4. For our discussion only the values without an asterisk (\*) are considered. For more details on the meson states see [54].

### 5.3 Possible improvements

As we have seen, the mass spectra as well as the obtained values for  $a_\mu^{\text{HVP,LO}}$  are not always well described by the holographic QCD models we considered in this thesis. One possible idea would be to use more advanced hQCD models. Of course we did only cover a few specific (and somehow also very simple) hQCD models. There are also a few even more advanced models out there which would be worth investigating. Another possible improvement would be to include higher order corrections which are not accessible by our current holographic framework. Admittedly, this is not a trivial task to do.

These improvements are both beyond the scope of this thesis and we leave them for the future.



## Appendix A

# Transformation into Liouville normal form

In this short appendix we are going to describe a transformation of an arbitrary Sturm-Liouville eigenvalue problem

$$\frac{d}{dz} \left[ p(z) \frac{d}{dz} \right] y(z) + [q(z) + \lambda \rho(z)] y(z) = 0, \quad (\text{A.1})$$

with eigenvalue  $\lambda$ , to the so called Liouville normal form

$$-\frac{d^2}{du^2} w(u) + [V(u) - \lambda] w(u) = 0, \quad (\text{A.2})$$

which contains no first order derivative term any more. The whole section is based on [38] and the appendix of [21]. The transformation can be achieved by first making a change of variables

$$u(z) = \int_0^z \sqrt{\frac{\rho(s)}{p(s)}} ds. \quad (\text{A.3})$$

Second we have to redefine the function we solve for by

$$w(u) = \sqrt[4]{p(z(u))\rho(z(u))} y(z(u)), \quad (\text{A.4})$$

as well as to introduce a new function

$$V(u) = \frac{1}{\rho} \left[ -q - \sqrt[4]{p\rho} \partial_z \left( p \partial_z \left( \frac{1}{\sqrt[4]{p\rho}} \right) \right) \right]. \quad (\text{A.5})$$

Note that from equation (A.3) we also know that

$$\frac{du}{dz} = \sqrt{\frac{\rho(z)}{p(z)}}. \quad (\text{A.6})$$

Since it will be important for most holographic models we discuss in this thesis, let us briefly focus on the case  $q(z) = 0$ . Also for convenience let us define

$$\Xi(u) := \sqrt[4]{p(z(u))\rho(z(u))}, \quad w(u) = \Xi(u) y(z(u)). \quad (\text{A.7})$$

Using

$$\partial_z = \sqrt{\frac{\rho(z)}{p(z)}} \partial_u, \quad (\text{A.8})$$

we can simplify equation (A.5) as

$$\begin{aligned} V(u) &= \frac{1}{\rho} \left[ -\Xi(u) \sqrt{\frac{\rho(z)}{p(z)}} \partial_u \left( p \sqrt{\frac{\rho(z)}{p(z)}} \partial_u \left( \frac{1}{\Xi(u)} \right) \right) \right] \\ &= - \left[ \frac{1}{\Xi(u)} \partial_u \left( \Xi(u)^2 \partial_u \left( \frac{1}{\Xi(u)} \right) \right) \right] \\ &= - \left[ \frac{1}{\Xi(u)} \partial_u \left( \Xi(u)^2 (-\Xi(u)^{-2}) \partial_u (\Xi(u)) \right) \right] \\ &= \frac{1}{\Xi} \frac{d^2 \Xi}{du^2}. \end{aligned} \quad (\text{A.9})$$

This expression turns out to be quite useful for some of our calculations.

# Bibliography

- [1] L. Hong, “Holographic duality, MIT OpenCourseWare Lecture Notes.”  
<https://ocw.mit.edu/courses/physics/8-821-string-theory-and-holographic-duality-fall-2014/lecture-notes/>, 2014.
- [2] D. J. Gross and F. Wilczek, *Ultraviolet Behavior of Non-Abelian Gauge Theories*, *Phys. Rev. Lett.* **30** (1973) 1343.
- [3] H. D. Politzer, *Reliable Perturbative Results for Strong Interactions?*, *Phys. Rev. Lett.* **30** (1973) 1346.
- [4] G. 't Hooft, *A Planar Diagram Theory for Strong Interactions*, *Nucl. Phys. B* **72** (1974) 461.
- [5] E. Cremmer, B. Julia and J. Scherk, *Supergravity Theory in Eleven-Dimensions*, *Phys. Lett. B* **76** (1978) 409.
- [6] J. M. Bardeen, B. Carter and S. Hawking, *The Four laws of black hole mechanics*, *Commun. Math. Phys.* **31** (1973) 161.
- [7] R. Bousso, *The Holographic principle*, *Rev. Mod. Phys.* **74** (2002) 825 [[arXiv:hep-th/0203101](https://arxiv.org/abs/hep-th/0203101)].
- [8] K. G. Wilson, *Confinement of quarks*, *Phys. Rev. D* **10** (1974) 2445.
- [9] C. R. Stephens, G. 't Hooft and B. F. Whiting, *Black hole evaporation without information loss*, *Class. Quant. Grav.* **11** (1994) 621 [[arXiv:gr-qc/9310006](https://arxiv.org/abs/gr-qc/9310006)].
- [10] L. Susskind, *The World as a hologram*, *J. Math. Phys.* **36** (1995) 6377 [[arXiv:hep-th/9409089](https://arxiv.org/abs/hep-th/9409089)].
- [11] A. M. Polyakov, *String theory and quark confinement*, *Nucl. Phys. B Proc. Suppl.* **68** (1998) 1 [[arXiv:hep-th/9711002](https://arxiv.org/abs/hep-th/9711002)].
- [12] J. M. Maldacena, *The Large  $N$  limit of superconformal field theories and supergravity*, *Int. J. Theor. Phys.* **38** (1999) 1113 [[arXiv:hep-th/9711200](https://arxiv.org/abs/hep-th/9711200)].
- [13] E. Witten, *Anti-de Sitter space and holography*, *Adv. Theor. Math. Phys.* **2** (1998) 253 [[arXiv:hep-th/9802150](https://arxiv.org/abs/hep-th/9802150)].
- [14] O. Aharony, S. S. Gubser, J. M. Maldacena, H. Ooguri and Y. Oz, *Large  $N$  field theories, string theory and gravity*, *Phys. Rept.* **323** (2000) 183 [[arXiv:hep-th/9905111](https://arxiv.org/abs/hep-th/9905111)].

- [15] M. Järvinen, *Recent progress in backreacted bottom-up holographic QCD*, *AIP Conf. Proc.* **1701** (2016) 090004 [[arXiv:1501.03693](#)].
- [16] T. Sakai and S. Sugimoto, *Low energy hadron physics in holographic QCD*, *Prog. Theor. Phys.* **113** (2005) 843 [[arXiv:hep-th/0412141](#)].
- [17] T. Sakai and S. Sugimoto, *More on a holographic dual of QCD*, *Prog. Theor. Phys.* **114** (2005) 1083 [[arXiv:hep-th/0507073](#)].
- [18] J. Erlich, E. Katz, D. T. Son and M. A. Stephanov, *QCD and a holographic model of hadrons*, *Phys. Rev. Lett.* **95** (2005) 261602 [[arXiv:hep-ph/0501128](#)].
- [19] A. Karch, E. Katz, D. T. Son and M. A. Stephanov, *Linear confinement and AdS/QCD*, *Phys. Rev. D* **74** (2006) 015005 [[arXiv:hep-ph/0602229](#)].
- [20] R. Casero, E. Kiritsis and A. Paredes, *Chiral symmetry breaking as open string tachyon condensation*, *Nucl. Phys. B* **787** (2007) 98 [[arXiv:hep-th/0702155](#)].
- [21] I. Iatrakis, E. Kiritsis and A. Paredes, *An AdS/QCD model from tachyon condensation: II*, *JHEP* **11** (2010) 123 [[arXiv:1010.1364](#)].
- [22] I. Iatrakis, E. Kiritsis and A. Paredes, *An AdS/QCD model from Sen's tachyon action*, *Phys. Rev. D* **81** (2010) 115004 [[arXiv:1003.2377](#)].
- [23] M. Kruczenski, D. Mateos, R. C. Myers and D. J. Winters, *Towards a holographic dual of large  $N(c)$  QCD*, *JHEP* **05** (2004) 041 [[arXiv:hep-th/0311270](#)].
- [24] F. Jegerlehner, *Quantum field theory and quantum electrodynamics*, in *The Anomalous Magnetic Moment of the Muon*, (Cham), pp. 23–161, Springer International Publishing, (2017),  
[https://doi.org/10.1007/978-3-319-63577-4\\_2](https://doi.org/10.1007/978-3-319-63577-4_2).
- [25] T. Aoyama et al., *The anomalous magnetic moment of the muon in the Standard Model*, [arXiv:2006.04822](#).
- [26] S. Borsanyi, Z. Fodor, J. N. Guenther, C. Hoelbling, S. D. Katz, L. Lellouch et al., *Leading-order hadronic vacuum polarization contribution to the muon magnetic moment from lattice QCD*, [arXiv:2002.12347](#).
- [27] C. Lehner and A. S. Meyer, *Consistency of hadronic vacuum polarization between lattice QCD and the  $R$ -ratio*, *Phys. Rev. D* **101** (2020) 074515 [[arXiv:2003.04177](#)].
- [28] D. Grumiller, “Lecture notes: Black Holes II.”  
[http://quark.itp.tuwien.ac.at/~grumil/pdf/Black\\_Holes\\_II.pdf](http://quark.itp.tuwien.ac.at/~grumil/pdf/Black_Holes_II.pdf), 2018.
- [29] M. Ammon and J. Erdmenger, *Gauge/Gravity Duality: Foundations and Applications*. Cambridge University Press, 2015, DOI:10.1017/CBO9780511846373.
- [30] D. Tong, “Lecture notes: Lectures on Gauge Theory.”  
<http://www.damtp.cam.ac.uk/user/tong/gaugetheory.html>, 2018.
- [31] M. Kreuzer, “Lecture notes: Supersymmetry.”  
<http://up.itp.tuwien.ac.at/~rebhana/QFT/susy.pdf>, 2015.



- [32] Y. Kim and D. Yi, *Holography at work for nuclear and hadron physics*, *Adv. High Energy Phys.* **2011** (2011) 259025 [[arXiv:1107.0155](#)].
- [33] J. Erdmenger, *Introduction to Gauge/Gravity Duality*, *PoS TASI2017* (2018) 001 [[arXiv:1807.09872](#)].
- [34] MUON G-2, *Final Report of the Muon E821 Anomalous Magnetic Moment Measurement at BNL*, *Phys. Rev. D* **73** (2006) 072003 [[arXiv:hep-ex/0602035](#)].
- [35] F. Jegerlehner, *Lepton magnetic moments: Basics*, in *The Anomalous Magnetic Moment of the Muon*, (Cham), pp. 163–246, Springer International Publishing, (2017), [https://doi.org/10.1007/978-3-319-63577-4\\_3](https://doi.org/10.1007/978-3-319-63577-4_3).
- [36] D. K. Hong, D. Kim and S. Matsuzaki, *Holographic calculation of hadronic contributions to muon  $g-2$* , *Phys. Rev. D* **81** (2010) 073005 [[arXiv:0911.0560](#)].
- [37] W. Magnus, F. Oberhettinger and R. Soni, *Formulas and Theorems for the Special Functions of Mathematical Physics*, Die Grundlehren der mathematischen Wissenschaften in Einzeldarstellungen. Springer-Verlag, 1966, DOI:10.1007/978-3-662-11761-3.
- [38] K. Svozil, *Mathematical methods of theoretical physics*, [arXiv:1203.4558](#).
- [39] M. A. Shifman, A. Vainshtein and V. I. Zakharov, *QCD and Resonance Physics. Theoretical Foundations*, *Nucl. Phys. B* **147** (1979) 385.
- [40] L. Reinders, H. Rubinstein and S. Yazaki, *Hadron Properties from QCD Sum Rules*, *Phys. Rept.* **127** (1985) 1.
- [41] J. Hirn and V. Sanz, *Interpolating between low and high energy QCD via a 5D Yang-Mills model*, *Journal of High Energy Physics* **2005** (2005) 030 [[arXiv:hep-ph/0507049](#)].
- [42] H. J. Kwee and R. F. Lebed, *Pion form-factors in holographic QCD*, *JHEP* **01** (2008) 027 [[arXiv:0708.4054](#)].
- [43] H. Grigoryan and A. Radyushkin, *Structure of vector mesons in holographic model with linear confinement*, *Phys. Rev. D* **76** (2007) 095007 [[arXiv:0706.1543](#)].
- [44] D. K. Hong, D. Kim and S. Matsuzaki, *Holographic calculation of hadronic contributions to muon  $g-2$* , *Phys. Rev. D* **81** (2010) 073005 [[arXiv:0911.0560](#)].
- [45] S. Afonin, *Generalized Soft Wall Model*, *Phys. Lett. B* **719** (2013) 399 [[arXiv:1210.5210](#)].
- [46] S. Afonin and T. Solomko, *Low and high energy constraints in AdS/QCD: not synergetic, but interchangeable?*, [arXiv:2006.14439](#).
- [47] H. J. Kwee and R. F. Lebed, *Pion Form Factor in Improved Holographic QCD Backgrounds*, *Phys. Rev. D* **77** (2008) 115007 [[arXiv:0712.1811](#)].
- [48] D. Li, M. Huang and Q.-S. Yan, *A dynamical soft-wall holographic QCD model for chiral symmetry breaking and linear confinement*, *Eur. Phys. J. C* **73** (2013) 2615 [[arXiv:1206.2824](#)].

- [49] D. Li and M. Huang, *Dynamical holographic QCD model for glueball and light meson spectra*, *JHEP* **11** (2013) 088 [[arXiv:1303.6929](#)].
- [50] A. Sen, *Dirac-Born-Infeld action on the tachyon kink and vortex*, *Phys. Rev. D* **68** (2003) 066008 [[arXiv:hep-th/0303057](#)].
- [51] E. Witten, *Anti-de Sitter space, thermal phase transition, and confinement in gauge theories*, *Adv. Theor. Math. Phys.* **2** (1998) 505 [[arXiv:hep-th/9803131](#)].
- [52] M. Davier, A. Hoecker, B. Malaescu and Z. Zhang, *A new evaluation of the hadronic vacuum polarisation contributions to the muon anomalous magnetic moment and to  $\alpha(m_Z^2)$* , *Eur. Phys. J. C* **80** (2020) 241 [[arXiv:1908.00921](#)].
- [53] A. Keshavarzi, D. Nomura and T. Teubner,  *$g - 2$  of charged leptons,  $\alpha(M_Z^2)$ , and the hyperfine splitting of muonium*, *Phys. Rev. D* **101** (2020) 014029 [[arXiv:1911.00367](#)].
- [54] PARTICLE DATA GROUP, *Review of Particle Physics*, *PTEP* **2020** (2020) 083C01.



TECHNISCHE  
UNIVERSITÄT  
WIEN  
Vienna | Austria

Institute for Theoretical Physics

**Title of work:**

Leading order HVP Contributions to the Anomalous Magnetic Moment of the Muon from Holographic QCD

**Thesis type and date:**

Master Thesis, December 2020

**Supervision:**

First Supervisor

Prof. Dr. Anton Rebhan

**Student:**

Name: Michael Stadlbauer

E-mail: michael.stadlbauer@24speed.at

Matr.-Nr.: 01609924

Semester: 9

**Statement regarding plagiarism:**

I, Michael Stadlbauer, declare that this thesis titled, "Leading order HVP Contributions to the Anomalous Magnetic Moment of the Muon from Holographic QCD" and the work presented in it are my own. I confirm that:

- This work was done wholly or mainly while in candidature for a research degree at this University.
- Where any part of this thesis has previously been submitted for a degree or any other qualification at this University or any other institution, this has been clearly stated.
- Where I have consulted the published work of others, this is always clearly attributed.
- Where I have quoted from the work of others, the source is always given. With the exception of such quotations, this thesis is entirely my own work.
- I have acknowledged all main sources of help.
- Where the thesis is based on work done by myself jointly with others, I have made clear exactly what was done by others and what I have contributed myself.

Vienna, 13. 12. 2020: \_\_\_\_\_